INFORMATION TO USERS

This manuscript has been reproduced from the microfilm master. UMI films the text directly from the original or copy submitted. Thus, some thesis and dissertation copies are in typewriter face, while others may be from any type of computer printer.

The quality of this reproduction is dependent upon the quality of the copy submitted. Broken or indistinct print, colored or poor quality illustrations and photographs, print bleedthrough, substandard margins, and improper alignment can adversely affect reproduction.

In the unlikely event that the author did not send UMI a complete manuscript and there are missing pages, these will be noted. Also, if unauthorized copyright material had to be removed, a note will indicate the deletion.

Oversize materials (e.g., maps, drawings, charts) are reproduced by sectioning the original, beginning at the upper left-hand corner and continuing from left to right in equal sections with small overlaps.

ProQuest Information and Learning
300 North Zeeb Road, Ann Arbor, MI 48106-1346 USA
800-521-0600

Université d'Ottawa · University of Ottawa

PERMISSION DE REPRODUIRE ET DE DISTRIBUER LA THÈSE

PERMISSION TO REPRODUCE AND DISTRIBUTE THE THESIS

NOM DE L'AUTEUR / NAME OF AUTHOR:	XU, Diancheng
ADRESSE POSTALE / MAILING ADDRESS:	9 DESJARDINS AVE OTTAWA ON K1N5N8
GRADE / DEGREE:	**ANNÉE D'OBTENTION / YEAR GRANTED**
M.A.Sc. (Mechanical Engineering)	2003
TITRE DE LA THÈSE / TITLE OF THESIS: "A FUZZY LOGIC APPROACH FOR CHATTER DETECTION AND SUPPRESSION IN END MILLING"	

L'auteur permet, par la présente, la consultation et le prêt de cette thèse en conformité avec les règlements établis par le bibliothécaire en chef de l'Université d'Ottawa. L'auteur autorise aussi l'Université d'Ottawa, ses successeurs et cessionnaires, à reproduire cet exemplaire par photograhie ou photocopie pour fins de prêt ou de vente au prix coûtant aux bibliothèques ou aux chercheurs qui en feront la demande.

Les droits de publication par tout autre moyen et pour vente au public demeureront la propriété de l'auteur de la thèse sous réserve des règlements de l'Université d'Ottawa en matière de publication de thèses.

The author hereby permits the consultation and the lending of this thesis pursuant to the regulations established by the Chief Librarian of the University of Ottawa. The author also authorizes the University of Ottawa, its successors and assignees, to make reproductions of this copy by photographic means or by photocopying and to lend or sell such reproductions at cost to libraries and to scholars requesting them.

The right to publish the thesis by other means and to sell it to the public is reserved to the author, subject to the regulations of the University of Ottawa governing the publication of theses.

N.B. LE MASCULIN COMPREND ÉGALEMENT LE FÉMININ

Dec. 17. 2002 — DATE

Diancheng Xu — (AUTEUR) SIGNATURE (AUTHOR)

Université d'Ottawa · University of Ottawa

Université d'Ottawa · University of Ottawa

FACULTÉ DES ÉTUDES SUPÉRIEURES ET POSTDOCTORALES

FACULTY OF GRADUATE AND POSTDOCTORAL STUDIES

XU, Diancheng

AUTEUR DE LA THÈSE - AUTHOR OF THESIS

M.A.Sc. (Mechanical Engineering)

GRADE - DEGREE

Mechanical Engineering

FACULTÉ, ÉCOLE, DÉPARTEMENT - FACULTY, SCHOOL, DEPARTMENT

TITRE DE LA THÈSE - TITLE OF THE THESIS

A Fuzzy Logic Approach for Chatter Detection and Suppression in End Milling

Ming Liang and Tet Yeap

DIRECTEUR DE LA THÈSE - THESIS SUPERVISOR

EXAMINATEURS DE LA THÈSE - THESIS EXAMINERS

M. Munro

X. Wang

J.-M. De Koninck, Ph.D.

LE DOYEN DE LA FACULTÉ DES ÉTUDES SUPÉRIEURES ET POSTDOCTORALES

SIGNATURE

DEAN OF THE FACULTY OF GRADUATE AND POSTDOCTORAL STUDIES

A Fuzzy Logic Approach for Chatter Detection and Suppression in End Milling

A thesis submitted to
the Faculty of Graduate and Postdoctoral Studies
in partial fulfilment of the requirements for the
degree of Master of Applied Science in
Mechanical Engineering

by

Diancheng Xu

Ottawa-Carleton Institute for Mechanical and Aerospace Engineering
University of Ottawa
Ottawa, Ontario, Canada, K1N 6N5

To my family

Abstract

In metal cutting processes, excessive vibration or chatter has an adverse effect on productivity and product surface quality. Various studies have been reported in the literature over the past few decades. However, the real application of the outcome of these studies has been very limited. A new system has been developed in this study for chatter detection and chatter suppression. The coherence function values of the frequency spectra from two accelerometers in orthogonal directions were used as a chatter indicator. The vibration energy was used to offset the over-vigilance behaviour of the coherence function. A fuzzy logic control approach was used for chatter suppression based on both the coherence function value and vibration energy level. To improve the adaptability of the fuzzy controller, a self-learning algorithm has also been developed for on-line updating the fuzzy rule base. A direct output tuning method was also proposed to improve the responsiveness of the system.

The proposed system has been tested using both steel and aluminium workpieces with and without thin-walls. The experimental results show that the proposed system worked reasonably well for on-line chatter detection and suppression.

The thesis also explored the possibility of using the coherence function for chatter prediction. The verification of its feasibility may be carried out in the future.

Acknowledgments

I would like to thank my supervisor, Dr. M. Liang, and my co-supervisor, Dr. T. Yeap, for their support and detailed guidance throughout my study. This thesis was part of a project initiated by them and was developed based on their continuous research, which have been done over the last eight years at the University of Ottawa's CNC Machining Lab.

The work carried out by several previous graduate students in related studies was very informative and useful in my research. The technical assistance of Mr. M. Makasare and other machine shop technicians is also appreciated.

Table of Contents

Abstract.....i

Acknowledgment.....ii

List of Figures.....vi

List of Tables.....ix

Nomenclature.....x

Chapter 1 Introduction.....1

1.1 Background.....1

1.2 Proposed Study.....1

1.3 Organization of the Thesis.....2

Chapter 2 Literature Review.....3

2.1 Chatter and Sensors for Chatter Detection.....3

2.1.1 Monitoring Tasks.....3

2.1.2 Chatter.....4

2.1.3 Sensors.....5

2.2 Feature Extraction.....5

2.2.1 Time Domain.....5

2.2.1.1 Time Series Modelling.....6

2.2.1.2 Real Time Signal Monitoring.....6

2.2.2 Frequency domain.....6

2.2.2.1 Fast Fourier Transform (FFT).....6

2.2.2.2 Wavelet Analysis.....7

2.3 Chatter Detection Mechanisms.....8

2.3.1 Cutting Parameter Measurements.....8

2.3.2 Damping Effects.....9

2.4 Control Strategy.....9
2.5 Chatter Avoidance and Suppression.....11
2.5.1 Chatter Avoidance.....11
2.5.2 Chatter Suppression.....12
2.6 Limitations of Previous Work and Motivation for the Proposed Study.....15
2.6.1 Chatter Detection.....15
2.6.2 Chatter Avoidance.....15
2.6.3 Chatter Suppression.....16
Chapter 3 Design of the Chatter Detection and System.....18
3.1 Method for Chatter Detection.....18
3.1.1 Coherence Function for Chatter Suppression.....19
3.1.2 Chatter Detection Using Mean Vibration Energy.....21
3.2 Chatter Prediction Based on Coherence Function.....21
3.2.1 Coherence Function.....21
3.2.2 Chatter Suppression Strategies.....24
3.2.3 Performance Indices.....25
3.2.4 Data Processing.....26
3.2.5 Windows Function.....27
3.2.6 Inputs and Input Scaling Factors.....28
3.3 The Structure of the Fuzzy Logic Controller.....29
3.3.1 Fuzzification and Membership Functions.....29
3.3.2 Rule Base.....32
3.3.3 Fuzzy Inference Engine and Defuzzification.....35
3.3.4 Scaling Factors.....39
3.3.4.1 Input Scaling Factors.....39
3.3.4.2 Output Scaling Factors.....40

3.3.5 Tuning Factors....42
3.3.5.1 Overshoot Suppression....42
3.3.5.2 Impact Suppression....42
3.3.5.3 Other Restricts....43
3.4 Self-learning and Direct Output Tuning Algorithms....43
3.4.1 Self-learning Algorithm for Rule Base Adjustment....44
3.4.2 Direct Outputs....46
Chapter 4 Experiments....54
4.1 Experiments Apparatus....54
4.1.1 CNC SERVO 2000 Milling Machine....55
4.1.2 Vibration Sensor....56
4.1.3 A/D Converter Card....57
4.2 Software and Algorithms....57
4.3 Experimental Set-up....57
4.4 Experimental Results....58
4.4.1 Flat Steel Workpieces—Full Immersion....62
4.4.2 Flat Steel Workpieces—Half Immersion....63
4.4.3 Double Thin-walled Steel Workpieces....63
4.4.4 Single Thin-walled Steel Workpieces....64
4.4.5 Aluminium Workpieces....64
4.4.6 Experimental Results Analysed in Frequency Domain....65
Chapter 5 Conclusion and Future Research....87
5.1 Conclusion....88
5.2 Future Research....88
References....90

List of Figures

Figure 3.1 Runout and vibration at a certain frequency.....23

Figure 3.2 Vibration and tool runout 24

Figure 3.3 Data modifications 29

Figure 3.4 Fuzzy logic control for chatter suppression 30

Figure 3.5 Illustration of fuzzification process.....30

Figure 3.6 Membership Functions.....31

Figure 3.7 Coherence ratio table: fuzzy rules for chatter suppression by adjusting spindle speed.....33

Figure 3.8 Coherence ratio table: fuzzy rules for chatter suppression by adjusting feed rate.....34

Figure 3.9 Energy table: fuzzy rules for chatter suppression by adjusting feed rate or spindle speed.....35

Figure 3.10 Illustration of input membership degrees with two triangular fuzzy sets....36

Figure 3.11a Calculation of the coefficients of output fuzzy values.....37

Figure 3.11b An illustrative rule base.....38

Figure 3.12 Defuzzification using singleton membership function.....39

Figure 3.13 Input scaling factors.....41

Figure 3.14 Fuzzy logic control with rule base self-learning for chatter suppression.....45

Figure 3.15 Feed rate adjustment with and without self-learning.....46

Figure 3.16 Rule base self-learning algorithm with different weights.....47

Figure 3.17 Coherence ratio table: fuzzy rules for chatter suppression by adjusting spindle speed using rule base self-learning algorithm.....48

Figure 3.18 Coherence ratio table: fuzzy rules for chatter suppression by adjusting feed rate using rule base self-learning algorithm.....49

Figure 3.19 Fuzzy logic control with direct outputs tuning for chatter suppression.....50

Figure 3.20 Schematic diagram for direct outputs tuning.....51

Figure 3.21 Direct outputs tuning.....52

Figure 4.1 Hardware configuration.....54

Figure 4.2 CNC SERVO 2000 milling machine.....55

Figure 4.3 The tri-axial accelerometer and thin-wall cutting.....56

Figure 4.4 Tool-workpieces with three cutting tests 59

Figure 4.5 Dimensions of the workpieces.....60

Figure 4.6 Experimental results using fuzzy logic control system (4.6).....66

Figure 4.7 Experimental results using rule base self-learning algorithm (4.7).....67

Figure 4.8 Experimental results using rule base self-learning algorithm (4.8).....68

Figure 4.9 Experimental results using rule base self-learning algorithm (4.9).....69

Figure 4.10 Experimental results using single direct output tuning algorithm (4.10).....70

Figure 4.11 Experimental results using single direct output tuning algorithm (4.11).....71

Figure 4.12 Experimental results using double direct output tuning algorithm (4.12).....72

Figure 4.13 Experimental results using double direct output tuning algorithm (4.13).....73

Figure 4.14 Experimental results using fuzzy logic control system (4.14).....74

Figure 4.15 Experimental results using single direct output tuning algorithm (4.15).....75

Figure 4.16 Experimental results using double direct output tuning algorithm (4.16).....76

Figure 4.17 Experimental results using fuzzy logic control system (4.17).....77

Figure 4.18 Experimental results using double direct output tuning algorithm (4.18).....78

Figure 4.19 Experimental results using fuzzy logic control system (4.19).....79

Figure 4.20 Experimental results using double direct output tuning algorithm (4.20).....80

Figure 4.21 Experimental results using fuzzy logic control system (4.21).....81

Figure 4.22 Experimental results using fuzzy logic control system (4.22).....82

Figure 4.23 Experimental results using fuzzy logic control system (4.23).....83

Figure 4.24 Experimental results using double direct output tuning algorithm (4.24).....84

Figure 4.25a Chatter suppression with self-learning algorithm (4.25a).....85

Figure 4.25b Chatter suppression with self-learning algorithm (4.25b).....86

Figure 4.25c Chatter suppression with self-learning algorithm (4.25c).....87

List of Table

Table 3.1 Other adjustment limits for safe operation.....43

Nomenclature

E_x	Mean vibration energy level in x-axis
E_y	Mean vibration energy level in y-axis
E_r	Resultant mean vibration energy level
E_{RMS}	Root mean square of vibration energy
$G_x(f)$	Auto-correlation spectrum of signal $x(t)$
$G_y(f)$	Auto-correlation spectrum of signal $y(t)$
$G_{xy}(f)$	Cross-correlation spectrum of signal $x(t)$ and signal $y(t)$
Im	Imaginary part of a complex value
$KI_{t,\gamma}$	Scaling factor for the maximum coherence ratio
$KI_{t,\Delta\gamma}$	Scaling factor for the change of maximum coherence ratio
$KI_{t,E}$	Scaling factor for energy level
KO_{os}	Overshooting tuning factor
KO_{imp}	Impact suppression factor
$KO_{t,f}$	Output tuning factor for feed rate
$KO_{t,v}$	Output tuning factor for spindle speed
Re	Real part of a complex value
$X(f)$	Fourier transform of $x(t)$
$Y(f)$	Fourier transform of $y(t)$
$X^*(f)$	Conjugate value of $X(f)$
$Y^*(f)$	Conjugate value of $Y(f)$
f	Feed rate
f_s	Spindle frequency
f_t	Tooth passing frequency
v	Spindle speed

w	Weight for rule base self-learning algorithm
w_t	Total weight for the direct output tuning algorithm
w_γ	Weight for coherence ratio in the direct output tuning algorithm
w_E	Weight for energy level in the direct output tuning algorithm
$x(t)$	Time-domain signal in x-axis
$y(t)$	Time-domain signal in y-axis
Δf	Feed rate adjustment
Δv	Spindle speed adjustment
$\Delta\gamma_{max}$	The change of the maximum value of the coherence ratio
$\Delta\hat{\gamma}$	Normalized $\Delta\gamma$
$\tilde{o}()$	Error
$\gamma(f)$	Coherence ratio
γ_{max}	The maximum value of the coherence ratio
$\hat{\gamma}$	Normalized γ
$m(x)$	Membership degree

Chapter 1

Introduction

1.1 Background

Further improvement in productivity and product quality in metal cutting processes machines has been a challenging issue due to the complexity of the machining process. The research studies show that the metal removal rate and surface quality are not usually limited by the cutting ability of the tools but rather by the severe vibrations, which is known as chatter.

How to avoid and suppress chatters has been studied for several decades and many different approaches have been attempted. However, due to various limitations as reviewed in Chapter 2, industrial application of those approaches is very limited, which calls for a further investigation of the chatter problem.

1.2 Proposed Study

To provide a chatter control system that is easy to implement for real application, the following research work was proposed:

1. *Develop a chatter detection mechanism.* In the chatter detection mechanism, the coherence function will be used due to its sensitivity to chatter. The coherence function values will be calculated based on the vibration signals from two accelerometers orthogonal to each other. The vibration energy signals obtained from the same accelerometers will be applied to offset the over-vigilance problem of the coherence function.

2. *Attempt to develop a chatter prediction method.* This prediction method will be derived from the coherence function. Pre-chatter actions will be taken to avoid the chatter occurrence.
3. *Develop a self-learning fuzzy chatter suppression system.* A fuzzy chatter suppression module will be developed based on the coherence function value, the change of the coherence function value and vibration energy. To improve the adaptability of the fuzzy module, a self-learning algorithm will be also developed.

1.3 Organization of the Thesis

The rest of the thesis is organized as follows. Chapter 2 provides a brief review of previous work in chatter detection and suppression in machining processes. Chapter 3 reports the proposed chatter detection, prediction and suppression methods. The implementation of the proposed chatter detection and suppression system and experimental results are presented in Chapter 4. Chapter 5 concludes the thesis and suggests some possible future work.

Chapter 2

Literature Review

Automated manufacturing enterprises are appealing in the aspects of the machine and condition monitoring systems as the means of increasing productivity of their machines, as well as improving the quality of their products. The condition monitoring systems can also provide the systematic and fast methods of monitoring and control of manufacturing systems in order to guarantee optimal operations and reduce inspection. The basic concepts of machine and the process condition monitoring are to obtain the real-time condition information of the machine tool, by so doing to exhibit intelligence in terms of being aware of its health and process conditions.

2.1 Chatter and Sensors for Chatter Detection

2.1.1 Monitoring Tasks

In the literature, the following parameters have been used for monitoring machining processes: machine tool power consumption (Altintas, 1992), spindle torque (Matsushima, 1982), cutting force (Ranganath *et al.*, 1999), and vibration (Yilmaz *et al.*, 2002). The use of other such as acoustic emission (Everson, 1998; Inasaki, 1999), optical, tool temperature, electrical resistance and radioactive methods has also been investigated.

Tool condition monitoring is obviously one of the important monitoring requirements of machining operations (Du *et al.*, 1992). Generally speaking, the monitoring tasks include the monitoring of tool breakage, tool wear, tool vibration and the chip forms. Most practical approaches to cutting tool condition monitoring have been developed using the indirect measurements. For example, the vibration measurement indirectly measures the tool properties such as the chip depth, because the most indirect

signal measurements are much easier to obtain than the direct measurements (Jensen, 1999).

Cutting force has been considered to be one of reliable indicators of the tool condition. In the past decade a number of researchers (e.g., Jensen, 1999; Ranganath, 1999; and Altintas *et al.*, 1999) have concentrated on the studies of cutting forces. However, because of the limitations of physical size and the high cost of dynamometers, the indirect evaluation approaches such as the spindle motor current, torque, vibration or sound are preferred in real applications (Lee and Tarng, 1999).

2.1.2 Chatter

Among the measurement approaches described above, vibration analysis is a widely used conditional monitoring tool. It is used as a means of monitoring the mechanical condition of a wide range of machines and processes (Prickett, 1999). Severe vibration, known as chatter, not only leads to a decrease of the metal removal rate and workpiece accuracy, but also shortens the tool life and may cause machine failures as well (Liao and Young, 1994). Regenerative chatter accounts for the major problems of machining stability. Recent years, many researchers have developed a variety of methods in the chatter analysis, prediction, detection and suppression.

At early stage, chatter was mostly attributed to the negative damping effect (Arnold, 1946). Later, Tlusty *et al.* (1967) recognized that the leading sources of chatter come from the regenerative and mode coupling effects. These effects stem from the interaction of the structural dynamics of the workpiece, machine tool, and the feedback of subsequent cuts of the tools. Other researchers presented that these factors can also cause chatters such as the variation of the chip thickness, changing orientation of cutting forces, process damping, runout and the possibility of the loose contact of the insert to the workpiece (Tlusty *et al.*, 1991; Altintas *et al.*, 1991).

2.1.3 Sensors

The sensor is a key element of any tool/process monitoring system. There is a variety of sensors, which are utilised in detecting power, torque, strain and distance. Other kinds of sensors are also employed in the different fields. They are the force transducer sensors, acoustic emission sensors, vibration and ultrasound sensors, laser sensors and cameras.

With the development of computer techniques, a multi-sensor approach has become increasingly popular because every single sensor has its own limits in obtaining information. And further, the combination of multi-sensor technique and the utilization of artificial intelligence make the machining control more effective. Choi *et al.* (2000) used both an acoustic emission sensor and a built-in force sensor for online tool condition monitoring during turning. This is called the sensor fusion method. Inasaki (1999) used different sensors in a machine in order to obtain more information.

2.2 Feature Extraction

Chatter of a machine tool is self-excited vibration, formed by undesirable relative oscillation between the cutting tool and the workpiece that is usually developed under a large metal removal rate. To avoid chatters and hence maintain good surface quality, the material removal rate has to be reduced by using conservative cutting parameters, such as feed rate, depth of cuts and spindle speed (Hadi and Ebrahimi, 2001).

To develop a chatter suppression system, chatter has to be detected based on the data obtained on-line. The following few sections provide a brief review of various techniques used for chatter detection.

2.2.1 Time Domain

2.2.1.1 Time Series Modelling

There are two common techniques: autoregressive time series and autoregressive moving average time series. These two models can be used to predict the cutting forces that could be used for chatter detection purpose. Actual sensor signals, measured over one revolution of the tool, are used as an input to the model, which then predicts the anticipated values for the following revolution.

2.2.1.2 Real Time Signal Monitoring

This is based on the time series modelling and has become a useful tool when a fault signature can be clearly identified within the monitored signals. Using this approach, Principe and Yoon (1991) developed a tool breakage detection algorithm based on the features of the spindle displacement. Altintas *et al.* (1990) developed a tool monitoring algorithm, which detected the changes in the cutting processes that may arise due to broken teeth of a cutter.

2.2.2 Frequency Domain

2.2.2.1 Fast Fourier Transform (FFT)

Fast Fourier Transform based analysis has been widely utilized for tool monitoring and chatter detection because it can be used to identify the causes of the severe vibrations based on the frequency distributions. This is an obvious advantage of frequency domain analysis in comparison to the time domain analysis. However, it is time consuming in data processing and this may cause sluggish response of a chatter suppression system particularly for high speed machining processes.

Tarng (1996) proposed a tool monitoring algorithm and considered the frequency domain content of the measured cutting force signals. Tool frequency and tooth

frequency were identified. The tool breakage was detected using FFT. However, the limitation of using FFT is that it may be necessary to re-evaluate the thresholds if the machining conditions vary.

2.2.2.2 Wavelet Analysis

A wavelet is a waveform of effectively limited duration that has an average value of zero. It can be more than sine waves, which are the basis of Fourier analysis. This difference means that the Fourier analysis is to break up a signal into sine waves of various frequencies while wavelet analysis is to break up a signal into shifted and scaled versions of the original wavelet.

Li (1997) used the continuous wavelet transform to decompose the spindle servo motor current signal to detect on-line tool breakage. The experimental results show that clear small differences between the normal and tool breakage can be observed above processed signals. It was confirmed that wavelet transform could reliably detect tool breakage. Wavelet transform has a good solution in the time-frequency domain so that it can extract more information in the time domain in different frequency bands (Kasashima, 1995).

Recently, Lee and Tarng (1999) used the discrete wavelet transform to decompose a signal into the approximation and detail of signal in monitoring the tool conditions. The approximation is the low-frequency components of the signal and the detail is the high-frequency components of the signal. This decomposition process can be iterated so that one signal can be broken down into a hierarchical set of approximations and details. This procedure can also be called multilevel signal decomposition. As a result, the manifestations of the tool failure in the time and frequency domains can be simultaneously obtained through multilevel signal decompositions.

2.3 Chatter Detection Mechanisms

2.3.1 Cutting Parameter Measurements

Hadi and Ebrahimi (2001) presented a method for chatter avoidance through a mathematical model. They stated that the cutting forces depended on the chip thickness in end milling. The equations are:

$$F_T = K_T A_d h \tag{2-1}$$

$$F_R = K_R F_T \tag{2-2}$$

where F_T and F_R are the tangential component and radial component of the cutting force, respectively, K_T and K_R specific cutting stiffness and force ratio, A_d the axial depth of cut, and h the instantaneous chip thickness, which is measured during the cutting tests.

Because of the complication in modelling, the runout (the offset of the cutter) is ignored in model formulations although it is an important contributing factor to chatter in end milling.

In the above equations, there are some constants depending on the workpiece and the milling cutter. It indicates that the mathematical model largely depends on the materials of the workpiece and the types of the cutter.

Ranganth *et al.* (1999) proposed a method for dynamic force prediction in peripheral milling by measuring the flank face interference volume. In their work, the basic mechanism was that the cutting forces depend on the cutting volume. When they used the model, cutter runout and tool deflection were considered. But the effects of cutting damping were not incorporated into the chip formation. Actually, positive cutting damping is believed to be another main source of chatter and has a significant effect on the cutting dynamics in milling.

Based on the relations between dynamics and chip thickness, Jensen and Shin (1999) developed a more comprehensive analytical model to predict the stability limits for face milling operation. The model can be used as a multi-degree of freedom structure.

The author stated that this model is capable of accounting for various non-linearities, such as variation of chip thickness, changing orientation of cutting forces, process damping, runout, and complex workpiece geometry, etc.

Many studies based on this mechanism have been carried out. For example, Altintas *et al.* (1999) used a dynamic model to predict stability in ball end milling.

However, it is often difficult to use this mechanism in real time due to the time-consuming computation involved in using this mechanism.

2.3.2 Damping Effects

Damping effect on chatter is discussed separately although it has been combined with the cutting parameters such as chip thickness in the papers on the previous topics.

Kwon *et al.* (1992) indicated that the problem of monitoring and forecasting tool life still remains unsolved because of the lack of a reliable correlation between the measured parameters and gradual tool wear. Recent research studies have been concentrated on the damping ratio (i.e., the increment) of the cutting dynamics. The measurement of the increase in the damping ratio provides a means for tool wear monitoring.

The real and imaginary parts of the complex frequency are the actual frequency of the motion and the decay rate, respectively. The decay rate is the velocity at which the amplitude of the oscillations grows (Genta, 1999). This decay rate actually is the damping ratio. Kwon *et al.* (2001) used the imaginary part of the inner modulation transfer function of the cutting process as the indicator of tool wear. The author also stated that the imaginary part of the inner modulation transfer function is proportional to the flank tool wear land width and tool wear grows when the damping effect increases.

2.4 Control Strategy

In the past decades, researchers have developed a variety of methods to make the machining more adaptive, flexible and intelligent. The following are some of the commonly used approaches.

a) Fixed Gain Feedback Control

Because the gain is fixed, this type of control may lead to poor control performance and the cutting process may become unstable during the time-varying machining processes. The control system becomes unstable if the gain is too high, and it responses too slow if the gain is too low.

b) Adaptive Control

Along this line, parameter adaptive control and model reference adaptive control were widely used. A parameter adaptive controller consists of two functions: online estimation of the parameters of the cutting process and real time control. The drawback is that it requires some material parameters obtained offline. This type of control is only used for the linearized cutting processes. For model reference adaptive control, it is very difficult to select an appropriate model and the control has no learning ability.

c) Neural Network Control

The main purpose of the neural network based controller is to construct a reverse function of the plant using the neural network so that the output of the system is the desired input. The disadvantage is that it limits the response speed of the control system.

d) Fuzzy Control

Fuzzy control has proven to be a powerful tool when it is applied to ill-defined and uncertain systems. Recently, many studies have been devoted to the theory of fuzzy control and its application to machining processes.

Most machining processes are non-linear and time-varying with random disturbances. The traditional adaptive controller depends greatly on an accurate model of the machining process. It is difficult for a traditional adaptive controller to achieve the effective control of the machining process. Artificial intelligence, such as neural networks, genetic algorithm, fuzzy logic and expert systems, is based on the operating principles of the human brain and natural biological evolution. It has received considerable and increasing interests over the past decade and has been applied to CNC machining control (Tarng *et al.*, 1994).

Du *et al.* (1992) developed a methodology for tool condition monitoring in turning using the fuzzy set theory. The relationship between tool conditions and monitoring indices was described by a linear fuzzy equation. The parameters in this equation were determined based on the possibility and the probability distributions of the learning samples. The experimental results indicate an overall reliability of approximately 90% in detecting the various tool conditions considered in this study. These results represent a significant improvement over those obtained using other decision-making strategies.

2.5 Chatter Avoidance and Suppression

2.5.1 Chatter Avoidance

There are two approaches for chatter avoidance. The first one is machine tool redesign. The chatter can be avoided or reduced by increasing the rigidity of the machine tool structure or through the use of dampers. However, machine tools with such redesigned features are very expensive and this approach cannot solve the chatter problem for millions of existing machine tools. The second approach is to identify the

stability lobes experimentally. Once the stability lobes are identified, the machining will be performed only in the stable zones by using properly selected cutting parameters. For example, Budak and Altintas (1998) developed stability lobes for milling processes, which specify the boundaries between chatter-free and unstable conditions with respect to the depth of cut. However, the application of such an approach is very difficult in practice since the stability lobes are developed for a particular machine-tool-workpiece combination. Any slight change in the three will shift the lobes.

2.5.2 Chatter Suppression

a) Spindle Speed Modulation

The main idea of this approach is to modulate the spindle speed by following or changing the waveform (e.g., frequency and phase) of the spindle speed variation pattern. By doing so, the regenerative cutting pattern will be interrupted and hence the chatters caused by regenerative cutting path can be suppressed.

Liao and Young (1996) developed a chatter suppression system based on this approach. In their system, the direct force signal from a dynamometer was passed through a low pass filter then digitised. Fast Fourier Transform was used to obtain corresponding power spectrum from the vibration. Chatter frequency was identified when the intensity of a certain frequency other than spindle speed and cutting frequency is exceeding a threshold. Based on this frequency a new spindle speed is calculated by applying the principle of keeping the phase between present and previous undulation to 90°.

However, they cautioned that there were two cases where the stable speed might not be found. The first case occurs when the width of cut is too large and exceeds the stability limit. The second is the situation when the system has multiple modes and the stability

lobes of the different modes are different. In such cases, the system cannot be brought to a stable condition by regulating the spindle speed alone.

b) R-value

Ismail and Kubica (1995) developed a chatter indicator that is suitable as a feedback signal for controlling instability in milling operations.

They separated the total cutting force into dynamic component due to vibration only and static component due to tooth engagements excluding the inertia in the system. A chatter indicator, termed R-value, is then computed by dividing the dynamic root mean square force component by the static root mean square force component. Obviously, R-value is an application of the dynamics mechanism.

The R-value is proportional to the level of vibration, and the range of value would be limited so a threshold value could be selected above which the chatter will occur.

c) Coherence Function

Li *et al.* (1997) proposed to use coherence function as a chatter detection indicator. The coherence function was defined as:

$$\gamma^2(f) = \frac{G_{xy}^2(f)}{G_x(f)G_y(f)} \tag{2-3}$$

where $G_{xy}(f)$ is the cross-correlated spectrum of the two signals $x(t)$ and $y(t)$, $G_x(f)$ and $G_y(f)$ are the auto-correlated spectra of signals $x(t)$ and $y(t)$, respectively.

At the onset of chatter, the distribution of the vibration energy converges to the frequency of the chatter. The vibration signal also undergoes a transition from random to periodic behaviour when the vibration of the tool shank in two perpendicular directions is coupled. The above effects lead to the change in the coherence function between the crossed accelerations of the tool shank. (Li *et al.*, 1997)

At the onset of chatter, the coherence function between the two accelerations has a value close to unity and their auto-correlated spectra have a single peak at the chatter frequency due to the transition of the vibration from random to harmonic behaviour.

Dong *et al.* (1992) used a method based on coherence analysis in the frequency domain to predict chatter. The experiments demonstrated that the machine tool chatter could be detected by monitoring the coherence function of two acceleration signals from two suitable locations on the machine tool.

From the experiments, the following phenomenon was found: The steady state cutting force during stable machining has a very weak influence on the two output acceleration signals and hence the coherence is low. Once chatter occurs, or even at its onset, the dynamic cutting force exerts a strong influence on the two accelerations and hence a high coherence value approaching unity at the chatter frequencies. However, due to the limited computing power at the time when the work was carried out, it took about one second for computing the coherence function value. Hence, the author mentioned only sub-real-time detection was achieved and also they claimed that this should be sufficient since one second was typically the time it took for chatter to grow to its full strength (Dong *et al.*, 1992).

d) Multi-level Random Spindle Speed Variation

Yilmaz *et al.* (2002) presented a new chatter suppression method using multi-level random spindle speed variation.

Multi-level random signal is a continuous signal with discrete amplitudes at uniform time steps. This technique eliminates parameter adjustment phase that is required by similar methods such as sinusoidal spindle speed variation. The stability improvements achieved by multi-level random spindle speed variation machining is

satisfactorily comparable with the improvements achieved by sinusoidal spindle speed variation (Yilmaz *et al.*, 2002).

This method improved the machining productivity due to the variation spindle adjustment instead of decreasing the spindle speed.

2.6 Limitations of Previous Work and Motivation for the Proposed Study

2.6.1 Chatter Detection

As chatter is a complex phenomenon, a single indicator may not be sufficient. The use of different sensors, for example, accelerometers, acoustic sensors, may provide more comprehensive information. However, this will complicate the system development process and make it difficult to implement. For this reason, it is proposed to use a single type of sensors to provide multiple indicators. In this study, a 3-axial accelerometer sensor is used. Both coherence ratio and vibration energy values can be derived from the single type of sensor for detection of chatters. Also, it may be unrealistic to rely on stability lobes because the lobes may shift during cutting due to changes in tool-workpiece structural dynamics (Yilmaz *et al.*, 2002).

2.6.2 Chatter Avoidance

a) Machine Structure Change

As mentioned earlier, this approach requires a change in the machine tool structure. Although it is an active method, it has a high cost and not applied in practice.

b) Stability Lobes

Stability lobes method has a narrow application range. Each type of cutting is based on a distinctive set of stability lobes. To get comprehensive information on the relationship between the cut depth and the spindle speed, a large amount of experiments are required. This is apparently not suitable for today's manufacturing environment featuring small and unpredictable production orders and frequent tool changes.

2.6.3 Chatter Suppression

a) Spindle Speed Modulation

The most significant difficulty in using spindle speed modulation is to determine the frequency and amplitude before adding the proper sinusoidal signal. Though this approach has been used by several authors, a systematic approach in selecting the waveforms has not been suggested.

b) R-value

The chatter suppression method using R-value is also based on the traditional stability lobes. For every single tool-workpiece structure, the stability lobe is unique. Therefore the application scope of the stability lobes is very limited.

c) Coherence Function

Our experiments indicate that the coherence function tends to be overly reactive. Large coherence function values can be observed even before actual cutting. This is certainly misleading indication of chatter, thereby causing unnecessary machine stops or slowdown. To alleviate this difficulty, the coherence function is jointly applied with the vibration energy content in this study.

d) Multi-level Random Spindle Speed Variation

This approach was only applied to turning operations so far. The feasibility in using it for milling and other machining processes remains to be seen. Also, due to the nature of randomness in selecting spindle speed for each following control loop, an optimal machining process cannot be expected.

Chapter 3

Design of the Chatter Detection and Suppression System

The proposed system consists of two major components, i.e., a chatter detection module and a chatter suppression module. To provide more comprehensive information for chatter detection, both coherence function and mean vibration energy have been used. An attempt has also been made to predict chatter using some criteria derived from the coherence function. The fuzzy logic approach is applied for chatter suppression. To enhance the adaptability of the fuzzy module, a self-learning algorithm and a direct outputs tuning algorithm are added to the fuzzy module. The details are described in the following sections.

3.1 Method for Chatter Detection

As reviewed in Chapter 2, a variety of indicators have been suggested in the literature for chatter detection. Among them, vibration energy, dynamic cutting force and peak value in the frequency spectra are most widely used. However, the values of these indicators depend on the machining parameters (such as spindle speed, feed, and depth of cut), workpiece materials, tools and machines used for the operations. It is therefore very difficult to define a threshold value for chatter detection that can be used in a wide range of machining processes. For this reason, the coherence function value, which is dimensionless and is always between [0, 1] is adopted as a chatter indicator. The coherence function value is calculated based on the data from two accelerometers in orthogonal to each other. However, our experiments show that the coherence function is often over-reactive and it may reach a high value even if the cutting has not really started.

To avoid the mis-judgment caused by this phenomenon, the mean vibration energy is jointly used with the coherence function.

3.1.1 Coherence Function for Chatter Suppression

The coherence function is mathematically defined as:

$$\gamma^2(f)=\frac{|G_{xy}(f)|^2}{G_x(f)G_y(f)} \tag{3-1}$$

Assume signal $x(t)$ and $y(t)$ are the time-domain signals respectively obtained from two accelerometers in perpendicular directions. $X(f)$ and $Y(f)$ are the Fourier transforms of $x(t)$ and $y(t)$, respectively. $G_{xy}(f)$ is the cross-spectrum of the two signals $x(t)$ and $y(t)$, $G_x(f)$, $G_y(f)$ are the auto-spectra of signal $x(t)$ and $y(t)$, respectively. According to Neve (1996), the coherence function can be written as follows:

$$\gamma^2(f)=\frac{|X^*(f)\cdot Y(f)|^2}{[X^*(f)\cdot X(f)]\cdot[Y^*(f)\cdot Y(f)]}$$

$$=\frac{|[\mathrm{Re}(X(f))-i\,\mathrm{Im}(X(f))]\cdot[\mathrm{Re}(Y(f))+i\,\mathrm{Im}(Y(f))]|^2}{[\mathrm{Re}^2(X(f))+\mathrm{Im}^2(X(f))]\cdot[\mathrm{Re}^2(Y(f))+\mathrm{Im}^2(Y(f))]}$$

$$=\frac{[\mathrm{Re}(X(f))\cdot\mathrm{Re}(Y(f))+\mathrm{Im}(X(f))\cdot\mathrm{Im}(Y(f))]+i[\mathrm{Re}(X(f))\cdot\mathrm{Im}(Y(f))-\mathrm{Im}(X(f))\cdot\mathrm{Re}(Y(f))]^2}{[\mathrm{Re}^2(X(f))+\mathrm{Im}^2(X(f))]\cdot[\mathrm{Re}^2(Y(f))+\mathrm{Im}^2(Y(f))]}$$

$$=1 \tag{3-2}$$

where $X^*(f)$ and $Y^*(f)$ are the conjugate value of $X(f)$ and $Y(f)$, respectively, and $Re(\,)$ and $Im(\,)$ are the real and imaginary parts of a complex value, respectively. The result above can be separated into real and imaginary parts:

$$\mathrm{Re}(\gamma^2(f))=\frac{\mathrm{Re}^2[G_{xy}(f)]}{G_x(f)\cdot G_y(f)} \tag{3-3}$$

$$\mathrm{Im}\left(\gamma^2(f)\right)=\frac{\mathrm{Im}^2\left[G_{xy}(f)\right]}{G_x(f)\cdot G_y(f)} \tag{3-4}$$

In real applications, the equation used to calculate the coherence function (Neve 1996) is:

$$\mathrm{Re}\left(\gamma^2(f)\right)=\frac{\mathrm{Re}^2\left[G_{xy}(f)\right]}{G_x(f)\cdot G_y(f)}=\frac{\left[\mathrm{Re}(X(f))\cdot\mathrm{Re}(Y(f))+\mathrm{Im}(X(f))\cdot\mathrm{Im}(Y(f))\right]^2}{\left[\mathrm{Re}^2(X(f))+\mathrm{Im}^2(X(f))\right]\cdot\left[\mathrm{Re}^2(Y(f))+\mathrm{Im}^2(Y(f))\right]} \tag{3-5}$$

According to Li *et al* (1997), in a chatter free cutting process, the auto-spectra $G_x(f)$, $G_y(f)$ and the coherence function values spread over a wide frequency range and are characterized by lower level of stationary random signals. At the onset of chatter, the distribution of vibration energy converges to the chatter frequency. Predominantly high $G_x(f)$, and $G_y(f)$ values can be observed at the chatter frequency and consequently a coherence value quickly approaches unity. Since only the real part of the coherence function is to be used for chatter detection and prediction, hereafter notation $\gamma^2(f)$ will be used to indicate the real part of the coherence function and the term "coherence function" will mean the "real part of the coherence function" for simplicity.

The cross-spectrum $G_{xy}(f)$ and the auto-spectra $G_x(f)$, $G_y(f)$ are calculated on-line using FFT method. In a cutting process, two more spikes can be observed in the frequency domain FFT plots in addition to the one at the chatter frequency f_c. The two spikes are related to spindle frequency f_s and tooth passing frequency f_t and are calculated as: $f_s=\frac{v}{60}$, $f_t=\frac{m\cdot v}{60}$, where v is the spindle speed and m the number of cutting edges.

The chatter frequency in many cases (in particular in our test range) is different from f_s and f_t. For example, in our test scope, f_s is less than 20Hz and f_t is less than 80Hz whereas the observed chatter frequency is about 200 Hz. Therefore, f_s and f_t as well as the frequencies around them are ignored.

3.1.2 Chatter Detection Using Mean Vibration Energy

As mentioned earlier, to provide more comprehensive information, the mean vibration energy is also used. Another reason for using mean vibration energy is that the mean vibration energy has an aggregate effect on chatter detection and it may be used to predict chatters in later study. According to Thomson and Dahleh (1998), the mean vibration energy can be calculated as follows:

$$\bar{x} = \lim_{T\to\infty} \frac{1}{T} \int_0^T x(t)dt \tag{3-6}$$

For discrete variable, the mean vibration energy can be determined by:

$$E_x = \frac{1}{N} \sum_{i=1}^{N} |x_i|, \quad E_y = \frac{1}{N} \sum_{i=1}^{N} |y_i| \tag{3-7}$$

where N is the number of samples during a period over which the average is calculated.

In this thesis, the resultant mean vibration energy was calculated as:

$$E_r = \sqrt{E_x^2 + E_y^2} \tag{3-8}$$

3.2 Chatter Prediction Based on Coherence Function

3.2.1 Coherence Function

The significance of coherence function in the context of chatter analysis is described below.

According to Genta (1999), the real part of the Fourier transform function is the amplitude of the motion at a certain frequency and the imaginary part is the velocity of the motion at the frequency. These results can be explained in the following.

Recall the Fourier transformation:

$$X(f)=\sum_{t=0}^{N}x(t)\cdot e^{-i\frac{2\pi tf}{N}}=\sum_{t=0}^{N}x(t)\cdot\cos\frac{2\pi tf}{N}-i\sum_{t=0}^{N}x(t)\cdot\sin\frac{2\pi tf}{N}\qquad(f=0,1,\ldots f_{\max})\tag{3-9}$$

Separating $X(f)$ into real and imaginary parts gives:

$$\mathrm{Re}(X(f))=\sum_{t=0}^{N}x(t)\cos\frac{2\pi tf}{N}\qquad(f=0,1,\ldots f_{\max})\tag{3-10}$$

$$\mathrm{Im}(X(f))=\sum_{t=0}^{N}x(t)\sin\frac{2\pi tf}{N}\qquad(f=0,1,\ldots f_{\max})\tag{3-11}$$

Obviously, *Im(X(f))* is proportional to the derivative of *Re(X(f))* with respect to f (Genta, 1999). Suppose that *x(t)* is composed of a family of sine waves. Then *Re(X(f$_i$))* is the amplitude of the vibration at frequency f_i over a particular time window. The total amplitude at all frequencies is then $\sum_{f=1}^{f_{\max}}\mathrm{Re}(X(f))$, which is caused by the static force in the end milling process and reflects the average displacement of tool tip or the tool runout position. *Im(X(f$_i$))* is the change of the amplitude of the vibration at frequency f_i and $\sum_{f=1}^{f_{\max}}\mathrm{Im}(X(f))$ can be used to describe how severe the vibration is and how much the vibration deviates from the average displacement or from the average runout position. The total change of the amplitude is caused by dynamic forces during cutting as illustrated in Figure 3.1.

When the coherence function is equal to unity, i.e.,

$$\mathrm{Re}(\gamma^2(f))=\frac{[\mathrm{Re}(X(f))\cdot\mathrm{Re}(Y(f))+\mathrm{Im}(X(f))\cdot\mathrm{Im}(Y(f))]^2}{[\mathrm{Re}^2(X(f))+\mathrm{Im}^2(X(f))]\cdot[\mathrm{Re}^2(Y(f))+\mathrm{Im}^2(Y(f))]}=1$$

the following condition must hold:

$$\frac{\mathrm{Re}(X(f))}{\mathrm{Im}(X(f))}=\frac{\mathrm{Re}(Y(f))}{\mathrm{Im}(Y(f))}\tag{3-12}$$

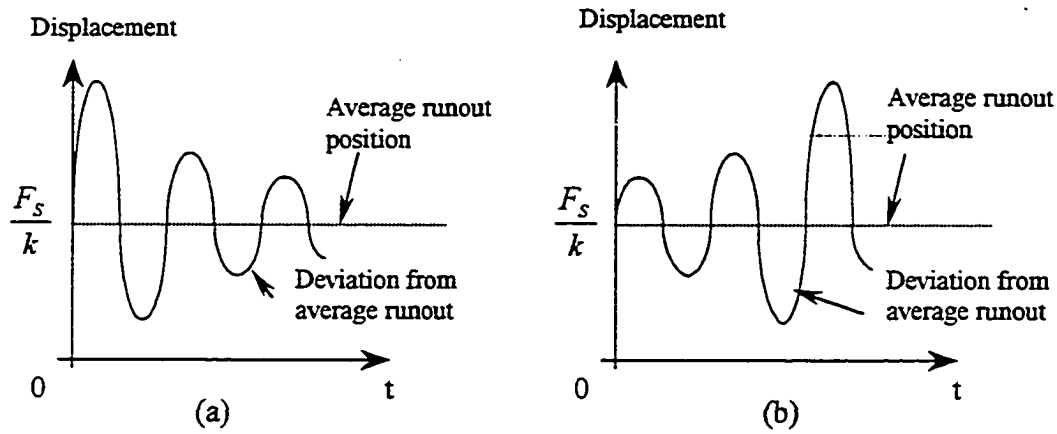

Figure 3.1 Runout and vibration at a certain frequency (F_s is the static cutting force, k is the stiffness of the tool, the curves represent the runout magnitude)
(a)runout converges to the average (b) runout diverges away from the average

The equation $\frac{\mathrm{Re}(X(f))}{\mathrm{Im}(X(f))}=\frac{\mathrm{Re}(Y(f))}{\mathrm{Im}(Y(f))}$ means the resultant amplitude is in the same direction as the resultant change of the amplitude (Figure 3.2a). Hence, the dynamic and static forces are collinear. As the static bending force always passes through the nominal center position of the cutter, the collinear dynamic force, when it is in the same direction as that of the static force, will have a maximum effect on the runout enforcement and consequently the largest contribution to chatter.

When the coherence function equals zero, i.e.:

$$\mathrm{Re}\left(\gamma^2(f)\right)=\frac{\left[\mathrm{Re}(X(f))\ \mathrm{Re}(Y(f))+\mathrm{Im}(X(f))\ \mathrm{Im}(Y(f))\right]^2}{\left[\mathrm{Re}^2(X(f))+\mathrm{Im}^2(X(f))\right]\left[\mathrm{Re}^2(Y(f))+\mathrm{Im}^2(Y(f))\right]}=0$$

The following condition holds:

$$\frac{\mathrm{Re}(X(f))}{\mathrm{Im}(X(f))}=-\frac{\mathrm{Im}(Y(f))}{\mathrm{Re}(Y(f))} \tag{3-13}$$

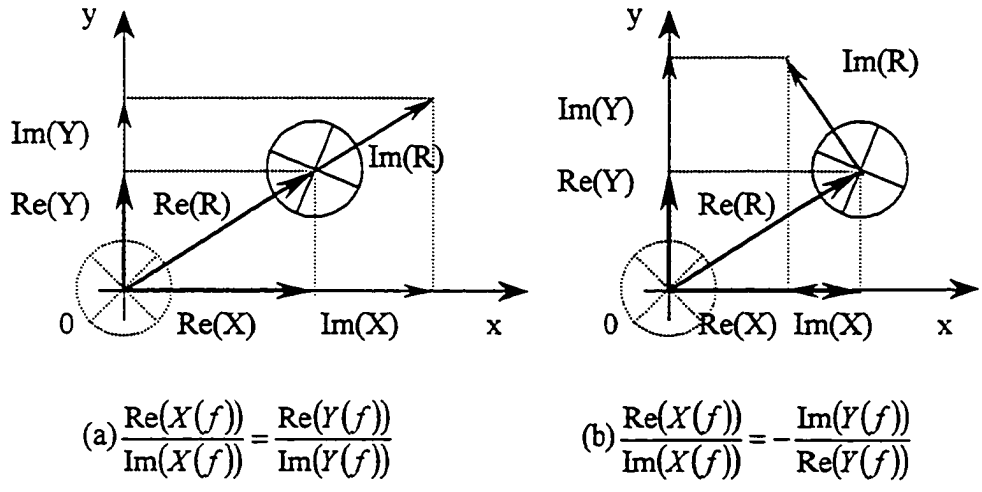

$$(a)\ \frac{\mathrm{Re}(X(f))}{\mathrm{Im}(X(f))} = \frac{\mathrm{Re}(Y(f))}{\mathrm{Im}(Y(f))} \qquad (b)\ \frac{\mathrm{Re}(X(f))}{\mathrm{Im}(X(f))} = -\frac{\mathrm{Im}(Y(f))}{\mathrm{Re}(Y(f))}$$

Figure 3.2 Vibration and tool runout
(a) The resultant vibration when Im(R) is collinear with the resultant runout Re(R)
(b) The resultant vibration when Im(R) is perpendicular to the resultant runout Re(R)
(R is the resultant vibration amplitude)

The equation $\frac{\mathrm{Re}(X(f))}{\mathrm{Im}(X(f))} = -\frac{\mathrm{Im}(Y(f))}{\mathrm{Re}(Y(f))}$ means the direction of the resultant change of the amplitude is perpendicular to the direction of the resultant amplitude (Figure 3.2b). This condition also means the dynamic force is perpendicular to the direction of the static force and hence perpendicular to the runout direction. The amplitude of the runout will virtually not be affected and the contribution will not as large as the one caused by the collinear dynamic force described above.

3.2.2 Chatter Suppression Strategies

The objective of chatter suppression is to maintain a stable cutting process. When chatter is detected, the system should be able to suppress it by regulating the spindle speed and feed rate based on the pre-determined rules.

The system should compensate for disturbances that would occur to cause controlled variables, i.e., the mean of vibration energy content, to deviate from the set level once a desired steady state is achieved. Due to the complex non-linear and time-variant nature of the cutting process as well as the lack of information and knowledge of cutting dynamics, the fuzzy logic approach is used in this study. The fuzzy logic control system is a real time expert system, which is based on a series of If-Then-Else linguistic rules. These rules can be obtained from well-experienced machine operators to regulate the cutting parameters such as feed rate and spindle speed without analysing the complex cutting dynamics (Tarng and Cheng, 1993; Driankov *et al.*, 1996).

3.2.3 Performance Indices

As we mentioned earlier, the following phenomena are observed from our experiments. On one hand, whenever there is a peak value in the cross-spectrum plot there must be a high peak of the coherence ratio occurring at the same frequency, which indicates that it is logic to use the coherence ratio as a chatter indicator. On the other hand, however, the opposite is not always true. When there is a peak value in the coherence ratio plot, there could be no dominated peak value in cross-spectrum plot observed immediately. Instead, a peak value always follows after a certain time delay, which means the coherence ratio could be used to predict the occurrence of the high peak in cross-spectrum value.

Performance Indices (PI's) that measure the deviations of both the coherence ratio and the mean vibration energy level from their reference levels are used as control criteria in this study. The PI's are calculated on-line from readily available data.

According to Liang (2001), the PI measuring the deviation of mean vibration energy from its reference level is defined as:

$$PI(EE)_i = \sqrt{\frac{\sum_{J=I-n_a+1}^{I} EE_J^2}{n_a}} \tag{3-14}$$

where n_a is the number of samples with which the RMS was calculated.

The performance index for coherence error is defined similarly.

3.2.4 Data Processing

In this thesis, the procedure of calculating the coherence ratio from the raw data is shown in Figure 3.2a.

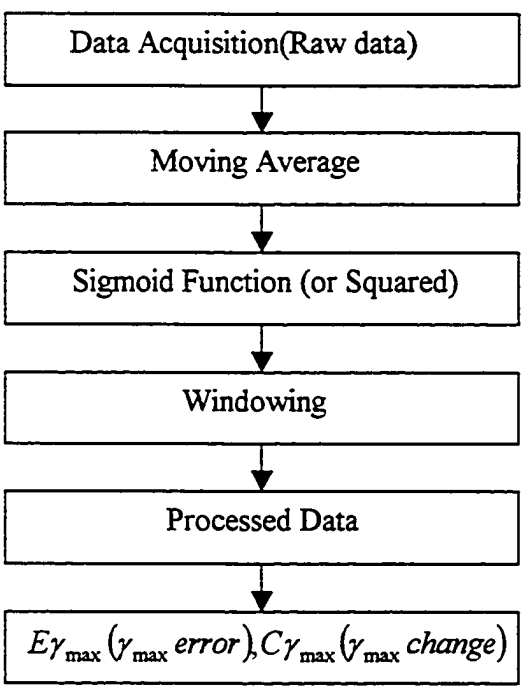

Figure 3.2a Steps for calculating coherence ratio

The steps are explained in detail as follows:

Two difficulties arise in the application of the coherence function: a) the coherence ratios plotted based on real cutting processes do not usually show a clear pattern, and b)

the coherence function tends to be overly vigilant. The thin line in Figure 3.3a is plotted using the raw coherence ratio from a typical cutting process. It is very difficult to pinpoint a dominant peak value. Figure 3.3a also shows that the ratios are too close to the maximum level in most cases, which shows the over-vigilant feature of the coherence ratio. To alleviate the first difficulty, the moving average value of the coherence values is used in our actual detection and suppression process. The moving average is calculated as follows:

$$\gamma_{f,smooth} = \frac{\sum_{p=f-n}^{f+n} \gamma_p}{2n+1} \tag{3-17a}$$

where γ_p is the original coherence value and $\gamma_{f,smooth}$ is the smoothed coherence value over a band of $(2n+1)$Hz. In this study, n is set to 2 and hence the bandwidth is 5Hz. To overcome the over-vigilance problem, a modified sigmoid function is used to enlarge the distinction between the coherence ratio and the maximum value. The modified sigmoid function is given as follows:

$$\gamma_e = \begin{cases} \dfrac{1}{e^{\frac{1-\gamma_{f,smooth}}{0.4}}} & if \quad \gamma_{f,smooth} > 0.5 \\ \dfrac{1}{e^{\frac{1-\gamma_{f,smooth}}{0.6}}} & if \quad \gamma_{f,smooth} \le 0.5 \end{cases} \tag{3-17b}$$

where γ_e is the adjusted coherence ratio using Equation 3-17b. The coherence ratio after processing is shown in the thick line in Figure 3.3a.

3.2.5 Windows Function

According to our experimental results, the chatter frequencies are always detected above 170 Hz. In order to eliminate the disturbances from the peak values below 170 Hz,

a window function is needed. To simplify the computing work, the following window function was employed to adjust the coherence ratio.

$$W(i)=\begin{cases}0.1 & i=0,1,\ldots 170\\ 0.9\times\dfrac{i-170}{187-170}+0.1 & i=171,172,\ldots 187\\ 1.0 & i=188,189,\ldots 233\\ 1.0-0.9\times\dfrac{i-233}{250-233} & i=234,235,\ldots 250\end{cases} \tag{3-18}$$

The coherence ratio after being adjusted by the windows function is shown in Figure 3.3b. The thicker line is the coherence ratio curve after being windowed and the thinner line is that before being windowed.

To simplify discussions, the coherence function modified using moving average, sigmoid function and window function is still called coherence function hereafter.

3.2.6 Inputs and Input Scaling Factors

The inputs to the fuzzy controller are $E\gamma_{\max}(\gamma_{\max} error)$, $C\gamma_{\max}(\gamma_{\max} change)$, and EE (mean vibration energy error). The $E\gamma_{\max}$, and $C\gamma_{\max}$ values are obtained from the data after smoothing and windowing.

They are defined as follows:

$$E\gamma_{\max}=\gamma_{\max}(i)-\gamma_{ref} \tag{3-19}$$

$$C\gamma_{\max}=\gamma_{\max}(i)-\gamma(i-1) \tag{3-20}$$

And

$$EE=E(i)-E_{ref} \tag{3-21}$$

where $\gamma_{max(i)}$ is the maximum value of the coherence ratio in time window i, γ_{up} and γ_{low} are the upper and lower limits of the coherence ratio, respectively, and γ_{ref} is the reference value based on experiments. According to Liang (2001), γ_{ref} was selected as 0.8.

3.3 The Structure of the Fuzzy Logic Controller

The structure of the fuzzy logic control system in this thesis for chatter suppression is schematically illustrated in Figure 3.4. The fuzzy logic control system consists of the following components: fuzzification module, membership function, rule base, fuzzy inference engine, defuzzification module, scaling factors and tuning factors.

These components will be explained in the following sections.

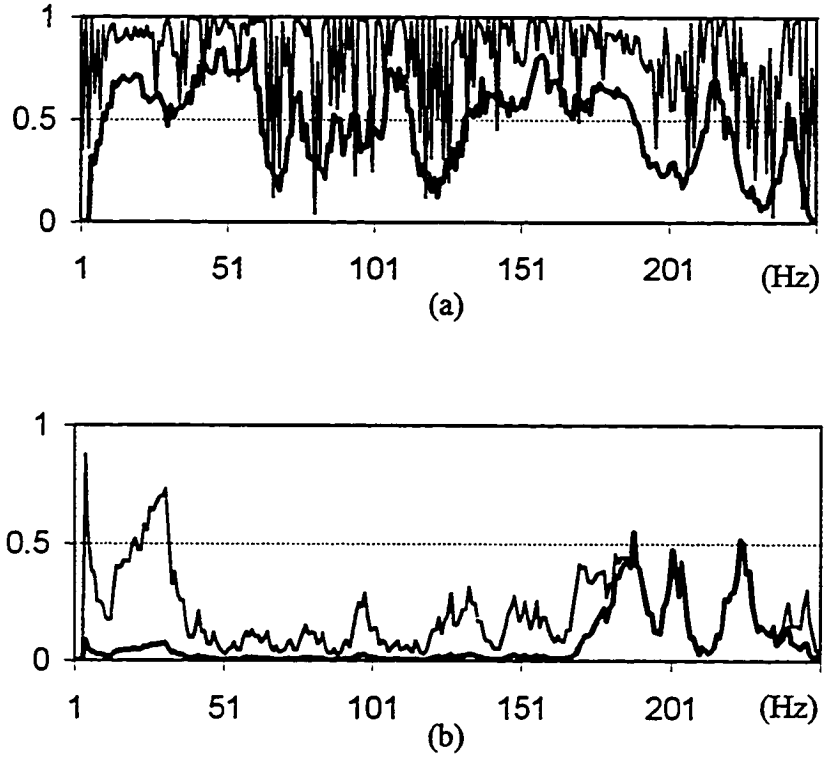

Figure 3.3 Data modifications (a) The coherence ratio is smoothed and the dominant peaks are shown clearly by taking moving average value and the sigmoid functions (b) The coherence ratio is windowed by window function

3.3.1 Fuzzification and Membership Functions

The fuzzification module performs an input normalization transformation, which maps the physical crisp values of the current process state variables into a normalized fuzzy domain.

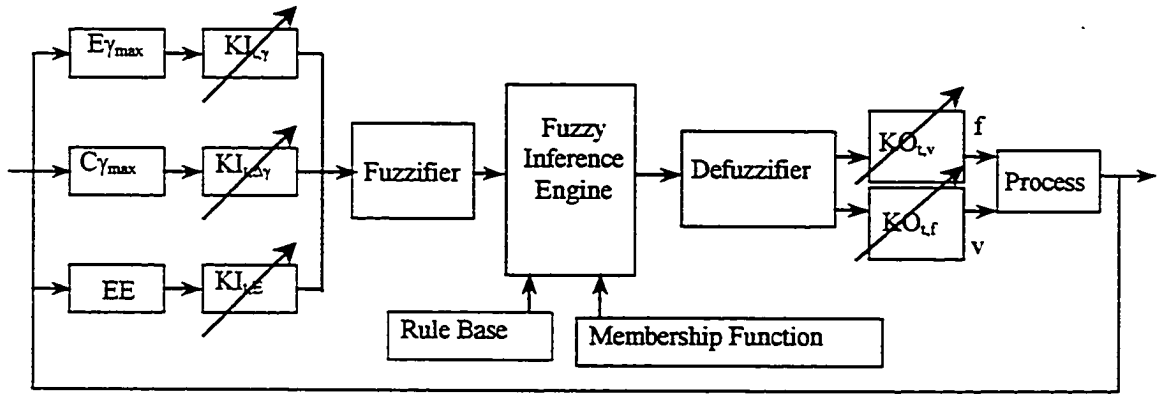

Figure 3.4 Fuzzy logic control for chatter suppression

In this thesis, three inputs are utilized. They are the maximum value of the coherence ratio $E\gamma_{max}$, the change of γ_{max}, $C\gamma_{max}$ and the mean vibration energy EE. After the computations, the physical values are converted into normalized values to the fuzzifier.

The crisp values are mapped into fuzzy domain. A number in the fuzzy domain may belong to one or several fuzzy sets. For example, in Figure 3.5, an input coherence ratio of 0.8 may be converted to a fuzzy value of 0.45, which may belong to two fuzzy sets: "positive small" (PS) and "positive medium" (PM) with degrees of belongingness 0.3 and 0.7 respectively.

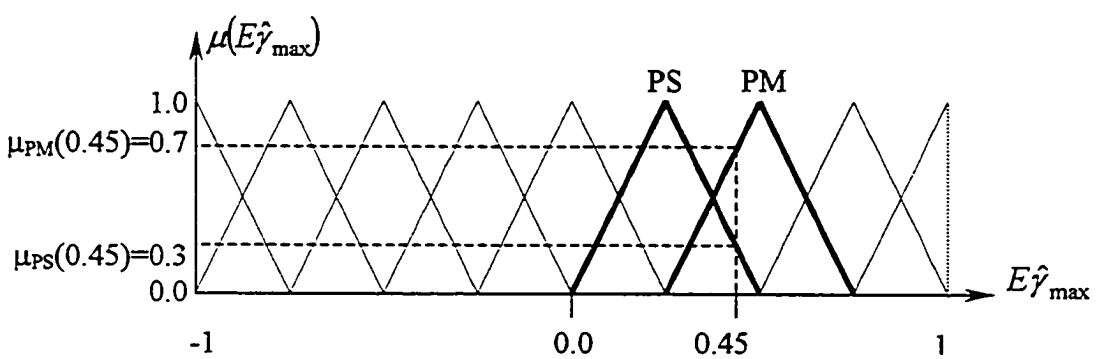

Figure 3.5 Illustration of fuzzification process

Triangular membership functions have been widely used for simplicity (e.g., Yeh *et al.* 1995, Hsu and Fann 1996). In this thesis, triangular fuzzy functions will be used for input variables. Nine fuzzy sets were used for inputs $E\gamma_{max}$ and $C\gamma_{max}$. The nine sets are NX (Negative Extra Big), NB (Negative Big), NM (Negative Medium), NS (Negative Small), ZE (Zero), PS (Positive Small), PM (Positive Medium), PB (Positive Big) and PX (Positive Extra Big).

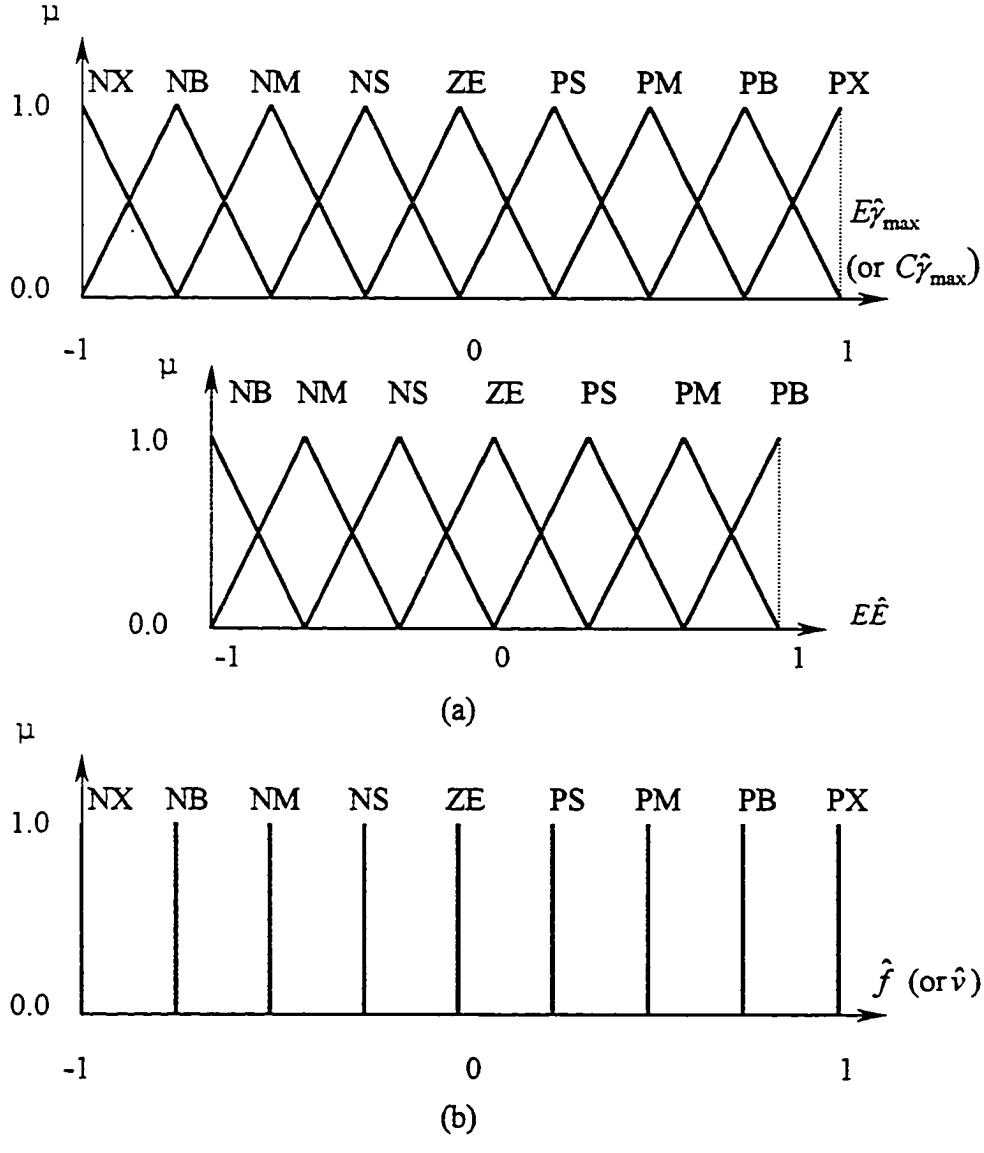

Figure 3.6 Membership functions
(a)Triangular membership functions of the inputs
(b)Spike membership functions of the outputs

For the third input EE, there are only seven fuzzy sets, i.e., NB, NM, NS, ZE, PS, PM, and PB. Figure 3.6 illustrates these membership functions.

Membership functions must also be specified for outputs feed rate f and spindle speed v to convert the fuzzy output values into physical values. To further reduce computing time, the Sugeno-type singleton membership functions as described by Gulley *et al.* (1995) and Driankov *et al.* (1996) are used for outputs (Figure 3.6b).

3.3.2 Rule Base

The control rule base is probably the most component in a fuzzy controller (Lee and Wang 1996). The fuzzy rules are obtained based on the experiences and control engineers' knowledge. Recently, different adaptive algorithms have been utilised to make the rule base more intelligence.

The basic rule is usually in linguistic format as illustrated by the following example:

IF $E\gamma_{max}$ is PB AND $C\gamma_{max}$ is PS, THEN f is NX AND v is NB.

The above rule means that if the maximum value of the coherence ratio $E\gamma_{max}$ is positive big and the change of this maximum value $C\gamma_{max}$ is positive small, then the value of the feed rate adjustment should be negative extra large and the value of the spindle speed regulation should be negative big.

Figures 3.7 (for spindle speed adjustment) and 3.8 (for feed rate adjustment) show the rule bases with $E\gamma_{max}$ and $C\gamma_{max}$ as inputs and Figure 3.9 shows the rule base with vibration energy as input for both spindle speed and feed rate adjustments.

Regular fuzzy logic control methods only require rule bases filled with fixed linguistic values. In this thesis, the self-learning algorithm is utilised. As a result, the linguistic values are updated online according to the real working conditions.

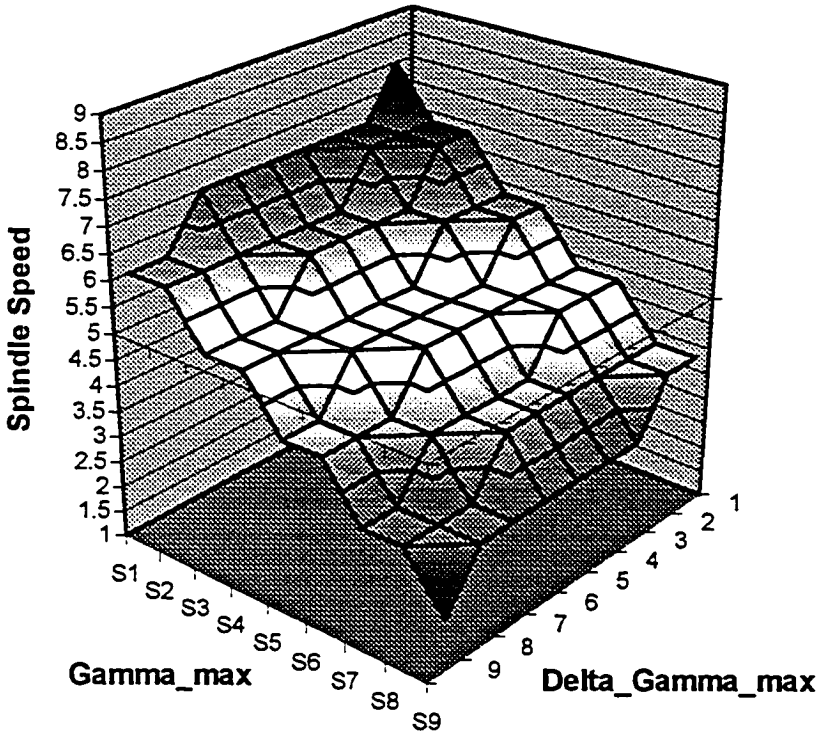

(a)

$C\gamma_{max}$ / $E\gamma_{max}$	NX	NB	NM	NS	ZE	PS	PM	PB	PX
NX	PB	PM	PM	PM	PM	PM	PM	PS	PS
NB	PM	PM	PM	PS	PS	PS	PS	PS	PS
NM	PM	PM	PS	PS	PS	PS	ZE	ZE	ZE
NS	PS	PS	PS	ZE	ZE	ZE	ZE	ZE	ZE
ZE	PS	PS	ZE	ZE	ZE	ZE	ZE	NS	NS
PS	ZE	ZE	ZE	ZE	ZE	ZE	NS	NS	NS
PM	ZE	ZE	ZE	NS	NS	NS	NS	NM	NM
PB	NS	NS	NS	NS	NS	NS	NM	NM	NM
PX	NS	NS	NM	NM	NM	NM	NM	NM	NB

(b)

Figure 3.7 Coherence ratio table: Fuzzy rules for chatter suppression by adjusting spindle speed
(a)3-D plot (b)Fuzzy values in the rule table

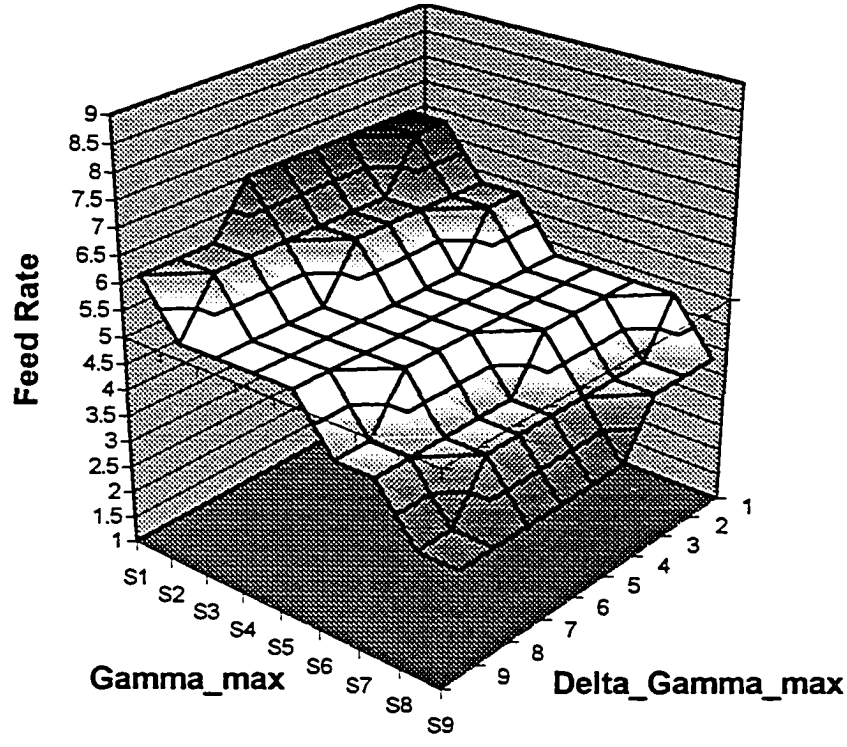

(a)

$E\gamma_{max}$ \ $C\gamma_{max}$	NX	NB	NM	NS	ZE	PS	PM	PB	PX
NX	PM	PM	PM	PM	PM	PM	PS	PS	PS
NB	PM	PM	PS	PS	PS	PS	PS	PS	ZE
NM	PS	PS	PS	PS	PS	ZE	ZE	ZE	ZE
NS	PS	PS	ZE	ZE	ZE	ZE	ZE	ZE	ZE
ZE	ZE	ZE	ZE	ZE	ZE	ZE	ZE	ZE	ZE
PS	ZE	ZE	ZE	ZE	ZE	ZE	ZE	NS	NS
PM	ZE	ZE	ZE	ZE	NS	NS	NS	NS	NS
PB	ZE	NS	NS	NS	NS	NS	NS	NM	NM
PX	NS	NS	NS	NM	NM	NM	NM	NM	NM

(b)

Figure 3.8 Coherence ratio table: Fuzzy rules for chatter suppression by adjusting feed rate
(a) 3-D plot (b)Fuzzy values in the rule table

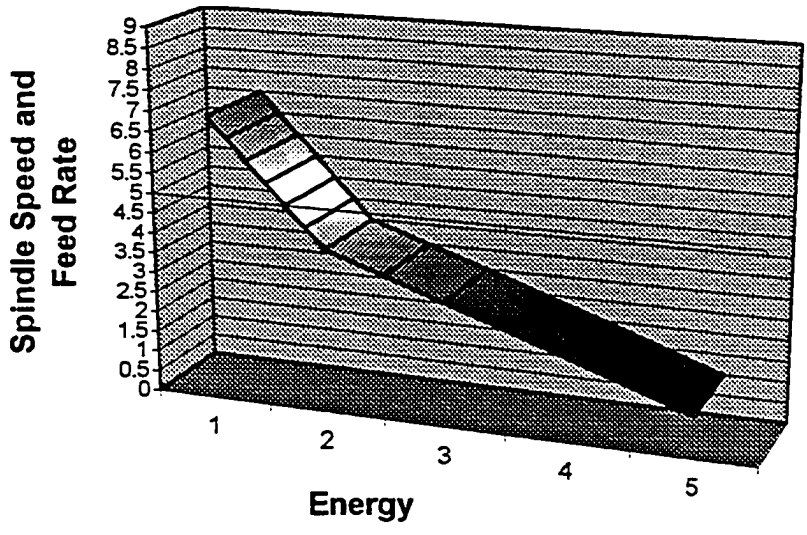

(a)

EE	Δf	Δv
NB	NB	NB
NM	NM	NM
NS	NS	NS
ZE	ZE	ZE
PS	PS	PS
PM	PM	PM
PB	PB	PB

(b)

Figure 3.9 Energy table: Fuzzy rules for chatter suppression by adjusting feed rate or spindle speed (a)3-D plot (b)Fuzzy values in the rule table

3.3.3 Fuzzy Inference Engine and Defuzzification

The fuzzy inference engine is used to determine fuzzy output based on each fuzzy input and control rules. In this thesis, the Sugeno-type inference is used which is

illustrated as follows. Suppose $E\hat{\gamma}_{max}$ and $C\hat{\gamma}_{max}$ inputs are 0.45 and -0.7. The two inputs triggers four rules which associated to four fuzzy-set combinations, i.e., ($E\gamma_{max} \subset$ PS| $C\gamma_{max} \subset$NB), ($E\gamma_{max} \subset$ PS| $C\gamma_{max} \subset$NM) ($E\gamma_{max} \subset$ PM| $C\gamma_{max} \subset$NB) ($E\gamma_{max} \subset$ PM| $C\gamma_{max} \subset$NM), as illustrated in Figures 3.10.

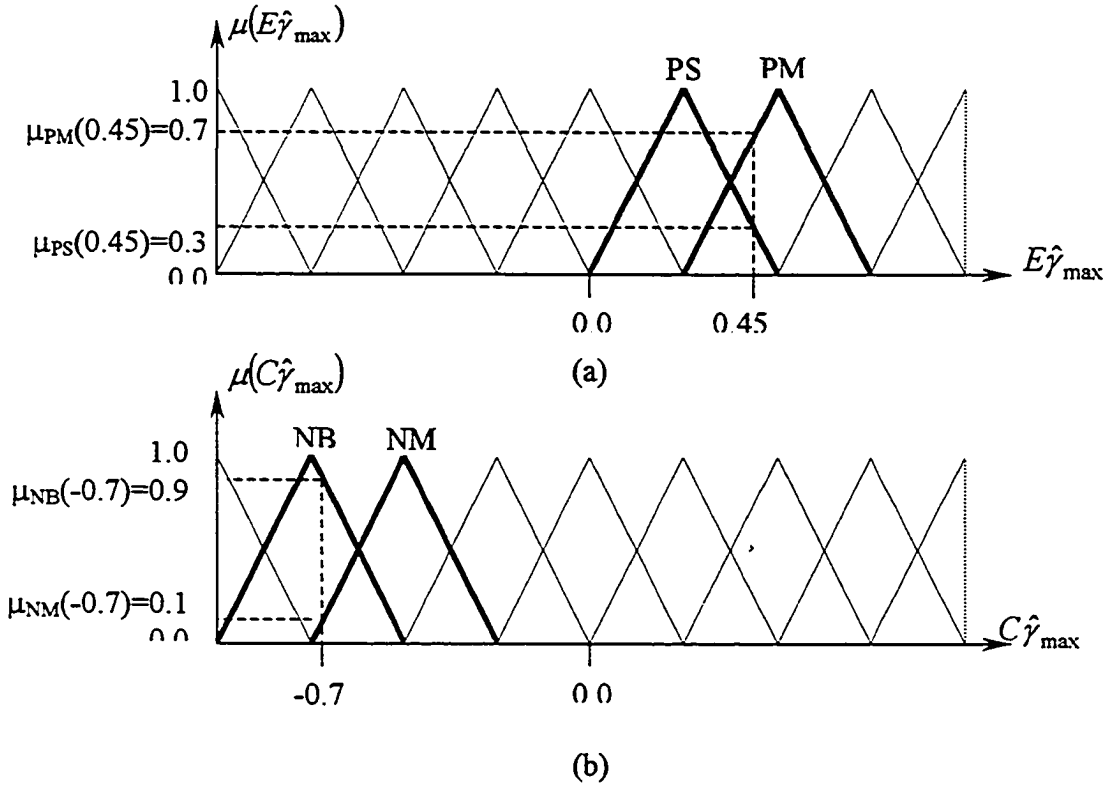

Figure 3.10 Illustration of input membership degrees with two triangular fuzzy sets
(a) Fuzzification for $E\gamma_{max}$, where $E\hat{\gamma}_{max}$ is the normalized $E\gamma_{max}$
(b) Fuzzification for $C\gamma_{max}$, where $C\hat{\gamma}_{max}$ is the normalized $C\gamma_{max}$

The output membership function value for each rule is determined according to the min-max rule as follows:

$$\mu_{Cij} = \min\left[\mu(E\hat{\gamma}_{max})_i, \mu(C\hat{\gamma}_{max})_j\right] \tag{3-22}$$

where μ_{Cij} is the output membership function value of associated with rule specified by inputs $(E\gamma_{max})_i$ and $(C\gamma_{max})_j$, $\mu[(E\gamma_{max})_I]$ and $\mu[(C\gamma_{max})_j]$ are the input membership function values.

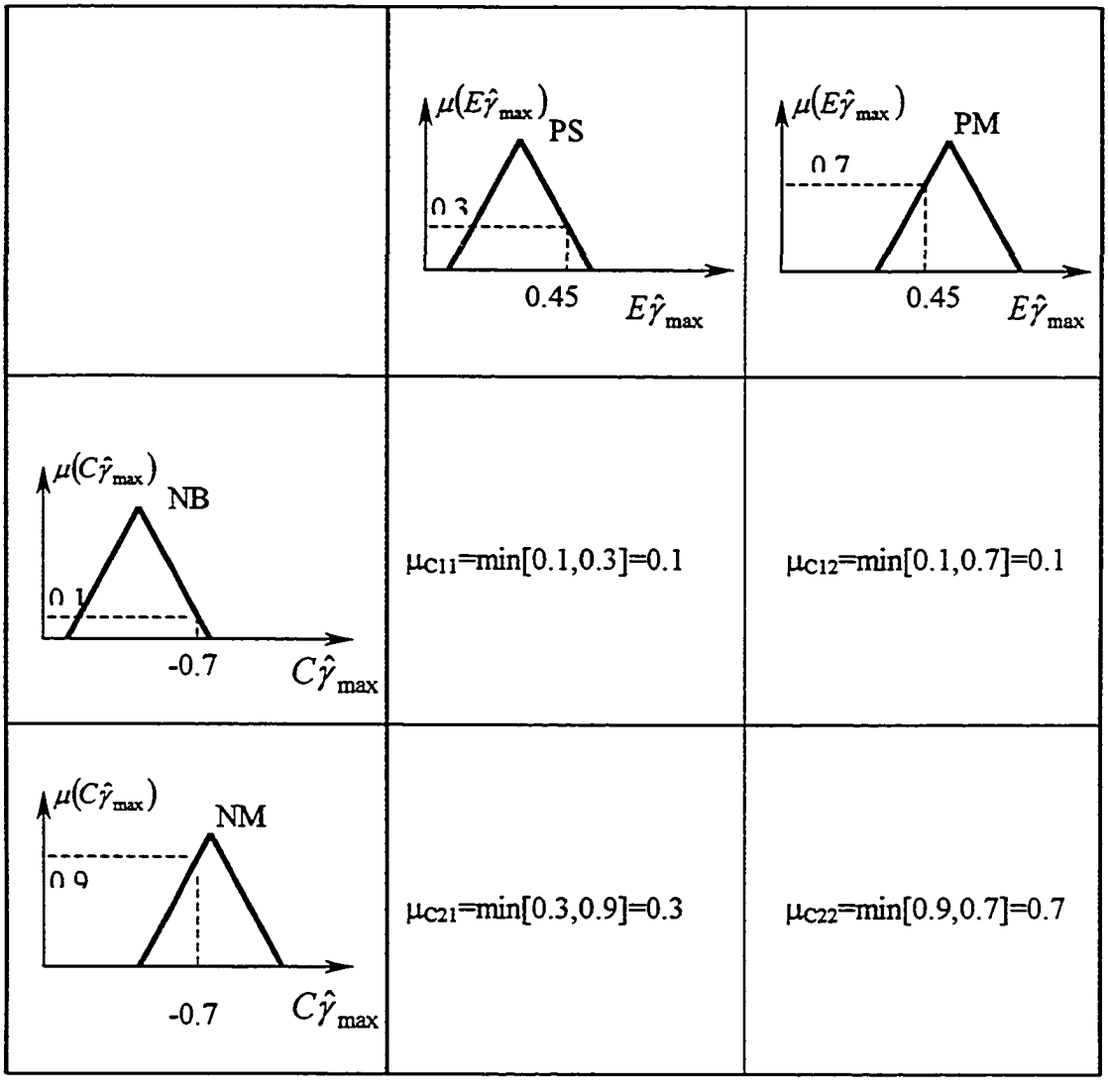

Figure 3.11a Calculation of the coefficients of output fuzzy values

Suppose the crisp output is spindle speed, the four output fuzzy sets can be located in the shaded area of an illustrative rule base shown in Figure 3.11b. The linguistic values of the four fuzzy sets are:

C_{11}=ZE, C_{12}=NS, C_{21}=ZE, and C_{22}=ZE.

The corresponding fuzzy values are 5, 5, 5, 4, respectively.

$C\gamma_{max}$ / $E\gamma_{max}$	NX	NB	NM	NS	ZE	PS	PM	PB	PX
NX	PB	PM	PM	PM	PM	PM	PM	PS	PS
NB	PM	PM	PM	PS	PS	PS	PS	PS	PS
NM	PM	PM	PS	PS	PS	PS	PS	ZE	ZE
NS	PS	PS	PS	ZE	ZE	ZE	ZE	ZE	ZE
ZE	PS	PS	ZE	ZE	ZE	ZE	ZE	NS	NS
PS	ZE	ZE	ZE	ZE	ZE	ZE	NS	NS	NS
PM	ZE	ZE	NS	NS	NS	NS	NS	NM	NM
PB	NS	NS	NS	NS	NS	NS	NM	NM	NM
PX	NS	NS	NM	NM	NM	NM	NM	NM	NB

Figure 3.11b An illustrative rule base

In the above, the output fuzzy set values and the corresponding coefficients have been determined. The fuzzy sets need to be converted into physical values before they could be used.

Defuzzification involves the process of converting the set of fuzzy control output values and mapping the inferred fuzzy control action to crisp control actions. The defuzzification strategy is aimed at producing a non-fuzzy control action that best represents the possibility distribution of the inferred fuzzy control action (Driankov *et al.*, 1999). The crisp output is calculated using weighted average method. (Driankov *et al.*, 1999)

$$u = \frac{\sum_{j=1}^{r} \mu_{C_j} \cdot C_j}{\sum_{j=1}^{r} \mu_{C_j}} \tag{3-23}$$

where r is the total number of rules, C_j is the value associated with the peak of output fuzzy set j, i.e., the suggested output value associated with the peak of fuzzy set j, and μ_{C_j} is the height which is given by

$$\mu_{C_j} = \min\left[\mu_{1_j}, \mu_{2_j}, \ldots, \mu_{k_j}\right] \qquad j = 1,2,\ldots,r \tag{3-24}$$

where r is the number of rules and k is the number of inputs.

The calculation of the crisp output value for the above illustrative example is illustrated in Figure 3.12 and the output value is:

$$u = \frac{0.1\times5+0.1\times5+0.3\times5+0.7\times4}{0.1+0.1+0.3+0.4} \approx 5.88$$

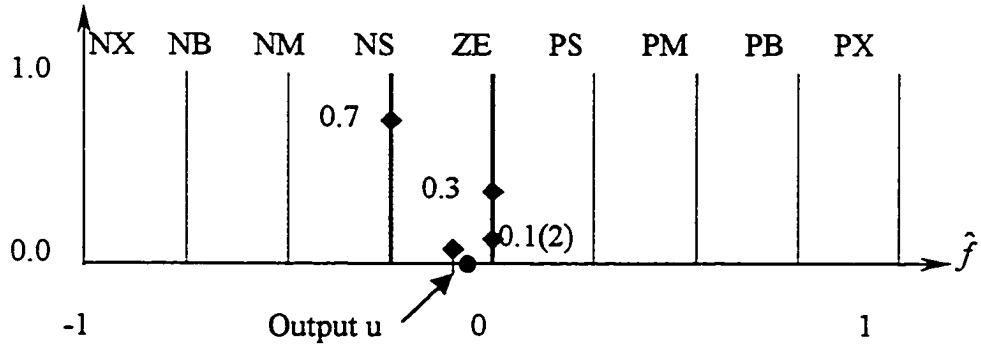

Figure 3.12 Defuzzification using singleton membership function

3.3.4 Scaling Factors

Scaling factors are used for mapping data from physical values of the process state variables into normalized value, knows as normalization, and they are also used for mapping normalized output domains into their physical values, which is called denormalization. Scaling factors also play a significant role in the overall performance of the control system, such as response, overshoot and stability. Hence, the proper selection of these factors is very important.

3.3.4.1 Input Scaling Factors

Driankov *et al.* (1996) claimed that the input scaling factors play an important role similar to that of the gain coefficients in a conventional controller.

According Liang (2001), the scaling factors for the three fuzzy engine inputs are defined as following:

The scaling factor for the error of the maximum coherence ratio is:

$$KI_{E\gamma} = \begin{cases} \dfrac{1}{\gamma_{up} - \gamma_{ref}} & if \quad (\gamma_{\max})_i \geq \gamma_{ref} \\ \dfrac{1}{\gamma_{ref} - \gamma_{low}} & if \quad (\gamma_{\max})_i < \gamma_{ref} \end{cases} \tag{3-25}$$

The scaling factor for the change of the maximum coherence ratio is:

$$KI_{C\gamma} = \frac{1}{\gamma_{up} - \gamma_{low}} = 1 \quad (\gamma_{up} = 1, \gamma_{low} = 0) \tag{3-26}$$

The scaling factor for the error of vibration energy level is:

$$KI_E = \begin{cases} \dfrac{1}{E_{up} - E_{ref}} & if \quad E_i \geq E_{ref} \\ \dfrac{1}{E_{ref} - E_{loe}} & if \quad E_i < E_{ref} \end{cases} \tag{3-27}$$

The scaling factors are further tuned based on real machining condition. For example, $KI_{E\gamma}$ is tuned as follows:

$$KI_{E\gamma t} = B_i KI_{E\gamma}$$

where, $B_i = \left[\dfrac{PI(EE)_i}{\varepsilon_E} \right]^{\alpha_E}$

$KI_{C\gamma}$ and KI_E are tuned in similarly.

As an example, the energy scaling factors are illustrated in Figure 3.13.

3.3.4.2 Output Scaling Factors

The output scaling factors map the normalized output data into their physical values. The physical values of the outputs, i.e., the spindle speed and the feed rate have their upper and lower limits. For example, the upper and lower limit values of the spindle speed used in this study are 500 rpm and 1200 rpm, respectively.

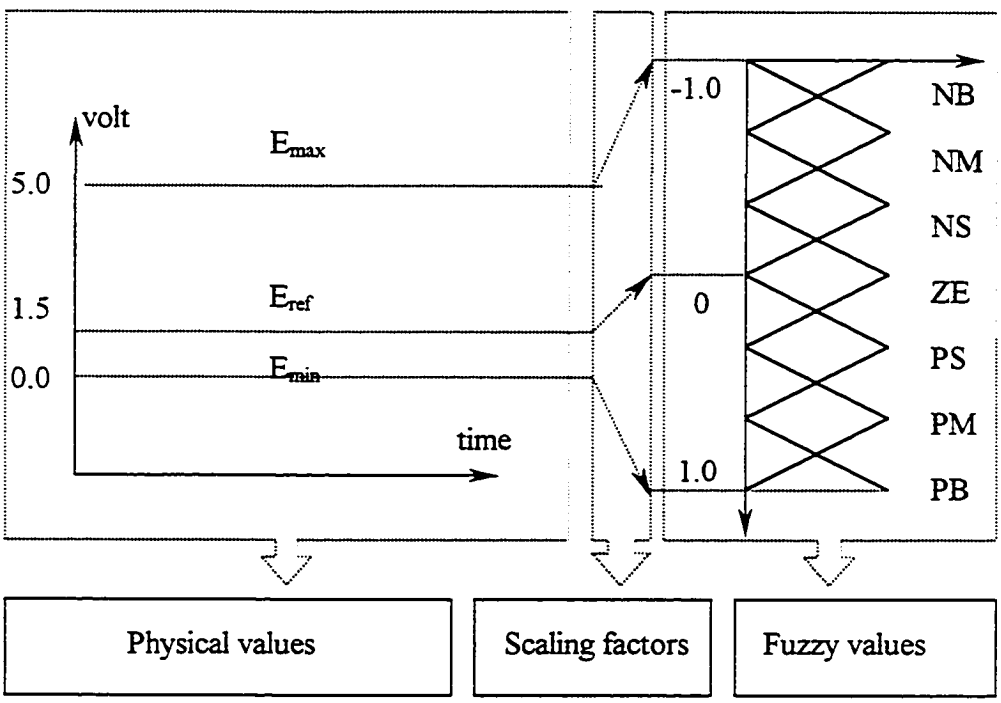

Figure 3.13 Input scaling factors

In order to prevent the abrupt change in output command that cannot be followed by the machine, a relation between control cycle and maximum allowable machine adjustment is established in this thesis. They are called the feed step and spindle speed step, namely the feed rate change and spindle speed change during a single control cycle as defined below (Liang, 1999):

$$Feed\ Step = \frac{FeedOutputRange}{CyclesPerSecond} \tag{3-28}$$

$$Speed\ Step = \frac{SpeedOutputRange}{CyclesPerSecond} \tag{3-29}$$

where *FeedOutputRange* and *SpeedoutputRange* are the voltage values associated with the feed rate adjustment range and spindle speed adjustment range, respectively. *CyclesPerSecond* is the number of control cycles per second. With these restrictions, the machine system is limited to make a full range adjustment within one second.

3.3.5 Tuning Factors

The tuning factors are used to enhance system response and stability. The few tuning factors used in this thesis are detailed as follows.

3.3.5.1 Overshoot Suppression

Overshoot often lead to severe vibrations during cutting. When a certain consecutive energy overshoot samples are observed, a special control method must be used to control the machine's performance. Overshoot-tuning factors are added to the regulation values of spindle speed and feed rate using the suppression algorithm:

If $|E_i| > |E_{i-1}| > |E_{i-2}| > \varepsilon$, set $m = m + 1 \quad KO_{os,i} = KO_{os,i-1} \cdot \alpha^m$

Else, set $m = 0 \quad KO_{os,i} = 1.0$

where ε is a threshold value, $KO_{os,i}$ is overshoot-tuning factor (Liang, 1999), α is a constant.

3.3.5.2 Impact Suppression

Impact is defined as the abrupt change in cutting energy. When impact happens, the change of the energy value is tremendous. To avoid the tool breakage, the adjustments of feed rate and spindle speed need to be regulated.

A dynamic impact suppression factor KO_{imp} (Hermansyah 2000) is added to Equations 3-28 and 3-29:

$$Feed\ Step = KO_{imp} \cdot \frac{FeedOutputRange}{CyclesPerSecond} \tag{3-30}$$

$$Speed\ Step = KO_{imp} \cdot \frac{SpeedOutputRange}{CyclesPerSecond} \tag{3-31}$$

Whenever $|E_i|$ is larger than a safe value a, the impact suppression factor is weighed by a gain g (g>1). Hence, the spindle speed and feed rate could drop faster.

3.3.5.3 Other Restrictions

To prevent tool breakage and machine overload, the following restrictions to feed rate and spindle speed are defined:

Restriction	Condition
$(f,v)=(f,v)_{min}$	$E>E_{max}$
$(f,v)=(f,v)_{max}$	$E<E_{min}$
$(f,v)=0$	$E>E_{upperlimit}$
$(f,v)=(f,v)_{lowelimit}$	$(f,v)<(f,v)_{lowerlimit}$
$(f,v)=(f,v)_{upperlimit}$	$(f,v)>(f,v)_{upperlimit}$

Table 3.1 Other adjustment limits for safe operation

3.4 Self-learning and Direct Output Tuning Algorithms

By utilizing the fuzzy control system, machine operations can be regulated according to the real-time behaviour of the system. These real cutting performances are affected by many predictable and unpredictable factors.

In this study, a self-learning algorithm and a direct output tuning algorithm are used to achieve a better control performance.

Self-learning is an adaptive control strategy. Since cutting processes are non-linear and time-varying dynamic system, an adaptive fuzzy logic controller thus has the potential to achieve a better control performance than the model-based controllers (Hsu and Fann, 1996). The fuzzy controller can be updated online by mapping the given current working state to a target state set until the machine runs on a desired working performance. In this thesis, the rule base is selected. A direct output tuning approach is also suggested to enhance the system performance

3.4.1 Self-learning Algorithm for Rule Base Adjustment

The rule base adjustment is done according to the maximum coherence ratio, $E\gamma_{max}$.

Based on the fuzzy control system in Figure 3.4, the structure of the rule base self-learning approach illustrated on a schematic diagram is shown in Figure 3.14.

In Figure 3.14, the self-learning approach consists of two steps. First, the error of the maximum coherence ratio, $\delta(E\gamma_{\max})$ is calculated as:

$$\delta(E\gamma_{\max}) = w \cdot (E\gamma_{\max} - E\gamma_n) \tag{3-32}$$

where w is the weight, which represents the learning rate of the system, $E\gamma_n$ is a neutralized coherence ratio, at which no machine regulations are needed. The w value has a direct impact on system performance. Generally, a larger w will increase the responsiveness of the system but decrease the system's robustness (Hsu *et al.*, 1996) as shown in Figure 3.16.

From Figure 3.16, it is observed that, when w=0.2, the system almost does not sense the change of the input $E\gamma_{max}$, and when w=0.7 or 0.8, the stability of the system is too

low which causes severe fee rate fluctuations. In this thesis, w is selected in the range of [0.3, 0.5] for responsiveness and robustness concerns.

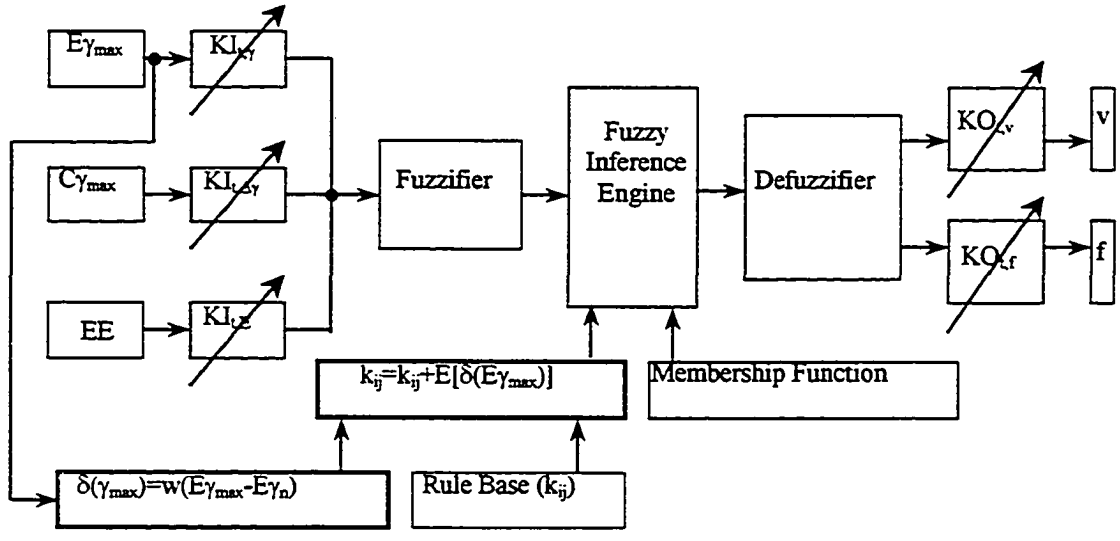

Figure 3.14 Fuzzy logic control with rule base self-learning for chatter suppression

Secondly, update the rule base by adding the error to all the nodes or rules:

$$k_{ij} \Leftarrow k_{ij} + E[\delta(E\gamma_{\max})] \tag{3-33}$$

where k_{ij} is a node in the rule base. There are 81 nodes in each coherence ratio rule base in this thesis. $E[\ ]$ denotes the average value of several errors. The actual self-learning algorithm does not need to update the rule base in every control cycle. In this thesis, the rule base updating interval is set to 6 control cycles to reduce computing time.

If the learning rate is properly selected, the self-learning algorithm generally improves the response of the system. Figure 3.15 shows the difference in feed rate adjustment with or without self-learning.

Figure 3.17 and 3.18 show two rule bases modified by the learning algorithm.

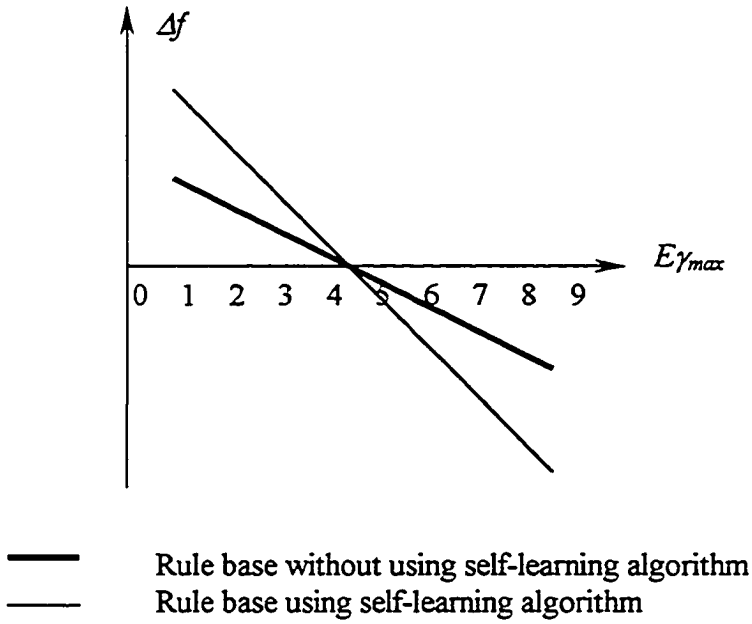

Figure 3.15 Feed rate adjustment with and without self-learning

3.4.2 Direct Output Tuning

According to the experimental results, the rule base self-learning algorithm proven to be an efficient tool for chatter control. However, it has its disadvantages. The spindle speed and feed rate are not adjusted successively because the rule values are discrete values, such as 1, 2, ..., 9. This may cause instability when the rule base is adjusted with a large weight. Hence, it is proposed in this study to directly fine-tune the output based the monitored process values, i.e., EE and $E\gamma_{max}$.

The structure of the direct output tuning approach is illustrated in a schematic diagram is shown in Figure 3.19. In this thesis, two types of direct tuning are tested. One is the output tuning according to the maximum coherence ratio, $E\gamma_{max}$, alone, the other is the output tuning based on both the maximum coherence ratio, $E\gamma_{max}$, and the energy level, EE.

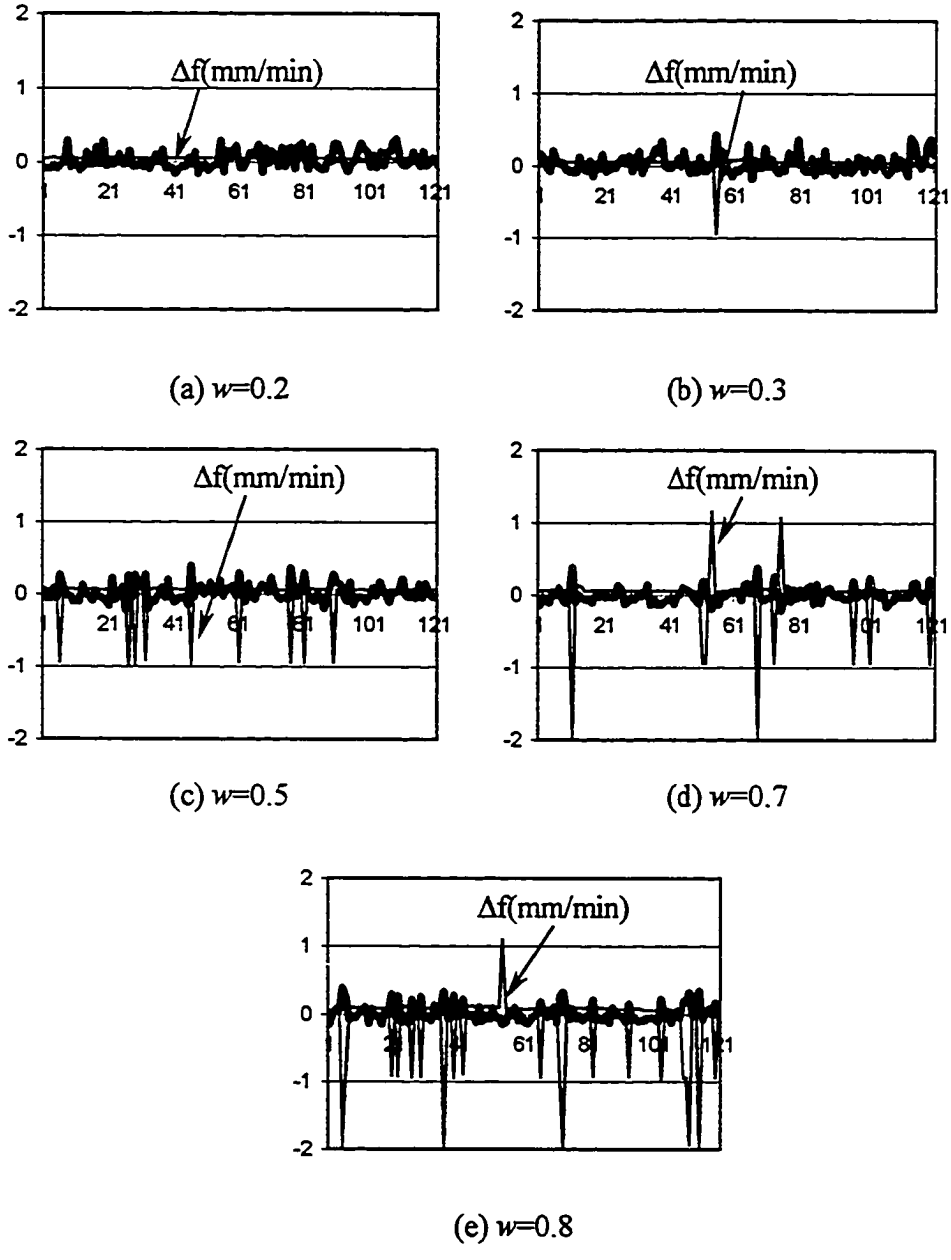

(a) w=0.2

(b) w=0.3

(c) w=0.5

(d) w=0.7

(e) w=0.8

Figure 3.16 Rule base self-learning algorithm with different weights (Thinner lines represent output Δf (mm/min), thicker lines represent input $E\gamma_{max}$)

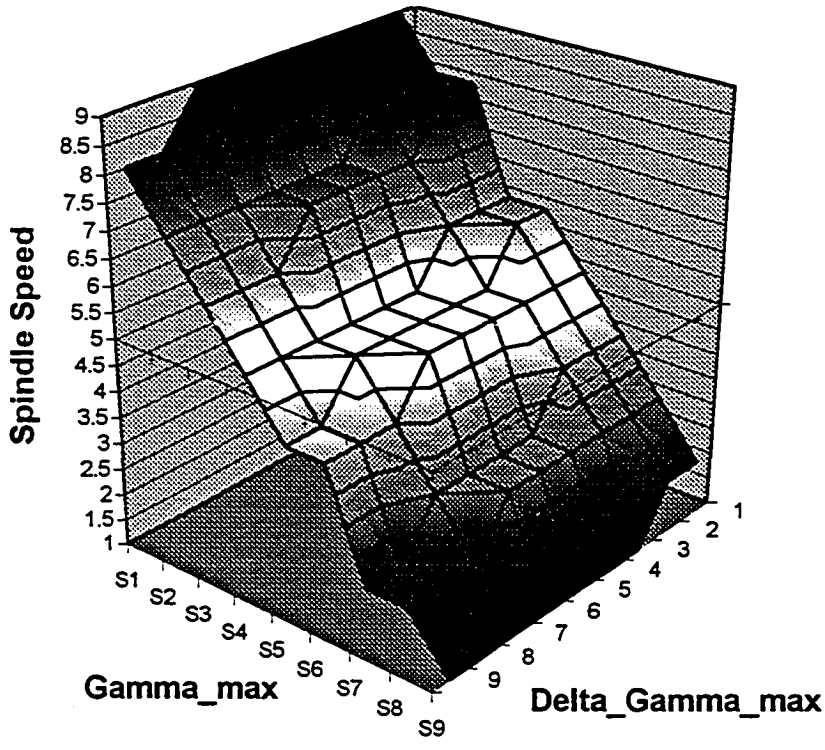

(a)

$E\gamma_{max}$ \ $C\gamma_{max}$	NX	NB	NM	NS	ZE	PS	PM	PB	PX
NX	PX	PX	PX	PX	PX	PX	PX	PB	PB
NB	PB	PB	PB	PM	PM	PM	PM	PM	PM
NM	PB	PB	PM	PM	PM	PM	PS	PS	PS
NS	PS	PS	PS	ZE	ZE	ZE	ZE	ZE	ZE
ZE	PS	PS	ZE	ZE	ZE	ZE	ZE	NS	NS
PS	ZE	ZE	ZE	ZE	ZE	ZE	NS	NS	NS
PM	NS	NS	NS	NM	NM	NM	NM	NB	NB
PB	NM	NM	NM	NM	NM	NM	NB	NB	NB
PX	NB	NB	NX	NX	NX	NX	NX	NX	NX

(b)

Figure 3.17 Coherence ratio table: Fuzzy rules for chatter suppression by adjusting spindle speed using rule base self-learning algorithm
(a)3-D plot (b)Fuzzy values in the rule table

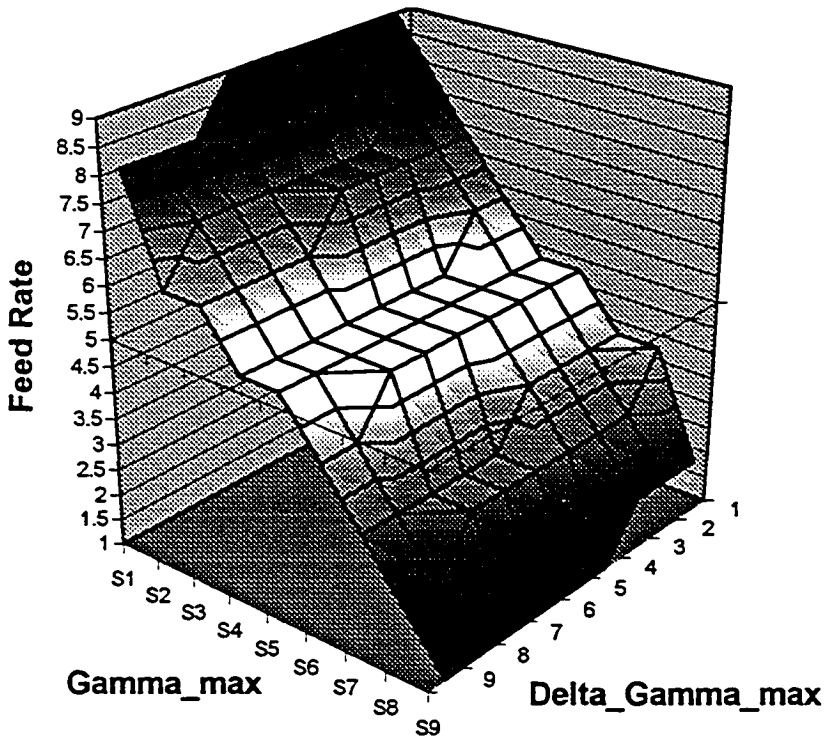

(a)

$C\gamma_{max}$ / $E\gamma_{max}$	NX	NB	NM	NS	ZE	PS	PM	PB	PX
NX	PX	PX	PX	PX	PX	PX	PB	PB	PB
NB	PB	PB	PM	PM	PM	PM	PM	PM	PS
NM	PM	PM	PM	PM	PM	PS	PS	PS	PS
NS	PS	PS	ZE	ZE	ZE	ZE	ZE	ZE	ZE
ZE	ZE	ZE	ZE	ZE	ZE	ZE	ZE	ZE	ZE
PS	ZE	ZE	ZE	ZE	ZE	ZE	ZE	NS	NS
PM	NS	NS	NS	NS	NM	NM	NM	NM	NM
PB	NS	NM	NM	NM	NM	NM	NM	NB	NB
PX	NB	NB	NB	NX	NX	NX	NX	NX	NX

(b)

Figure 3.18 Coherence ratio table: Fuzzy rules for chatter suppression by adjusting feed rate using rule base self-learning algorithm
(a) 3-D plot (b) Fuzzy values in the rule table

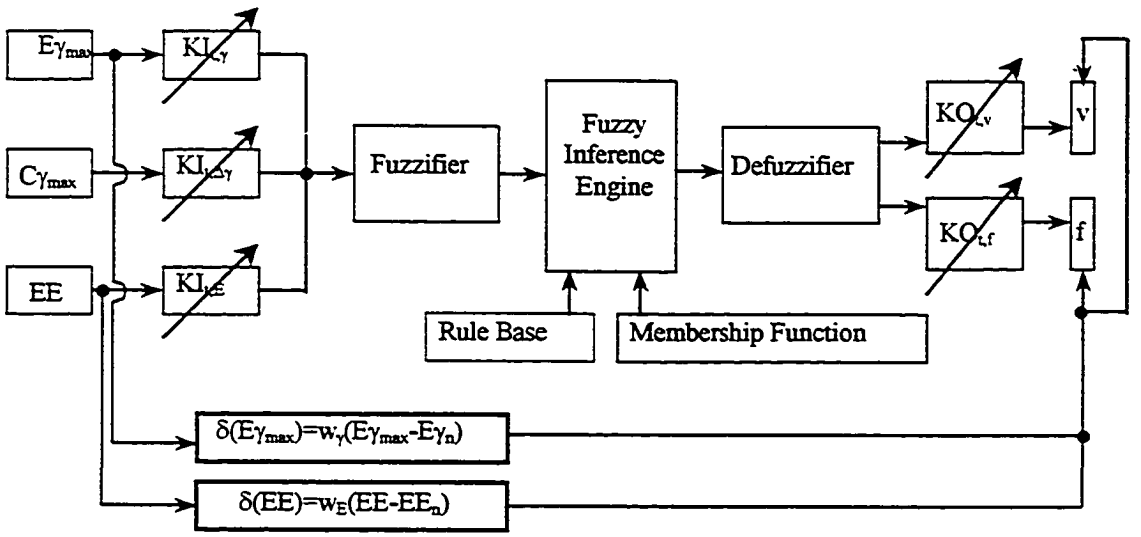

Figure 3.19 Fuzzy logic control with direct outputs tuning for chatter suppression

Similar to the rule base self-learning algorithm, in the first step, the errors of the coherence ratio and energy level are calculated using Equations 3-33 and 3-34:

$$\delta(E\gamma_{\max}) = w_\gamma \cdot (E\gamma_{\max} - E\gamma_n) \tag{3-34}$$

$$\delta(EE) = w_E \cdot (EE - EE_n) \tag{3-35}$$

where, w_γ is the weight for coherence ratio selected in the range of [0.5, 0.8], w_E is the weight for energy level selected in the range of [1.0, 1.5], EE_n is the reference value, selected as 1.5.

The second step is to fine-tune the feed or spindle speed increments using the following two equations:

$$\begin{cases} \Delta f_{adjust} = \Delta f \cdot w_t \cdot [\delta(E\gamma_{\max}) + \delta(EE)] \\ \Delta v_{adjust} = \Delta v \cdot w_t \cdot [\delta(E\gamma_{\max}) + \delta(EE)] \end{cases} \tag{3-36}$$

$$\begin{cases} \Delta f_{adjust} = \Delta f \cdot \delta(E\gamma_{\max}) \\ \Delta v_{adjust} = \Delta v \cdot \delta(E\gamma_{\max}) \end{cases} \tag{3-37}$$

where w_t is a positive constant and is fixed at 1.0 in this study.

The experimental results show that the adjustment made by the direct output tuning algorithm is more responsive and smoother in some cases as compared to that using the rule base self-learning approach.

Advantages of using the direct output tuning may be explained as follows. When the performance indices are close to their reference values, the outputs are adjusted to a smaller value. This helps to avoid the large vibration caused by over adjustments of spindle speed and feed rate. When the performance indices are far away from the reference values, the output adjustments are strengthened by using a larger multiplier. Figure 3.20 illustrates the relation between Δf and $E\gamma_{max}$ with different w_r values.

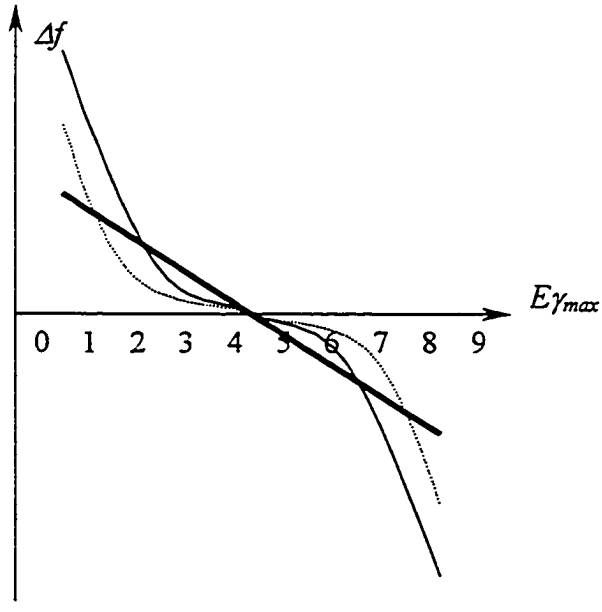

Output without using self-learning algorithm
Output using self-learning algorithm with a larger weight
Output using self-learning algorithm with a smaller weight

Figure 3.20 Schematic diagram for direct outputs tuning

An experimental result was shown in Figure 3.21, which compares the feed rate adjustment processes with and without direct output tuning.

When the mean vibration energy level is above a threshold value E_{th}, which is around 0.4, the absolute value of the adjusted output $|\Delta f_{adjust}|$ is larger than the absolute value of the output $|\Delta f|$. When energy level is below E_{th}, then the absolute value of the adjusted output $|\Delta f_{adjust}|$ is smaller than the absolute value of the output $|\Delta f|$.

The threshold value of E is determined by the selection of weight w_i. The larger the weight is selected, the smaller the threshold value is, so that a larger weight makes the control system more sensitive and a smaller weight makes the control system more stable.

In the real application, the threshold value of E and the threshold values of other inputs are jointly used to determine the output adjustments.

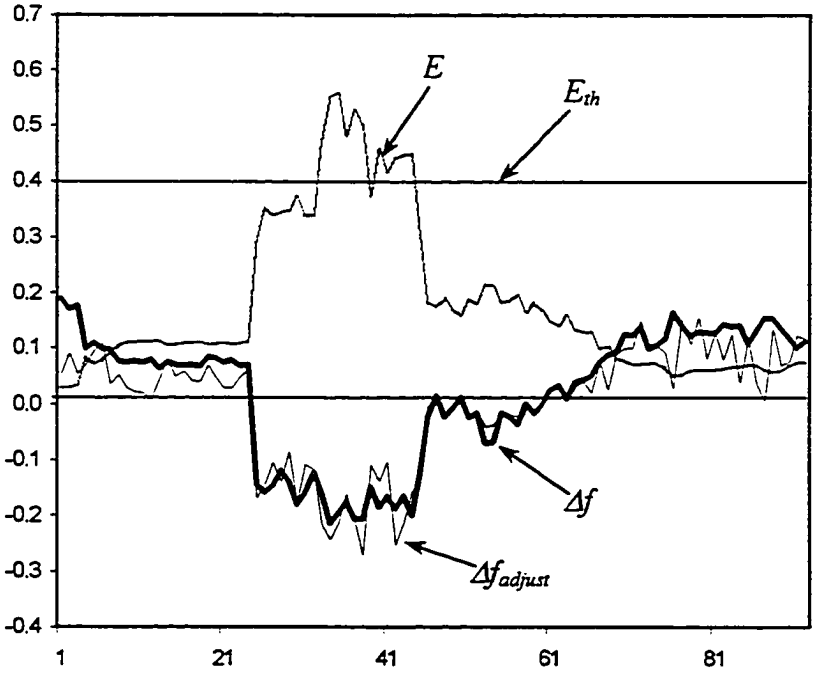

Figure 3.21 Direct outputs tuning

Unlike the rule base self-learning algorithm, which is carried out in the fuzzy domain, the direct output tuning is conducted in the physical domain. Without direct output tuning, the fuzzy controller would execute the commands based on a rule base that with some time delay and hence the commands do not necessarily reflect the real-time machining conditions. The direct output tuning is more responsive to the on-line cutting conditions and therefore should improve the performance of the fuzzy system.

Chapter 4

Experiments

4.1 Experimental Apparatus

The schematic configuration of the system is illustrated in Figure 4.1. The chatter suppression system consists of the following hardware components:

- CNC SERVO 2000 milling machine
- Wilcoxon 993B-6 hermetic tri-axial accelerometer
- Wilcoxon P703BT power unit
- National Instrument DAQ AT-MIO-16DE-10 data acquisition card
- Intel Pentium III PC

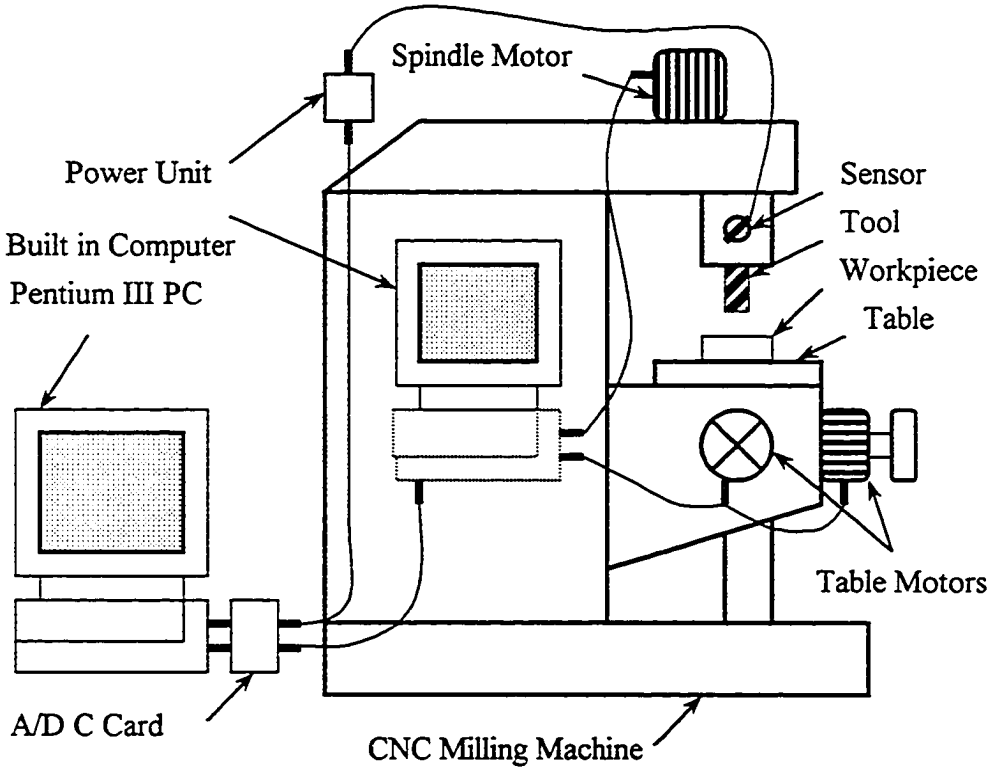

Figure 4.1 Hardware configuration

4.1.1 CNC SERVO 2000 Milling Machine

The CNC SERVO 2000 milling machine is a tri-axial vertical CNC milling machine with NC control in x- and y- axes built by Servo Product Company (Figure 4.2). The three-HP spindle motor is driven by a three-phase G3 adjustable frequency AC drives built by Saftronics.

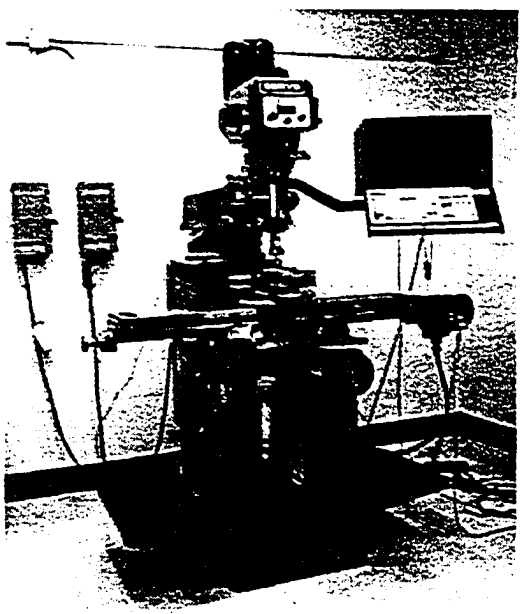

Figure 4.2 CNC SERVO 2000 milling machine

Driven by the spindle motor, the spindle speed can be adjusted either by the commands from the built-in computer, i.e., system operation console, or by regulating the meter manually on the spindle speed panel. In this study, the spindle speed is controlled by an external computer as shown in Figure 4.1. After being converted into analog signals by the A/D card, the digital signals from the external computer can be used to adjust the spindle speed. The NC machine has two speed range selections. The range of low gear is from 50rpm to 500rpm and that of high gear is from 500rpm to 5000rpm.

CNC SERVO 2000 has a three-axes sliding table, which can drive the workpiece moving in a specified direction.

The movements along x-axis (table direction) and y-axis (crossing table direction) are controlled by SERVO II axis drive motors. The movements along z-axis (vertical direction) is operated manually by the operators. The feed rate adjustment commands from the built-in computer control the table speed. The feed rate can also be changed manually from the teaching pendant. The override range of feed rate on the teaching pendant is from 0 to 150%. The teaching pendant was also modified to be able to switch to an "automatic" button to accept the control commands from the external PC.

4.1.2 Vibration Sensor

The vibration sensor in this thesis is a hermetic tri-axial accelerometer, 993B-6 provided by Wilcoxon. The sensor is shown in Figure 4.3.

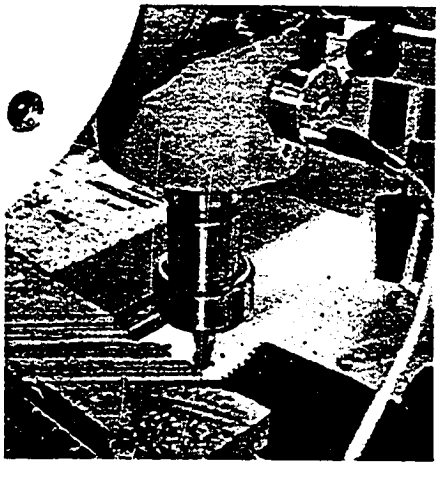

Figure 4.3 The tri-axial accelerometer and thin-wall cutting

This vibration sensor is mounted near the tool holder, where the vibration signals of the tool-workpiece system can be obtained. Wilcoxon 993B-6 sensor can detect

vibrations from three axes with the frequency responses 2-10,000Hz in z-axis and 2-7,000Hz in x-axis and y-axis. This sensor is accompanied with a power unit, P703BT, which has three identical outputs in x, y and z directions.

4.1.3 A/D Converter Card

The DAQ card is a multifunction input-output with up to 100ks/sec reading capability. It also features a 12-bit analog-to-digital converter for 16 single ended or 8 differential analog inputs, two 12-bit analog outputs, two 24-bit counter/timers, and 32 digital I/O lines.

The analog signal from the vibration sensor is digitized at 4,096 samples/second for each direction using double buffering method to ensure data integrity. The digital commands from PC are converted to analog voltage output signals in the range of [1.3, 4.8V] for feed (represents 0 to 150% feed rate override) and 1 to 10V for spindle speed (represents 50 to 500 rpm for low gear and 500 to 5000 rpm for high gear), respectively.

4.2 Software and Algorithms

• Development tools

LabWindows/CVI is used for building the "projects" for chatter detection and suppression with resource code written in C. The fuzzy logic toolbox of MATLAB is used for generating the fuzzy engine.

• DAQ Card Configuration

NI-DAQ Utility is used to specify the DAQ card configuration.

4.3 Experimental Set-up

• Cutter

High Speed Steel (HSS) 9/16"(14.3mm) end-milling cutter with four helical flutes and 30° helix angles

• Workpiece materials

1018 cold rolled steel and aluminium

• Spindle Speed Range

500 rpm to 1200 rpm

• Feed rate Range

0 to 150 mm/min

• Cutting direction

45° from either x- or y- axis (Figure 4.5).

• Profile of workpiece

Flat cutting, single thin-wall cutting and double thin-wall cutting (See Figure 4.4 and Figure 4.5 for the geometric dimensions and the cutting depth or width)

• Immersion and use of coolant

Full immersion with coolant

• Control method

Fuzzy control with and without self-learning algorithm

4.4 Experimental Results

During the end milling operations, chatter is detected either when the mean vibration energy E is above its reference value E_{ref} or the γ_{max} is above its reference level γ_{ref}. The control target is to maintain the mean vibration energy E at or around the reference value and the γ_{max} value below its reference level by adjusting the spindle speed v and the feed rate f. Based on a series of tests, the reference value of the mean vibration energy is selected as E_{ref}= 1.5 volt, with the upper limit E_{upper}= 5.0 volt, and γ_{ref}= 0.8.

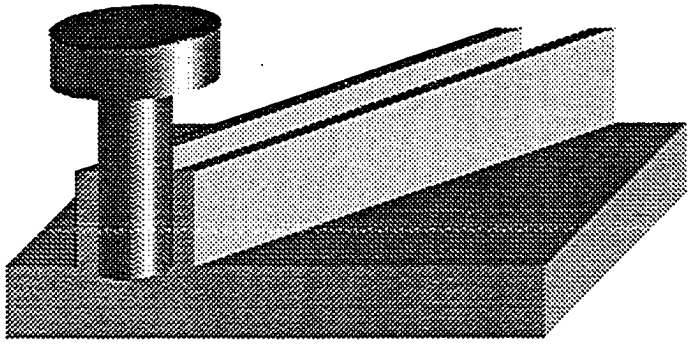

(a) Sinking Generation with Double Thin-wall

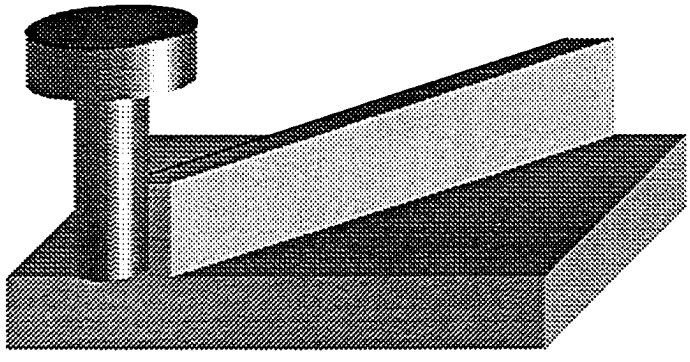

(b) Side Generation with Single Thin-wall

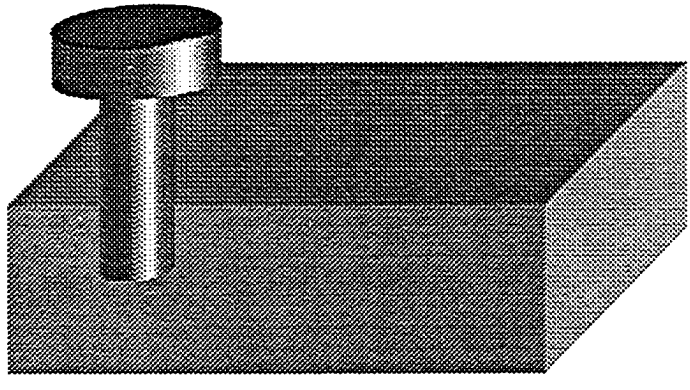

(c) Regular Flat Cutting

Figure 4.4 Tool-workpieces with three cutting tests

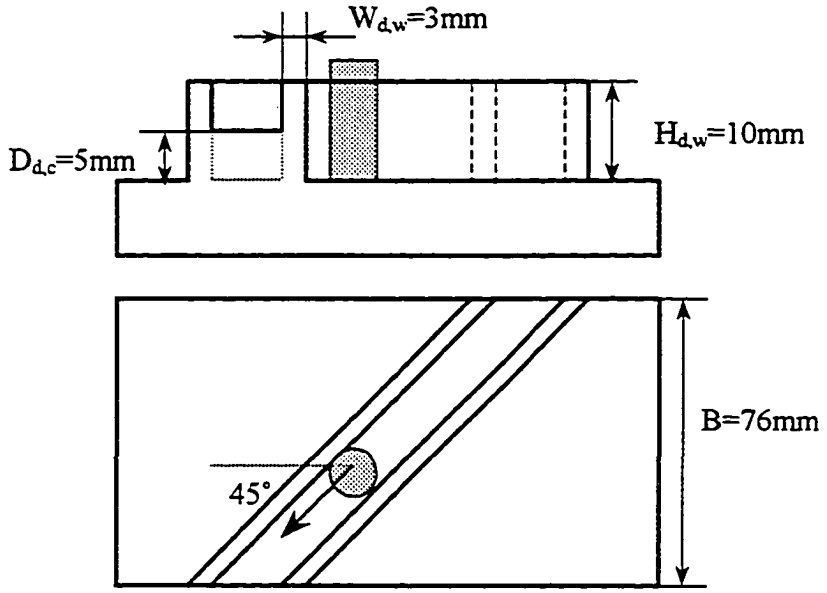

(a) Dimensions for Sinking Generation

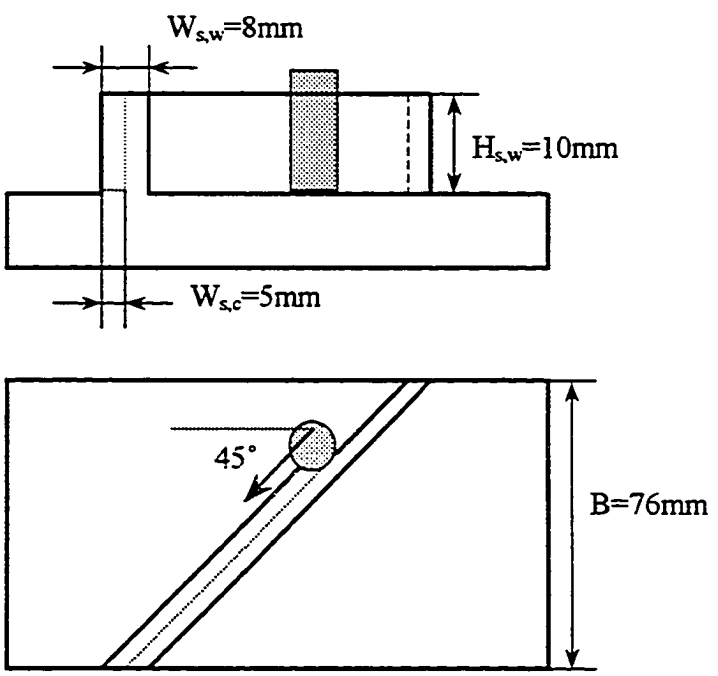

(b) Dimensions for Side Generation

Figure 4.5 Dimensions of the workpieces
(a) $H_{d,w}$ is the height of the double thin-wall, $W_{d,w}$ is the width of the double thin-wall, $D_{d,c}$ is the depth of cut in double thin-wall cutting, and B is the width of the workpiece (b)$H_{s,w}$ is the height of the single thin-wall, $W_{s,w}$ is the width of the single thin-wall, and $D_{d,c}$ is the depth of cut in single thin-wall cutting

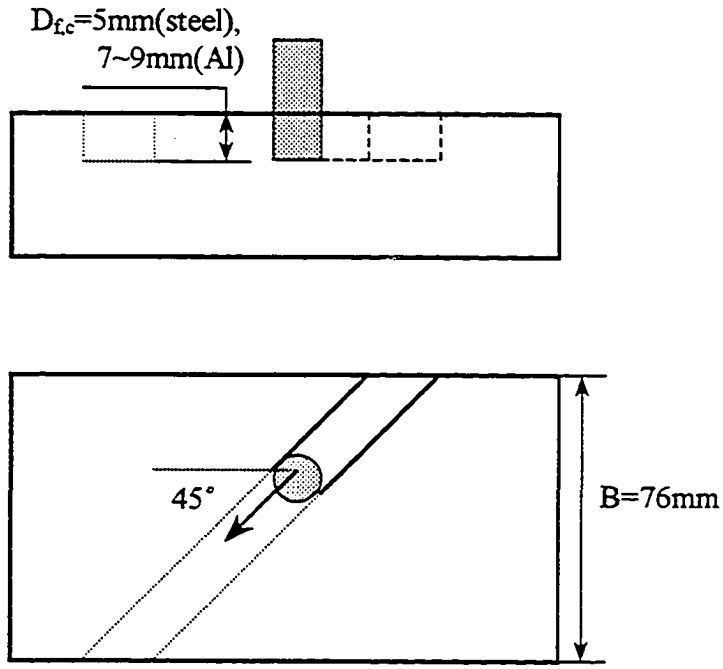

(c) Dimensions for Flat Cutting

Figure 4.5 Dimensions of the workpieces
(c) $D_{f.c}$ is the depth of cut in flat cutting

In the experimental results, the root mean square values of the mean vibration energy E is also plotted to observe the behaviour of the control system which is defined as follows:

$$E_{RMS,i} = \sqrt{\frac{\sum_{j=i-N_e}^{i} E_j^2}{N_e}} \qquad i = 0,1,\ldots \tag{4-1}$$

where E_j is the vibration energy level measured in control cycle j, N_e is the number of control cycles over which $E_{RMS,i}$ is calculated, in this thesis N_e is selected as 10. For each experimental result, the root mean square value of E_{RMS} is plotted together with E.

Figures 4.6 through 4.24 show the experimental results with different cutting situations and different control methods. For clarity concern, the feed rate adjustment Δf and the spindle speed adjustment Δv are displayed separately in different parts of each figure, and the maximum coherence ratio $E\gamma_{max}$ and the change of maximum coherence ratio $C\gamma_{max}$ are also plotted separately for the same reason. The discussions are given below.

4.4.1 Flat Steel Workpieces—Full Immersion

The results for the full immersion cutting of flat steel workpieces are plotted in Figures 4.6 through 4.13. Figure 4.6 shows the experimental results of flat cutting without using self-learning algorithms. Severe vibration was observed at the beginning of cut, leading to a high level mean vibration energy EE which was above the reference value E_{ref} though the coherence function value was still below its reference level. This triggered the suppression action and both the spindle speed v and the feed rate f were reduced. It was noticed that the suppression took about 10 seconds to suppress the chatter for the initial cutting period. For the chatters occurred after the initial cutting period, the suppression took much shorter time to complete. As shown in the figure, no long lasting chatters were observed after the initial period and the $E\gamma_{max}$ and EE values were well maintained around the reference levels. As discussed in Chapter 3, the coherence function value could be used for chatter prediction and also our experiments show that higher coherence ratios were often observed before the chatter onset. Hence maintaining the coherence function value below the reference level will likely prevent chatters. This may partially explain why no severe and long lasting chatters were observed after the initial cutting period.

In Figures 4.7 and 4.9, rule base self-learning algorithm was used with the weights of 0.2, 0.3, and 0.4 respectively. As shown in Figures 4.7 and 4.8, the smaller weights

(0.2 and 0.3) tend to smooth out both vibration energy and coherence function values and hence the feed and spindle speed adjustment processes are also smoother. As shown in Figure 4.9, when a larger weight is used (0.4 in this case), the suppression response is faster (as shown in the initial cutting period) but the process is much less stable featured with large fluctuations of feed and speed adjustments.

Figures 4.10 to 4.13 show the results using direct output tuning. The single (using the coherence signal only) direct tuning results are presented in Figures 4.10 and 4.11, and double direct tuning results in Figures 4.12 and 4.13. In both cases the processes seem to be smoother as compared to the results without direct tuning. However the double direct tuning results appear to be smoother than those of the single direct tuning. As expected, it can also be observed that higher weights tend to improve system responsiveness and lower weights lead to a smoother process. In particular, the results shown in Figures 4.12 and 4.13 indicate that the processes were well controlled after the initial cutting period and only small amount of feed and spindle speed adjustments were made.

Excessive output adjustments may cause severe vibration. The use of the direct output tuning not only makes the output adjustment more effective but also helps avoid over adjustment unnecessarily when the cutting condition is already well regulated.

4.4.2 Flat Steel Workpieces—Half Immersion

Down-milling method is selected in the half immersion cutting. The flat half immersion cutting results are displayed in Figures 4.19 and 4.20. Figure 4.19 shows the result with the "plain" fuzzy controller without self-learning or direct tuning and Figure 4.20 shows the result obtained using double (both the vibration energy and coherence signals were used for the tuning) direct output tuning. It can be seen that the direct tuning slightly improved the responsiveness of the system.

4.4.3 Double Thin-walled Steel Workpieces

These results are plotted in Figures 4.14 through 4.16 corresponding to "plain" fuzzy control, single direct tuning and double direct tuning respectively. Of the three cases, the double direct tuning seems to be the best though some excessive feed and spindle speed adjustments were observed immediately after the initial cutting stage which causes some vibrations. This may be a result of a large weight (1.5) and a properly selected weight should correct this problem.

4.4.4 Single Thin-walled Steel Workpieces

Only two tests were conducted for this case, one was controlled using the "plain" fuzzy system (Figure 4.17) and the other with the double direct tuning (Figure 4.18). The direct tuning does not show obvious advantage because the vibration in this case was not as severe as compared to other previous cases.

In thin-wall cutting experiments the mean vibration energy could be lower than the threshold value. However, the spindle speed and the feed rate can be still very low because of the large value of coherence ratio which prevents further increasing spindle speed and feed rate. The experimental results of thin-wall cutting show that the coherence ratio is a reasonably effective tool for chatter detection.

4.4.5 Aluminium Workpiece

Figures 4.21 through 4.24 show the aluminium cutting results. The results for machining flat workpiece were in Figures 4.21 (depth of cut = 7 mm) and 4.22 (depth of cut = 9 mm). It is shown the vibration energy level was maintained below the threshold value (1.5) in both cases. The results for cutting double thin-walled worpiece were plotted in Figures 4.23 and 4.24. Again the vibration energy was maintained below the threshold level and the adjustment of feed and spindle speed was also reasonably smooth.

Although the maximum coherence ratio Ey_{max} and its change value Cy_{max} are not considered as the criterions on describing the cutting performances, they play significant roles in detecting and avoiding the chatters.

4.4.6 Experimental Results analysed in Frequency Domain

To further illustrate the chatter growing and suppression processes, some samples of the signals in frequency domain were also plotted in Figure 4.25 which was taken from a steel flat cutting data file (with rule base self-learning). The figure shows that the chatter growing process starting at time 4.5 seconds and reaches the threshold limit (0.8) of the coherence ratio at time 4.9 seconds. The suppression action was taken immediately and it took 0.5 second to suppress it (from 5.0 to 5.5 seconds).

The actual cutting time is different from the time shown in Figure 4.9 through 4.24. The time shown in the figures is approximately three times of the actual cutting time. The main reason is probably caused by insufficient computing power of the computer.

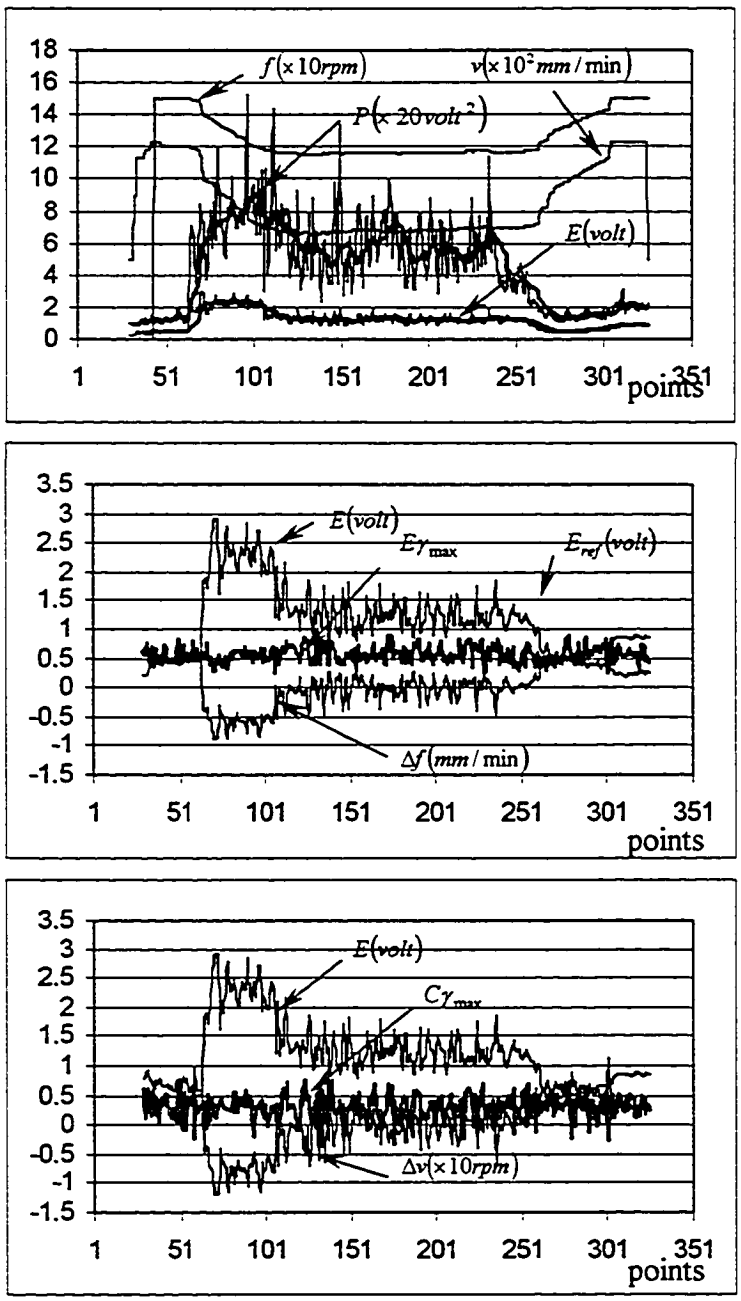

Figure 4.6 Experimental results using fuzzy logic control system (File:S_01, Steel, Flat Cut, Full Immersion)

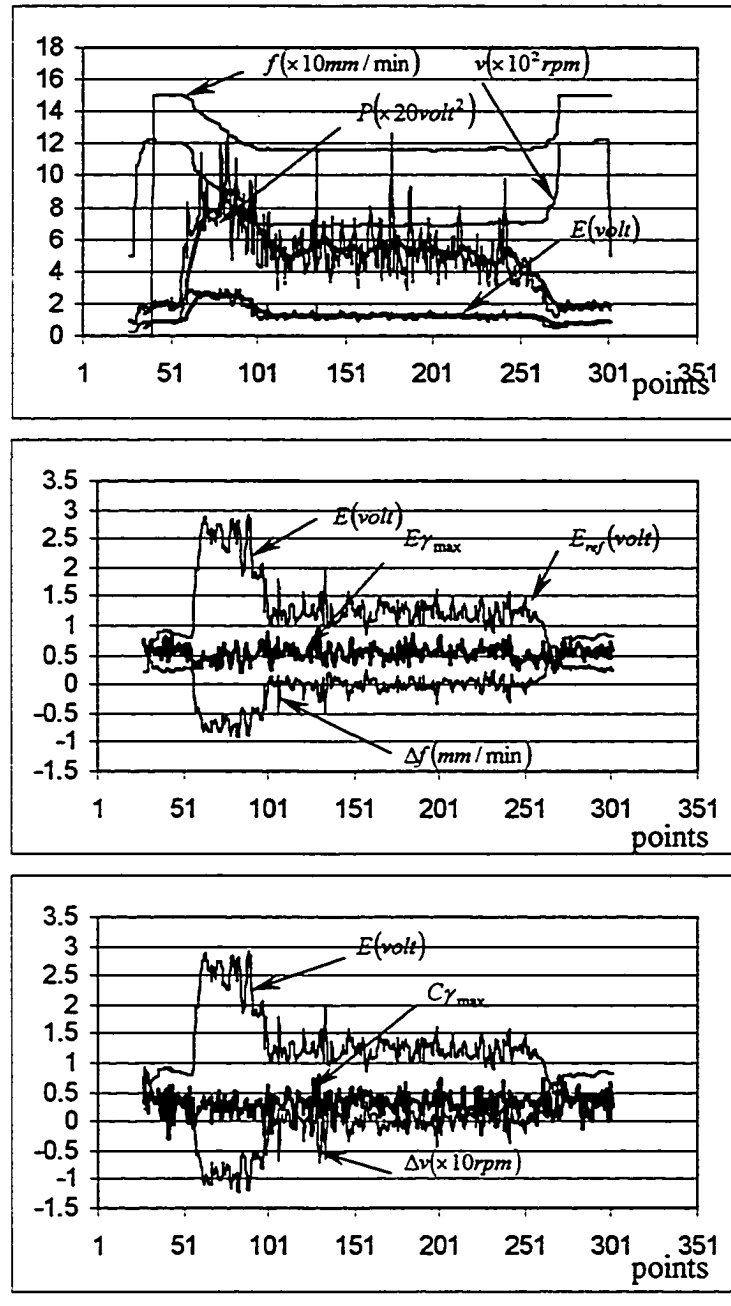

Figure 4.7 Experimental results using rule base self-learning algorithm (File:S_02, Weight=0.2, Steel, Flat Cutting, Full Immersion)

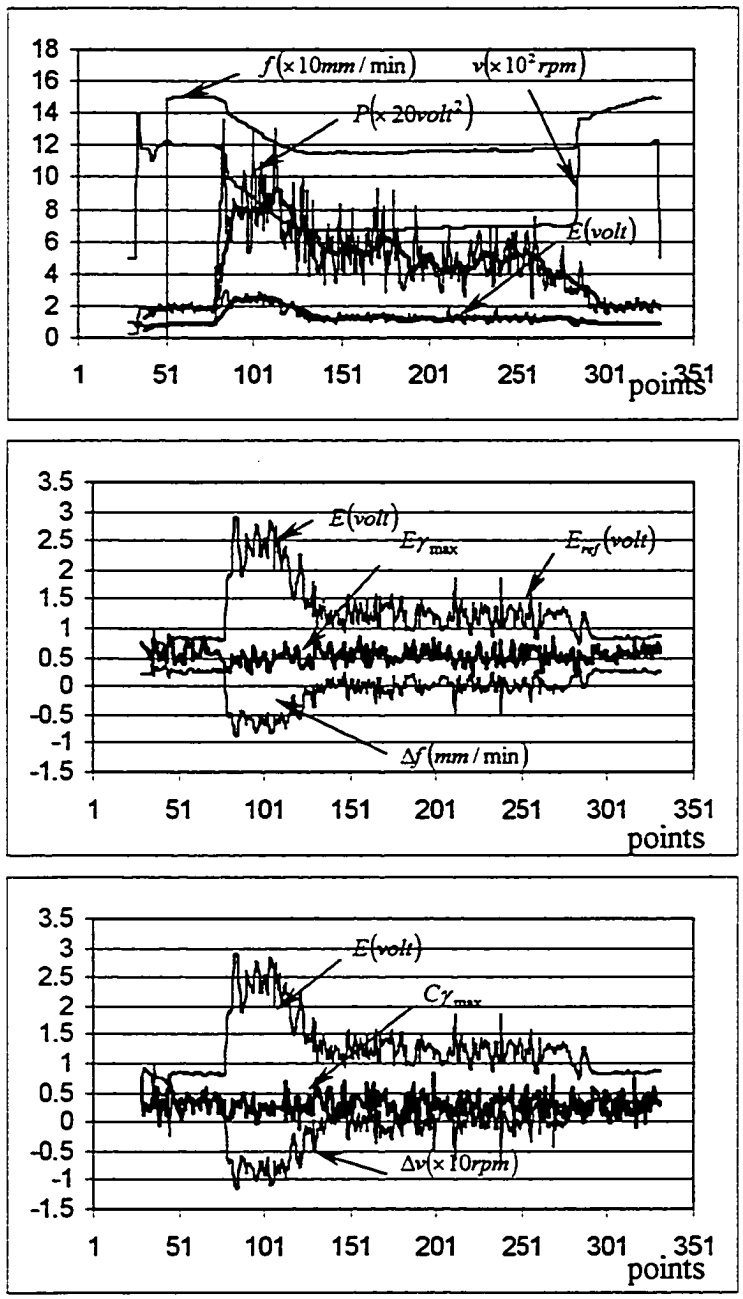

Figure 4.8 Experimental results using rule base self-learning algorithm (File:S_03, Weight=0.3, Steel, Flat Cutting, Full Immersion)

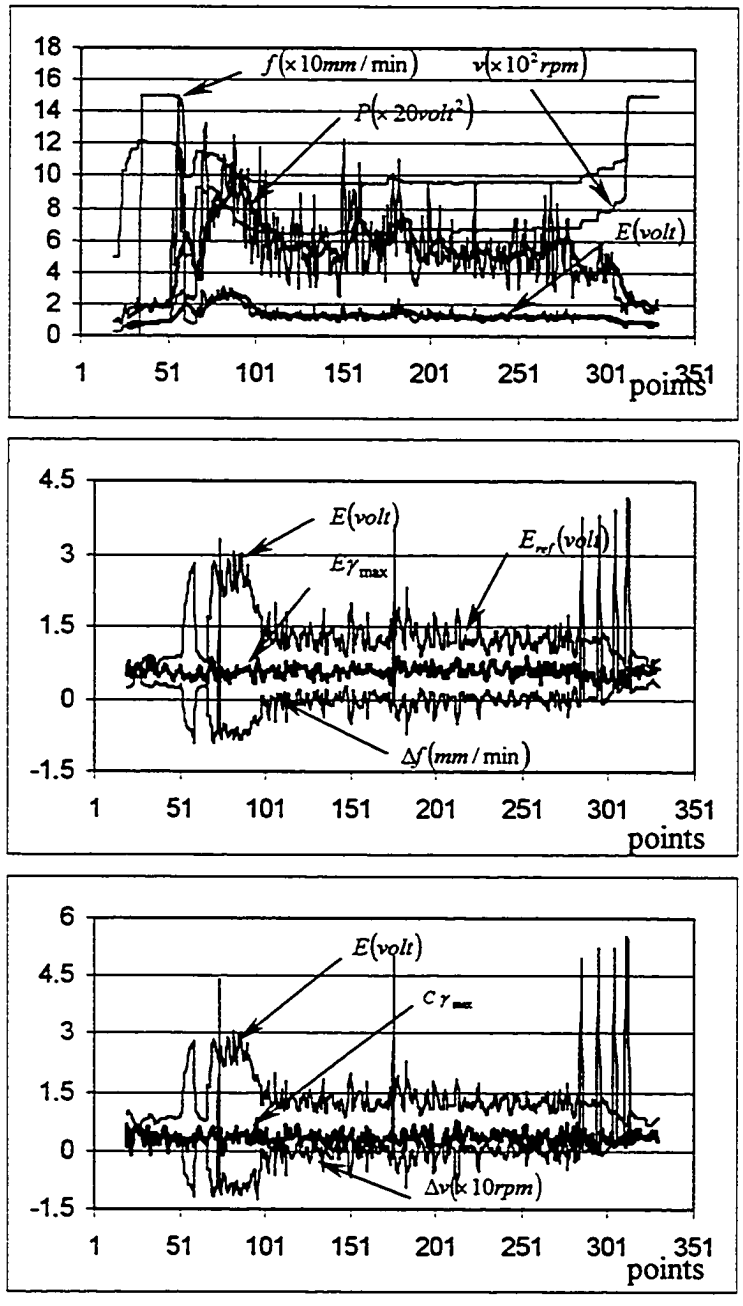

Figure 4.9 Experimental results using rule base self-learning algorithm (File:S_04, Weight=0.4, Steel, Flat Cutting, Full Immersion)

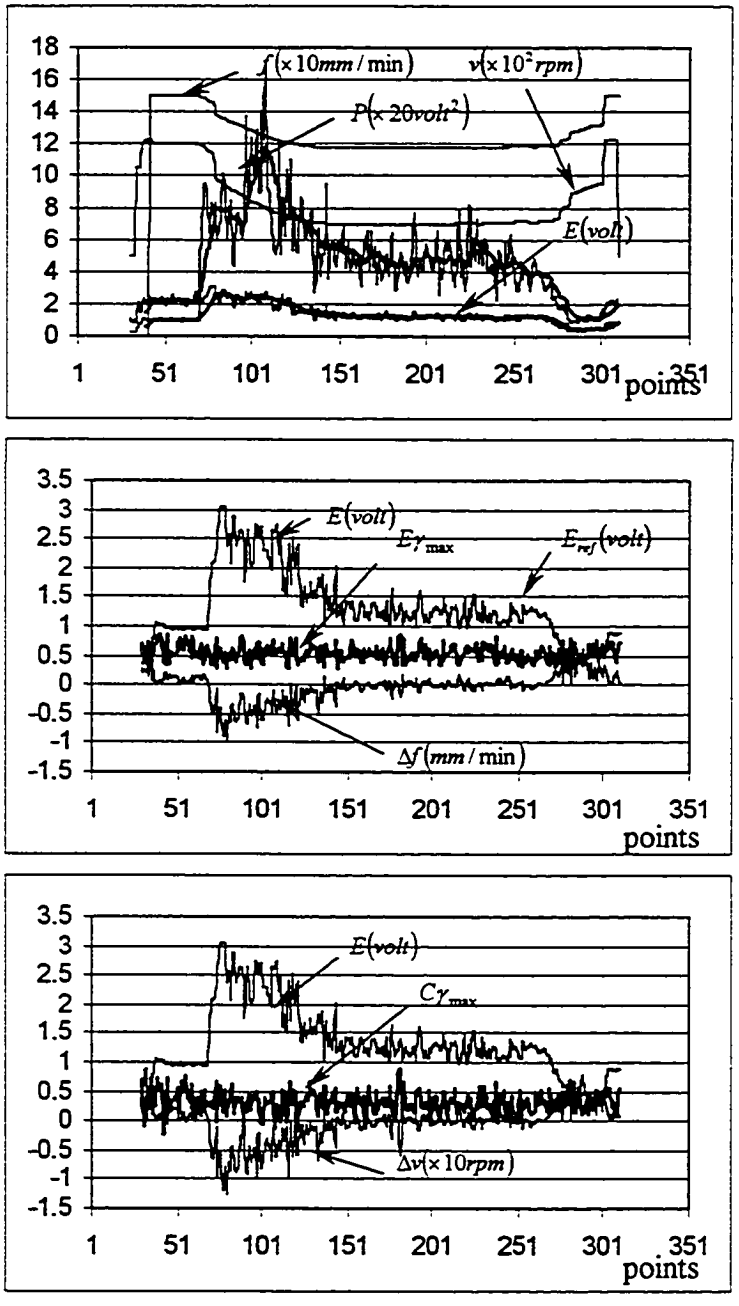

Figure 4.10 Experimental results using single direct output tuning algorithm (File:S_05, Weight=0.5, Steel, Flat Cutting, Full Immersion)

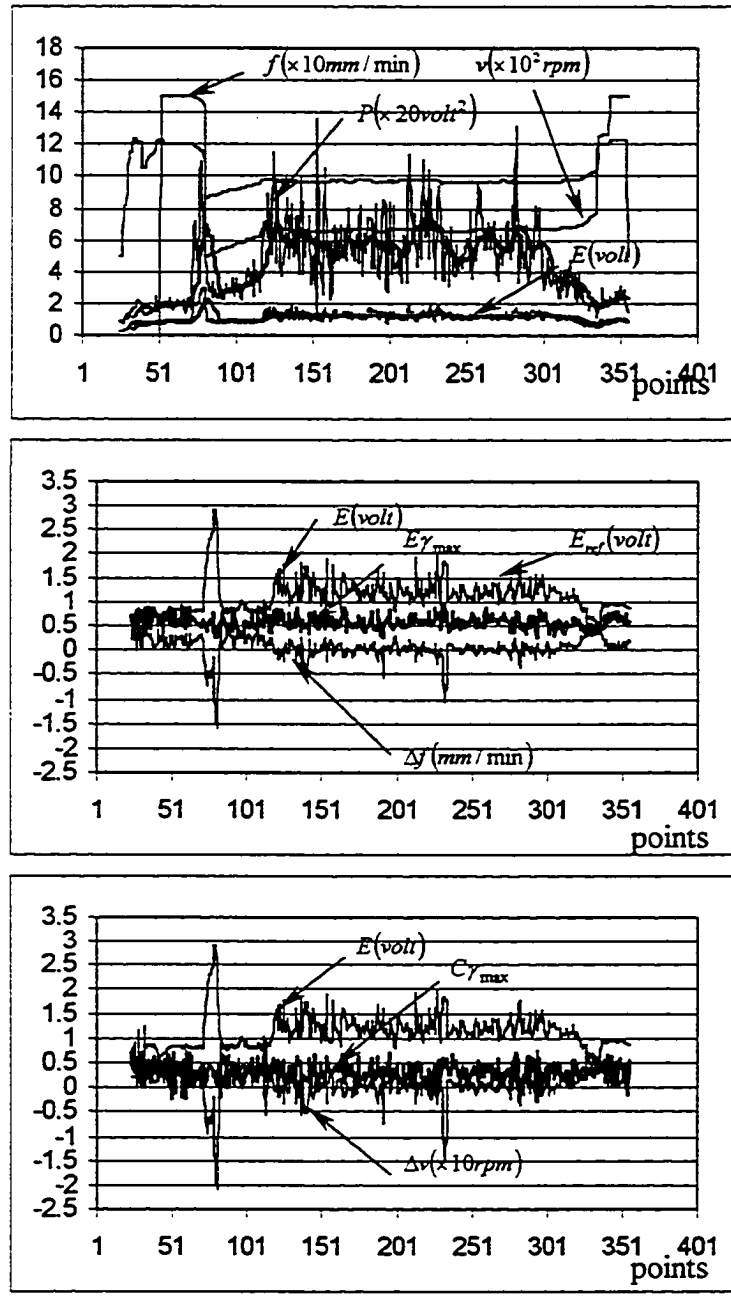

Figure 4.11 Experimental results using single direct output tuning algorithm (File:S_06, Weight=0.7, Steel, Flat Cutting, Full Immersion)

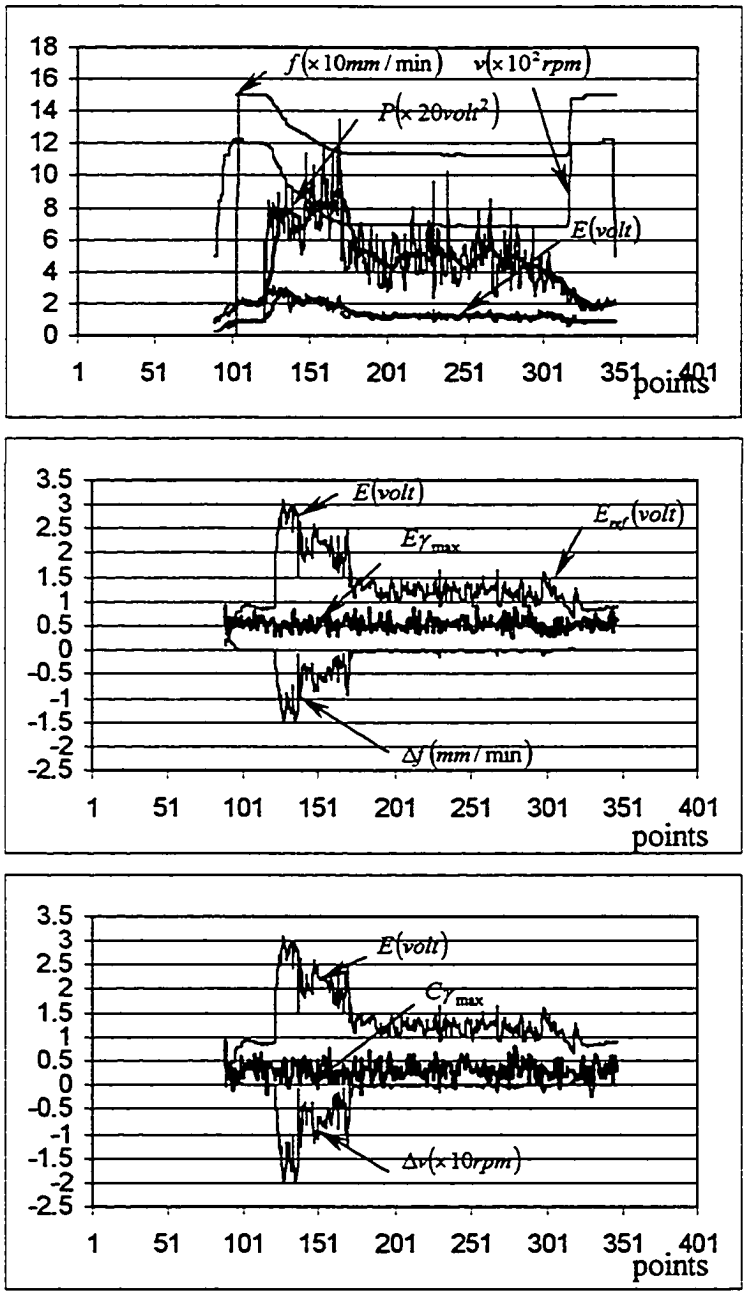

Figure 4.12 Experimental results using double direct output tuning algorithm (File:S_07, Weight=1.0, Steel, Flat Cutting, Full Immersion)

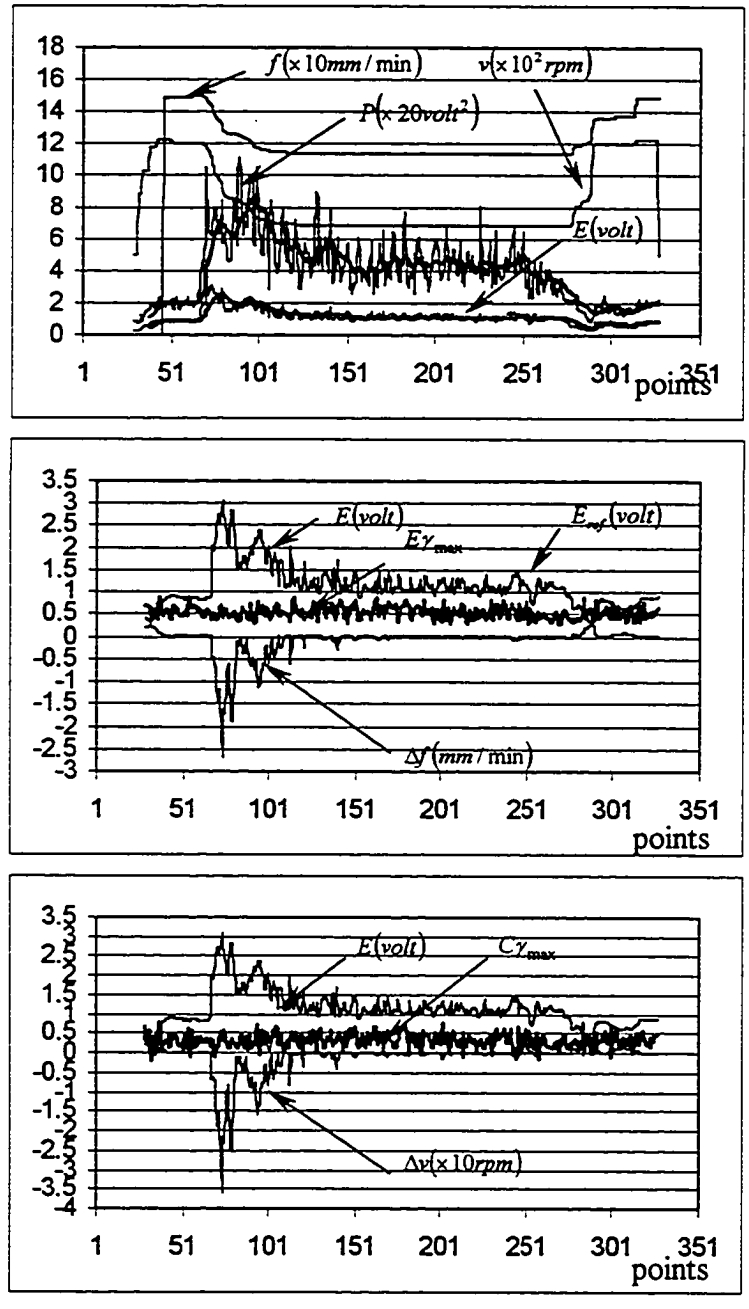

Figure 4.13 Experimental results using double direct output tuning algorithm (File:S_08, Weight=1.5, Steel, Flat Cutting, Full Immersion)

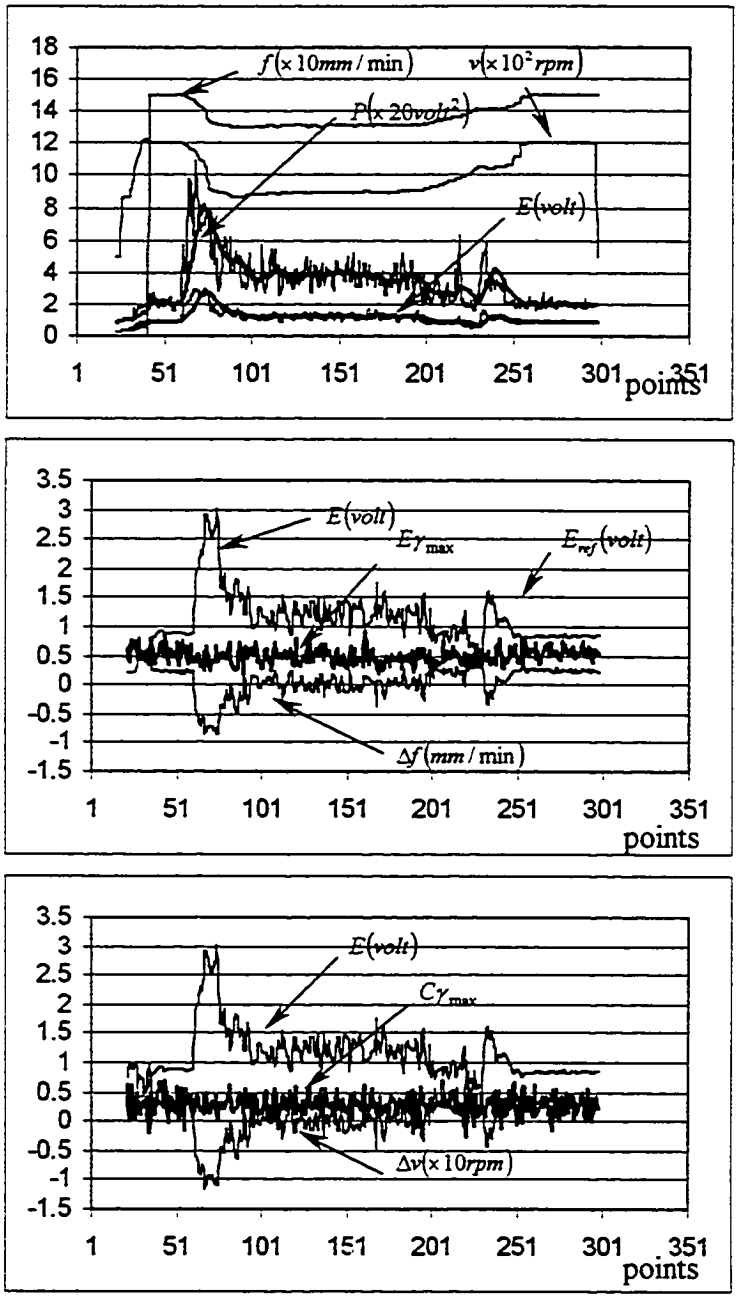

Figure 4.14 Experimental results using fuzzy logic control system (File:S_09, Steel, Double Thin-wall Cutting, 0-5mm, Full Immersion)

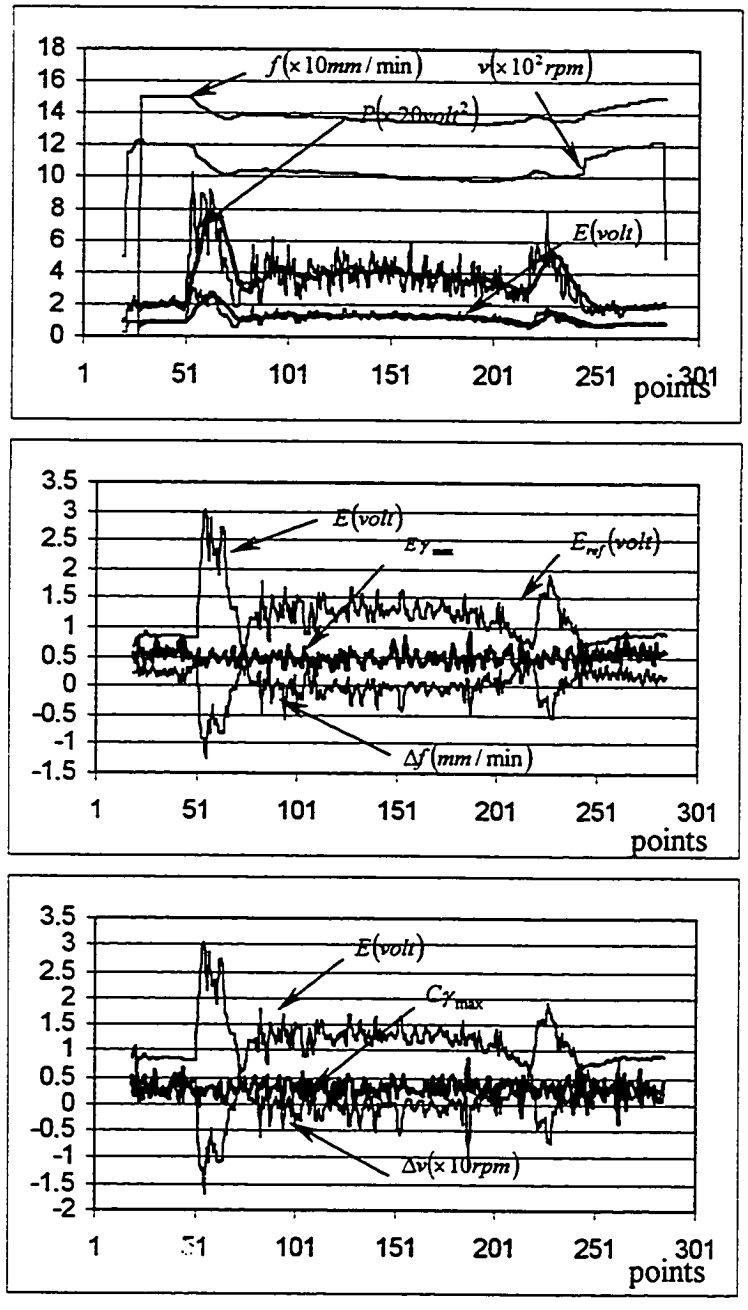

Figure 4.15 Experimental results using single direct output tuning algorithm (File:S_10, Weight=0.7, Steel, Double Thin-wall Cutting, 5-10mm, Full Immersion)

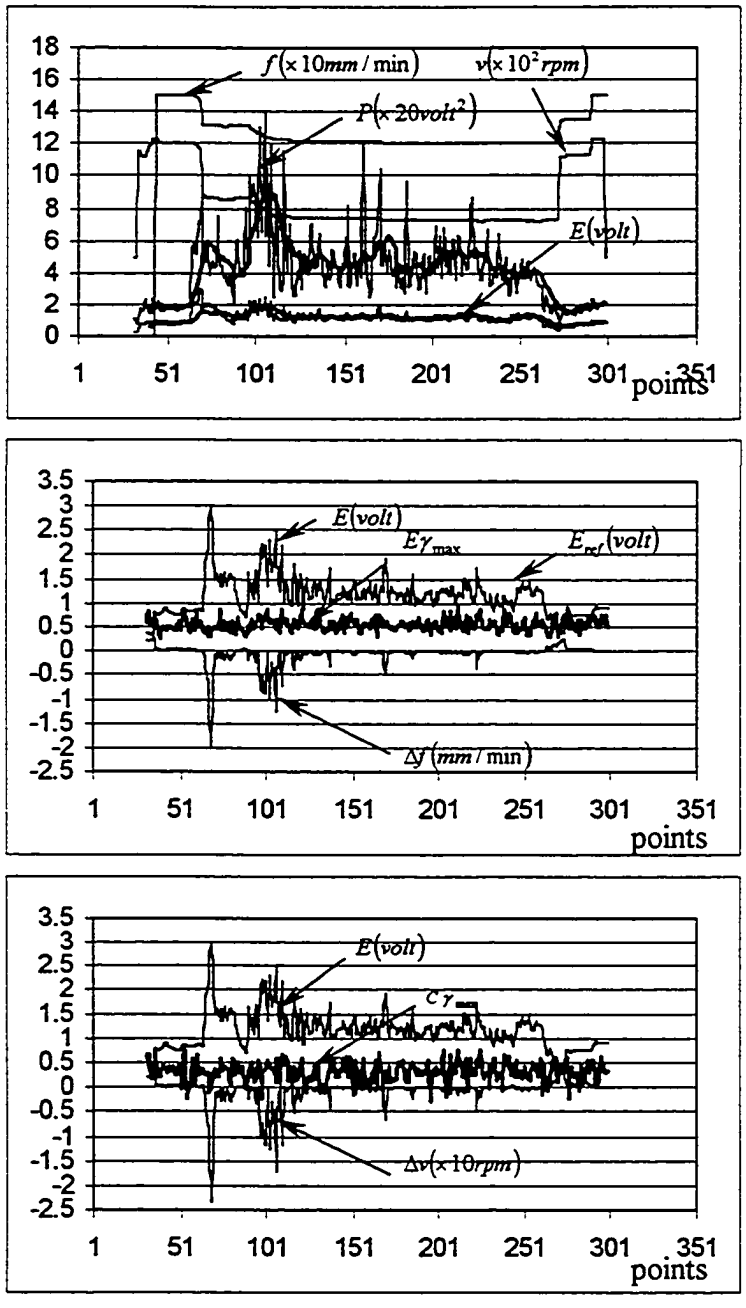

Figure 4.16 Experimental results using double direct output tuning algorithm (File:S_11, Weight=1.5, Steel, Double Thin-wall Cutting, 10-15mm, Full Immersion)

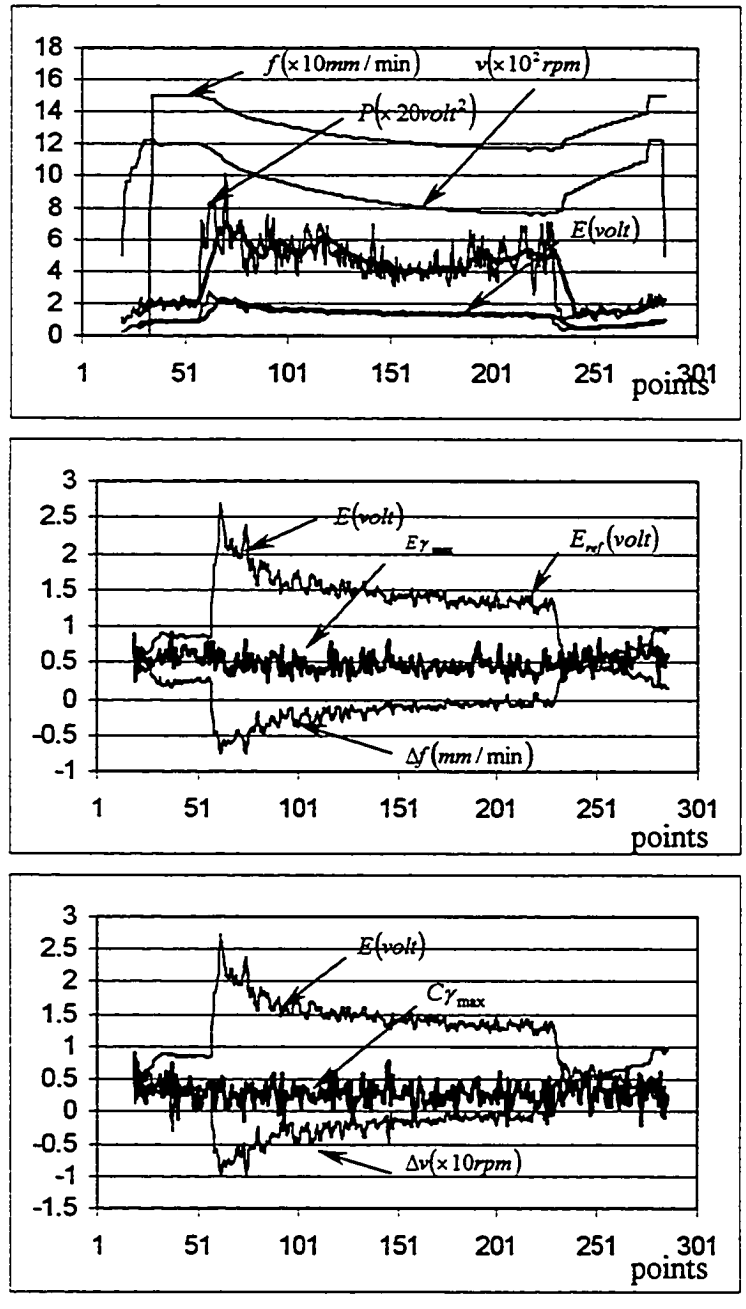

Figure 4.17 Experimental results using fuzzy logic control system (File:S_12, Steel, Single Thin-wall Cutting, 13-8mm)

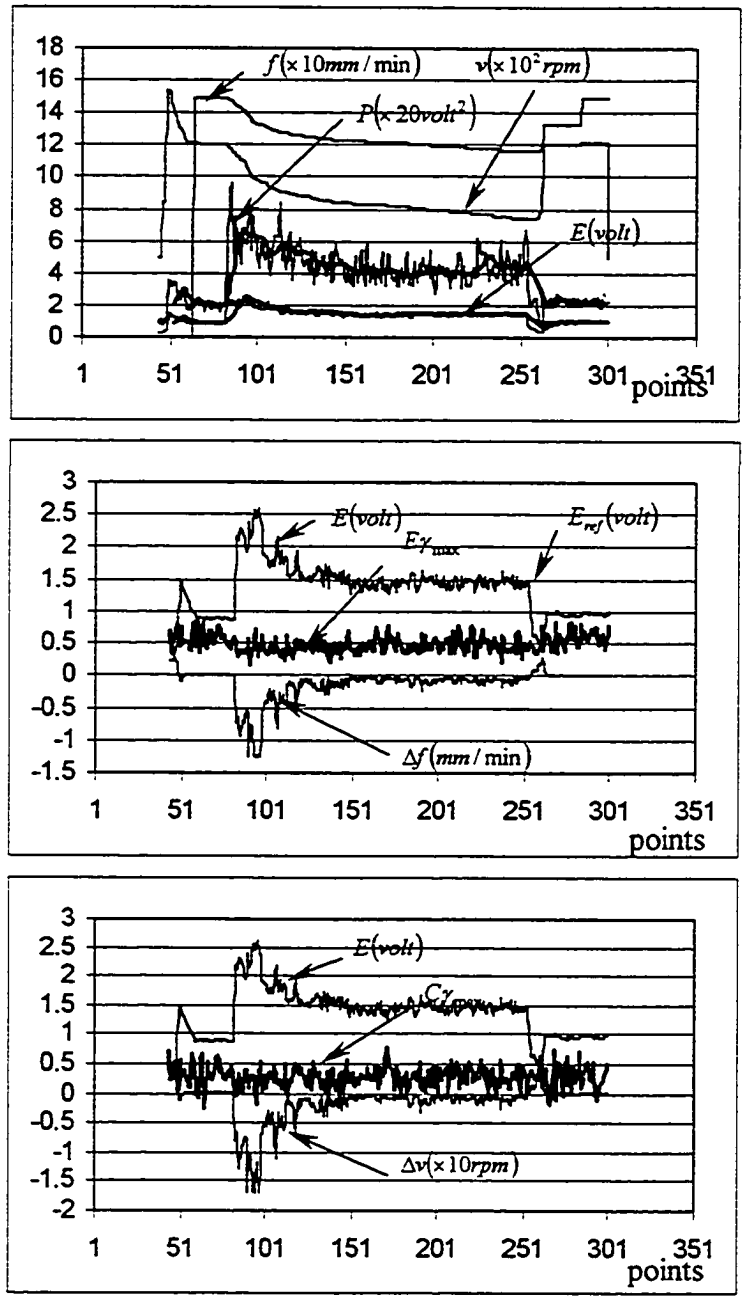

Figure 4.18 Experimental results using double direct output tuning algorithm (File:S_13, Weight=1.5, Steel, Single Thin-wall Cutting, 8-3mm)

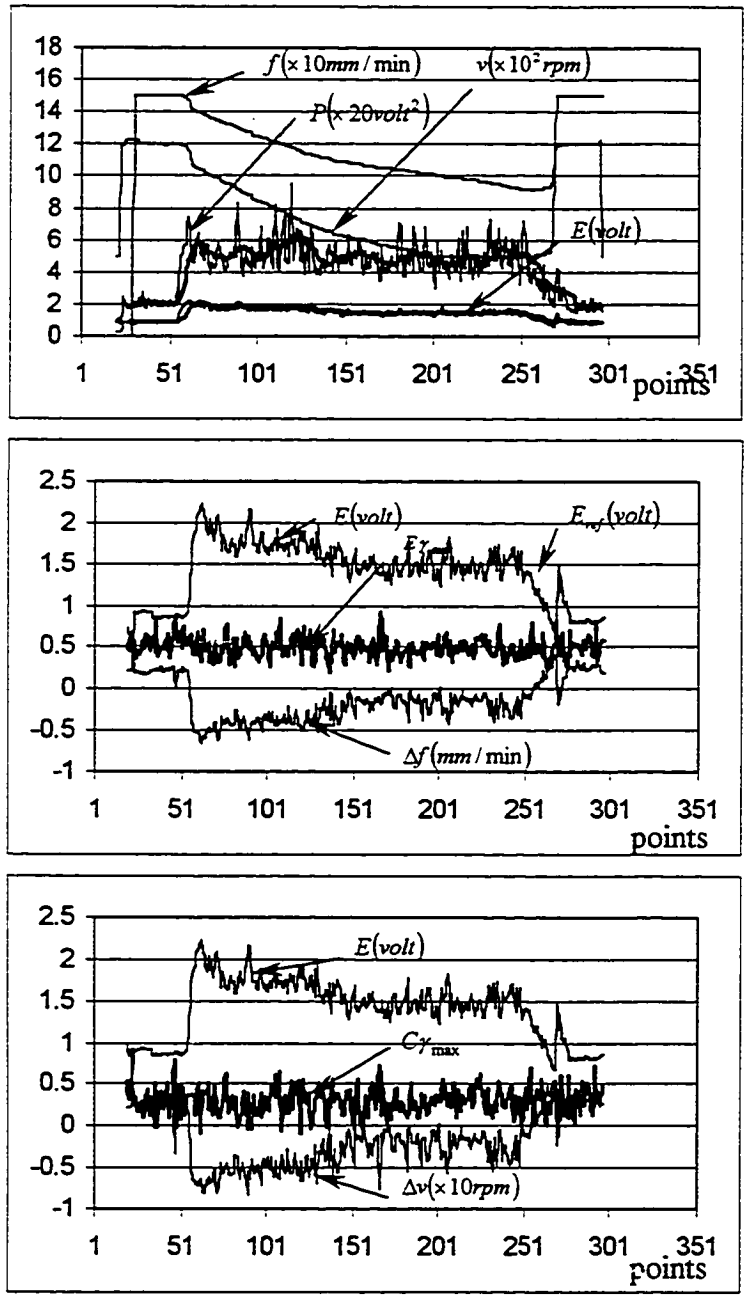

Figure 4.19 Experimental results using fuzzy logic control system (File:S_14, Steel, Flat Up Cutting, Half Immersion)

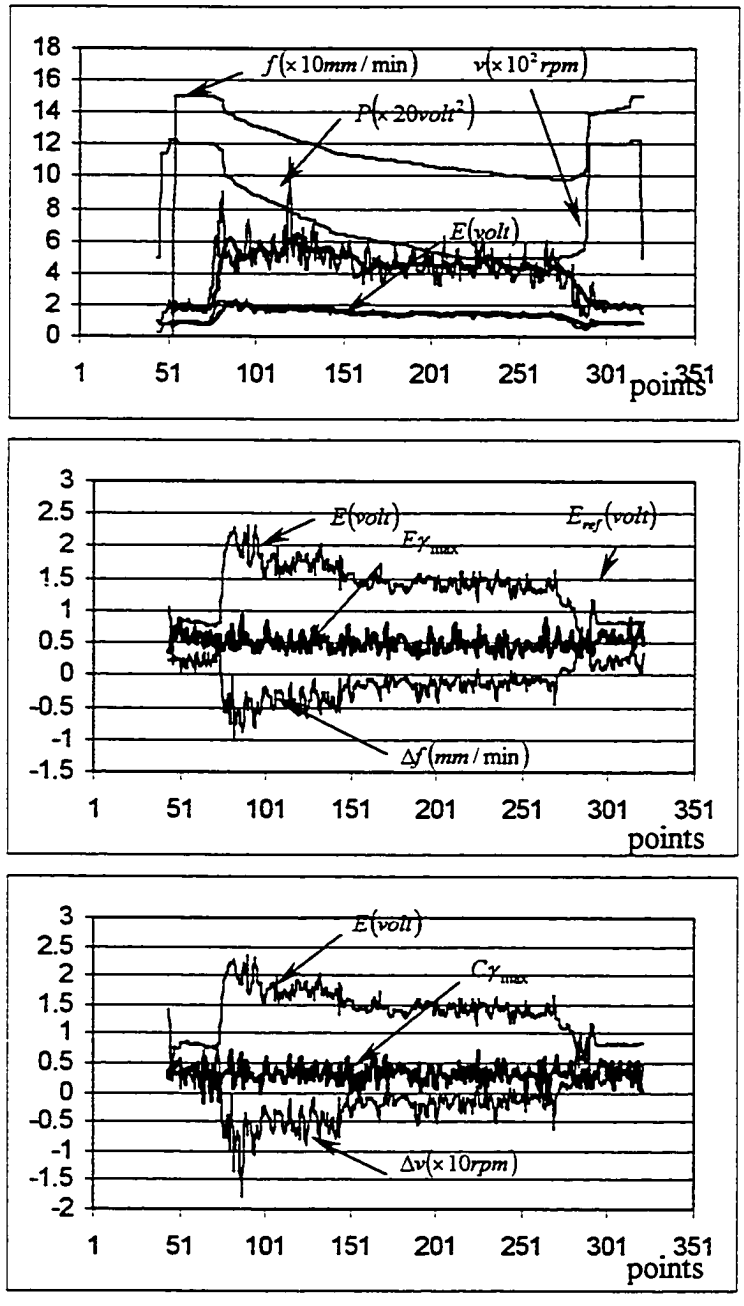

Figure 4.20 Experimental results using double direct output tuning algorithm (File:S_15, Weight=1.5, Steel, Flat Up Cutting, Half Immersion)

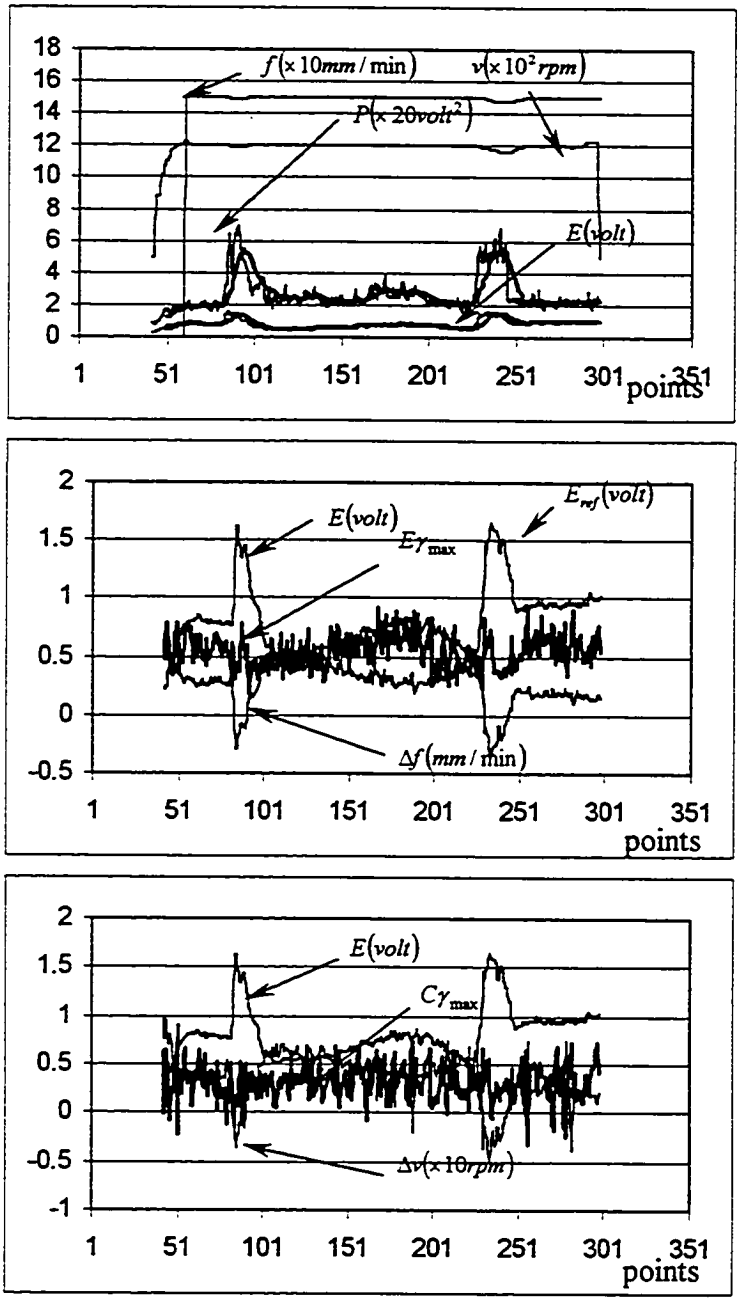

Figure 4.21 Experimental results using fuzzy logic control system (File:A_01, Aluminium, Flat Cutting, Depth=7mm, Full Immersion)

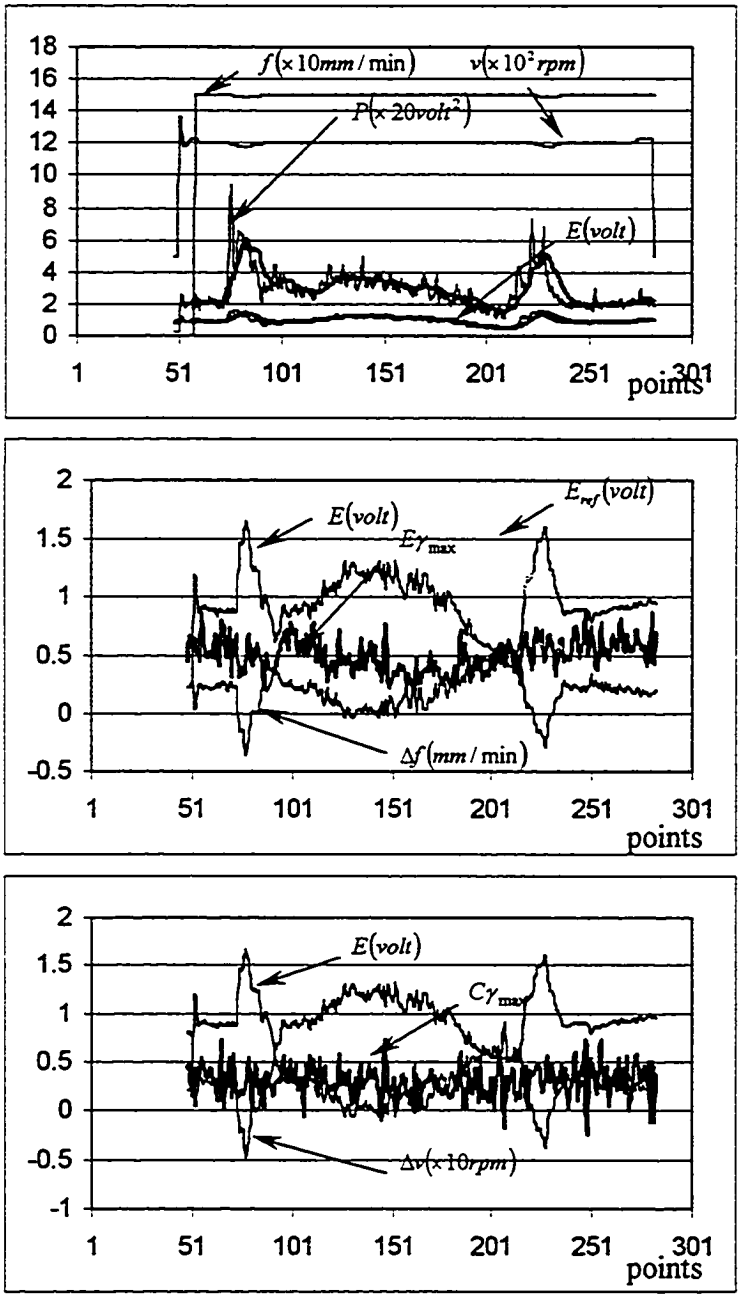

Figure 4.22 Experimental results using fuzzy logic control system (File:A_02, Aluminium, Flat Cutting, Depth=9mm, Full Immersion)

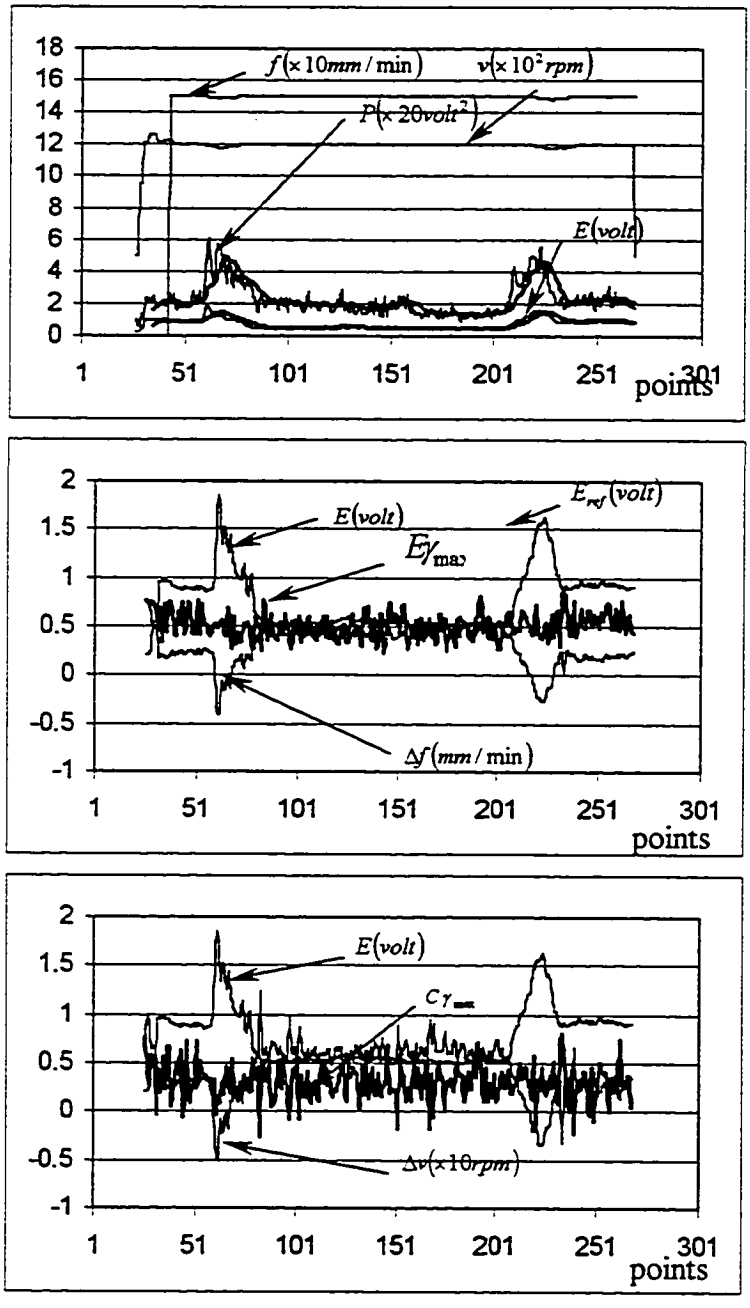

Figure 4.23 Experimental results using fuzzy logic control system (File:A_03, Aluminium, Double Thin-wall, Depth=0-5mm)

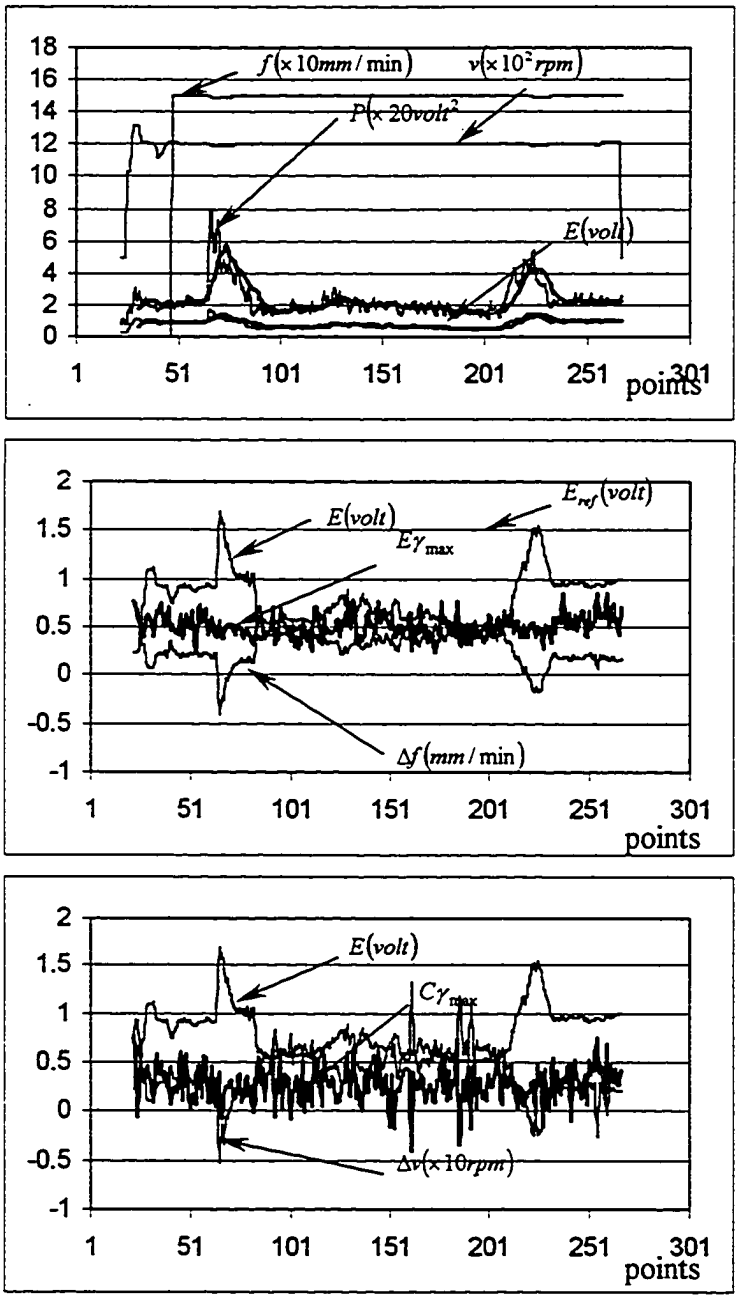

Figure 4.24 Experimental results using double direct output tuning algorithm (File:A_04, Aluminium, Double Thin-wall, Depth=5-10mm)

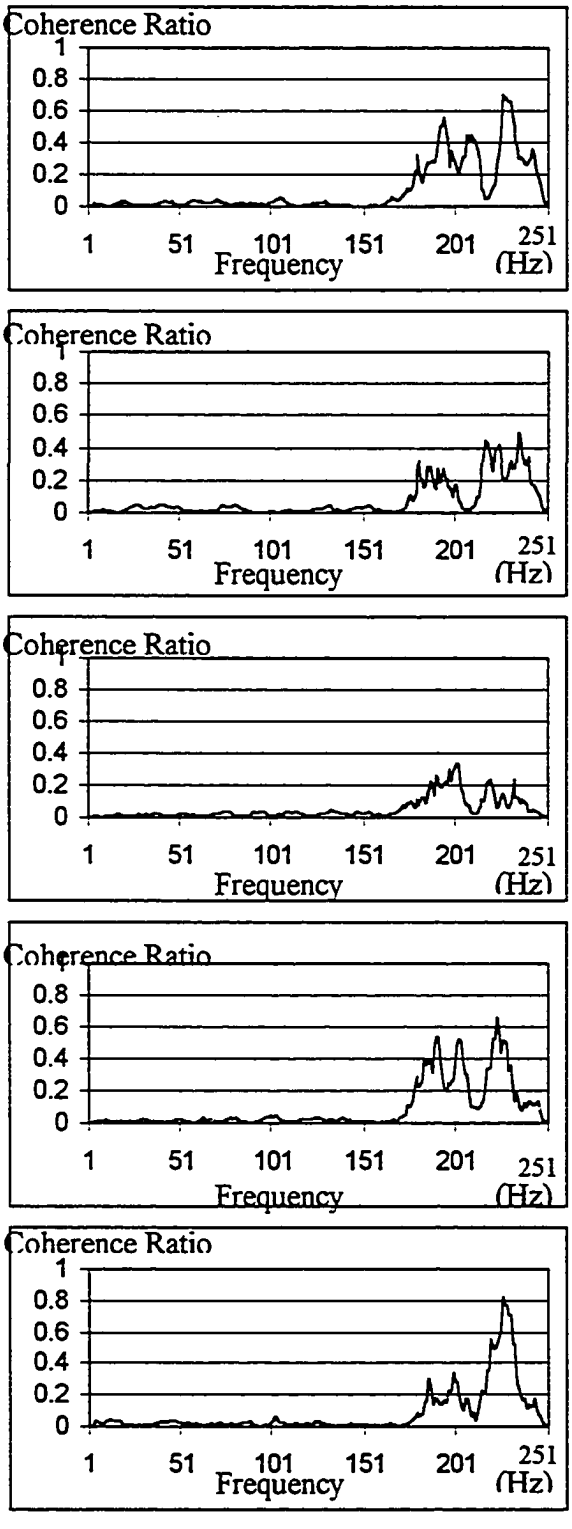

Figure 4-25a Chatter suppression with self-learning algorithm (Time:4.5 sec to 4.9 sec)

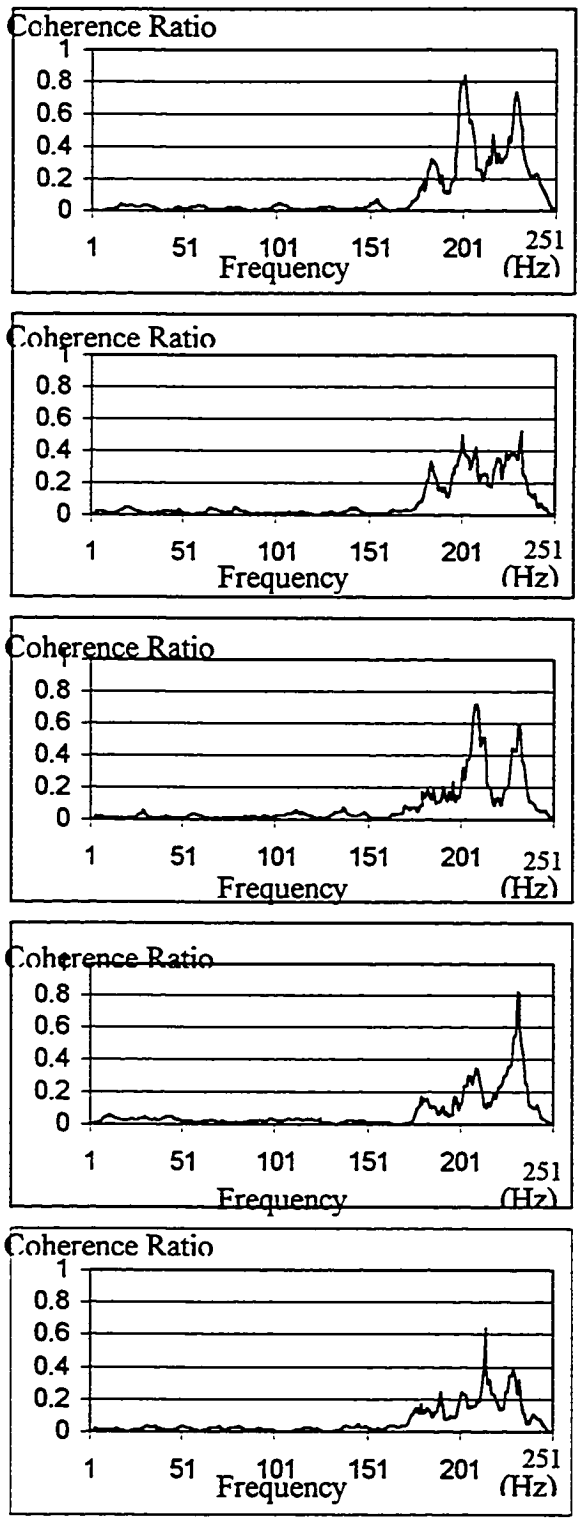

Figure 4-25b Chatter suppression with self-learning algorithm (Time:5.0 sec to 5.5 sec)

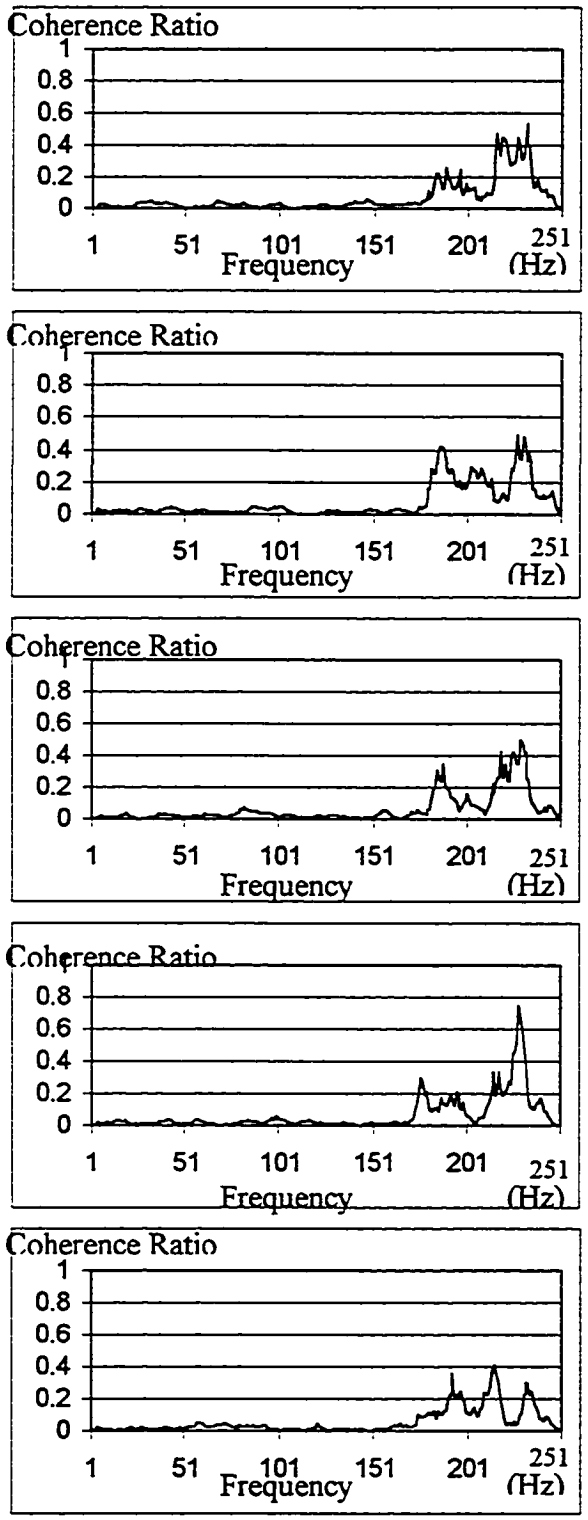

Figure 4-25c Chatter suppression with self-learning algorithm (Time:5.6 sec to 6.0 sec)

Chapter 5

Conclusion and Future Research

5.1 Conclusion

A fuzzy logic control system for chatter detection and suppression has been developed, which features the following:

1. Joint application of the mean vibration energy and coherence function for chatter detection. The experimental results show that the coherence function is sensitive to chatter but often over reactive. The use of mean vibration energy will complement this problem.
2. The use of a rule base self-learning algorithm to improve the adaptability of the fuzzy system and the use of and a direct output tuning algorithm to improve the responsiveness of the system.
3. Simultaneous adjustment of spindle speed and feed rate to enhance the chatter suppression process.

5.2 Future Research

Further studies may be carried out in the following directions:

1. Enhance the system performance for initial chatter suppression. It was observed that the system is less effective for suppressing the chatter in the initial cutting stage. The cause of such ineffectiveness remains to be investigated.
2. Investigate on-line chatter prediction. Our experiments show that the coherence function value often reaches a high value before the onset of chatter which indicates that the coherence function could be used for chatter prediction. Though some

preliminary analysis has been presented in the thesis, the application of the result is to be carried out in the future.

3. Develop an aggressive chatter suppression mechanism. Though the adjustment of feed and spindle speed was done in both directions (increase and decrease) in this study this was done in the near neighbourhood of a stability zone, which may not necessarily be the most productive one. To further improve the material removal rate, it is necessary to make feed and speed adjustment in a more productive stability zone. This may be done in conjunction with the study of stability lobes.

References

1. Al-Habaibeh, A., and Gindy, N., 2001, Self-learning Algorithm for Automated Design of Condition Monitoring Systems for Milling Operations, *The International Journal of Advanced Manufacturing Technology*, Vol.18, pp.448-459.

2. Altintas, Y., 1992, Prediction of Cutting Forces and Tool Breakage in Milling from Feed Drive Current Measurements, *Transaction of the ASME*, Vol.114, Nov., pp.386-392.

3. Altintas, Y., Shamoto, E., Lee P., and Budak, E., 1999, Analytical Prediction of Stability Lobes in Ball End Milling, *Transaction of the ASME*, Vol.121. Nov., pp.586-592.

4. Beggan, C., Woulfe, M., Young, P., and Byrne, G., 1999, Using Acoustic Emission to Predict Surface Quality, *The International Journal of Advanced Manufacturing Technology*, Vol.15, pp.732-742.

5. Bendat, J.S., and Piersol, A.G., 1980, Engineering Application of Correlation and Spectral Analysis, John Wiley, New York.

6. Brun-Picard, D., and Moraru, G., 2001, An Approach for the Control of the Self-vibrating Drilling Process, *Proceedings of the 3rd International Conference On Metal Cutting and High Speed Machining, June 27-29, Metz, France*, pp.163-168.

7. Budak,E., and Altintas, Y., 1995, Analytical Prediction of Chatter Stability in Milling: Part I General Formulation, *Proceedings of the ASME Dynamic Systems and Control Division*, Vol. 57-1,pp.545-556.

8. Budak,E., and Altintas, Y., 1995, Analytical Prediction of Chatter Stability in Milling: Part II Application of the General Formulation to Common Milling Systems, *Proceedings of the ASME Dynamic Systems and Control Division*, Vol. 57-1, pp.557-565.

9. Chang, Y.-F., and Chen, B.-S., 1998, The VSS Controller Design and Implementation for The Constant Turning Force Adaptive Control System, *International Journal of Machine Tools and Manufacturing*. Vol. 28, No.4, pp.373-387.

10. Choi, D., Kwon, W.T., and Chu, C.N., 1999, Real-time Monitoring of Tool Fracture in Turning Using Sensor Fusion, *The International Journal of Advanced Manufacturing Technology*, Vol.15, pp.305-310.

11. Choudhury, S.K., Goudimenko, N.N., and Kudinov, V.A., 1997, On-line Control of Machine Tool Vibration in Turning, *International Journal of Machine Tools and Manufacturing*. Vol. 37, No.6, pp.801-811.

12. Choudhury, S.K., Jain, V.K., and Rama Rao, Ch.V.V., 1999, On-line Monitoring of Tool Wear in Turning Using a Neural Network, *International Journal of Machine Tools and Manufacturing*, Vol.39, pp.489-504.

13. Curocak, H., November 1998, User-friendly Method for Tuning Fuzzy Logic Controllers, *Part of the SPIE Conference on Sensors and Controls for Intelligent Machining and Agile Manufacturing, Boston, Massachusetts.*

14. Dong, W., Joe, Y.H.Au, and Mardapittas, A., 1992, Machine Tool Chatter Monitoring by Coherence Analysis, *Int.J.Prod.Res.*,Vol.30, No.8, pp.1901-1924.

15. Driankov, D., Hellendoorn, H., and Reinfrank M., 1995, An Introduction to Fuzzy Control, Second, Revised Edition, Springer

16. Du, R.X., Elbestaw, M.A., and Li, S., 1992, Tool Condition Monitoring in Turning Using Fuzzy Set Theory, *International Journal of Machine Tools and Manufacturing*, Vol.32, No.6, pp.781-796.

17. Elbestawi, M.A., Ismail, F., Du, R., and Ullagaddi, B.C., 1994, Modeling Machining Dynamics Including Damping in the Tool-Workpiece Interface, *ASME, J. Ind.*, Vol. 116,pp.435-439.

18. Endres, W.J., DeVor, R.E., and Kapoor, S.G., 1995, A Dual Mechanism Approach to the Prediction of Machining Forces, Part 1, *ASME, J. Ind.* Vol. 117,pp.526-533.

19. Endres, W.J., DeVor, R.E., and Kapoor, S.G., 1995, A Dual Mechanism Approach to the Prediction of Machining Forces, Part 2 *ASME, J. Ind.* Vol. 117,pp.534-541.

20. Esterling, D. M., Buckner, G. D., and Caulfield, F. D., 2001, Integrated Chatter Prediction and Avoidance System, *Proceedings of the 3rd International Conference On Metal Cutting and High Speed Machining, June 27-29, Metz, France.*

21. Everson, C.E., and Hoessein Cheraghi, S., 1999, The Application of Acoustic Emission for Precision Drilling Process Monitoring, *International Journal of Machine Tools and Manufacturing,* Vol.39, pp.371-387.

22. Fdhi, E., and Hoshi, T., 2001, Mechanism and Prevention of High Frequency Chatter in Fine Boring, *The 3rd International Conference On Metal Cutting and High Speed Machining, June 27-29, Metz, France.*

23. Furness, R.J., Galip, U.A., and Wu, C.L., June 1993, Feed, Speed, and Torque Controllers for Drilling, *Proceedings of the America Control Conference, San Francisco, California*

24. Gehin, D., and Girot, F., 2001, Study of Radial Vibrations in High Speed Drilling, *Proceedings of the 3rd International Conference On Metal Cutting and High Speed Machining, June 27-29, Metz, France.*

25. Genta, G., 1999, Vibration of structures and Machines, Practical Aspects, Springer.

26. Gradisek, J., Govekar, E., Grabec, I., Mehnen, J., Kalveran, M., and Weinert, K., 2001, Analysis of High-speed Milling Dynamics: Chatter vs. Chatter-free Cutting,

Proceedings of the 3rd International Conference On Metal Cutting and High Speed Machining, June 27-29, Metz, France.

27. Gu, F., Kapoor, S.G., DeVor, R.E., and Bandopadhyay, P., 1997, An Enhanced Cutting Force Model for Face-Milling with Variable Cutter Feed Motion and Complex Workpiece Geometry, *ASME J. Manuf. Sci.Eng.*,119,pp.467-475.

28. Hadi, Y., and Ebrahimi, M., 2001, Effect of Sinusoidal and Quasi-mean Cutting Forces on the Occurrence of Chatter in End Milling Process, *Proceedings of the 3rd International Conference On Metal Cutting and High Speed Machining, June 27-29, Metz, France.*

29. Haykin, S., Adaptive Filter Theory, Third Edition, 1996, Prentice Hall

30. Schildt, H., 1992, Turbo C/C++: The Complete Reference, Second Edition, Osborne McGraw-Hill.

31. Hsu, Pau-Lo, and Fann, Wei-Ru, 1996, Fuzzy Adaptive Control of Machining Processes With a Self-learning Algorithm, *Transactions of the ASME*, Vol.188. Nov., pp.522-531.

32. Ibrahim Nur Tansel, 1994, Identification of the Prefailure Phase in Microdrilling Operations Using Multiple Sensors, *International Journal of Machine Tools and Manufacturing*, Vol.34, No.3, pp.351-364.

33. Inasaki, I., 1999, Sensor Fusion for Monitoring and Controlling Grinding Processes, *The International Journal of Advanced Manufacturing Technology*, Vol.15, pp.730-736.

34. Inman, Daniel J., Engineering Vibration, 1994, Prentice Hall, Englewood Cliffs, N.J.

35. Ismail, F., and Kubica, E.G., 1995, Active Suppression of Chatter in Peripheral Milling, Part 1: A Statistical Indicator to Evaluate the Spindle Speed Modulation Method, *The International Journal of Advanced Manufacturing Technology*, Vol.10, pp.299-310.

36. Jemielniak, K., 1999, Commercial Tool Condition Monitoring Systems, *The International Journal of Advanced Manufacturing Technology*, Vol.15, pp.711-721.

37. Jensen, S.A., and Shin, Y.C., November 1999, Stability Analysis in Face Milling Operations, Part 1: Theory of Stability Lobe Prediction, *Transactions of the ASME*, Vol.121, pp.600-605.

38. Jensen, S.A., and Shin, Y.C., November 1999, Stability Analysis in Face Milling Operations, Part 2: Experimental Validation and Influencing Factors, *Transactions of the ASME*, Vol.121, pp.606-614.

39. Kalinski, Krzysztof J., 2001, Chatter Vibration Surveillance by the Spindle Speed Optimal Control, *Proceedings of the 3rd International Conference On Metal Cutting and High Speed Machining, June 27-29, Metz, France*, pp.237-240.

40. Kalinski, K.J., Kucharski, T., and Sawiak, S., 2001, A new Method for Suppression of Chatter Vibration by Programmed Spindle Speed Control, *Proceedings of the 3rd International Conference On Metal Cutting and High Speed Machining, June 27-29, Metz, France.*

41. Kim, M.K., Cho, M.W., and Kim, K., 1994, Application of the Fuzzy Control Strategy to Adaptive Force Control of Non-minimum Phase End Milling Operations, *International Journal of Machine Tools and Manufacturing*, Vol.34, No.5, pp.677-696.

42. Kondo, E., and Kawagoishi, N., 2001, Feasibility Study on Criteria of detecting Mode-coupling Chatter, *Proceedings of the 3rd International Conference On Metal Cutting and High Speed Machining, June 27-29, Metz, France*, pp.131-134.

43. Kwon, W.-T., and Ehmann, K. F., 1994, Tool Wear Monitoring By Using the Imaginary Part of the Transfer Function of the Cutting Dynamics, *International Journal of Machine Tools and Manufacturing*, Vol.34, No.3, pp.393-406.

44. Lee, A.-C., and Liu, C.-S., 1991, Analysis of Chatter Vibration in the End Milling Process, *International Journal of Machine Tools and Manufacturing*, Vol.31, No.4, pp.471-479.

45. Lee, B.Y., and Tarng, Y.S., 1999, Application of the Discrete Wavelet Transform to the Monitoring of Tool Failure in End Milling Using the Spindle Motor Current, *The International Journal of Advanced Manufacturing Technology*, Vol.15, pp.238-243.

46. Li, X., 1999, On-line Detection of the Breakage of Small Diameter Drills Using Current Signature Wavelet Transform, *International Journal of Machine Tools and Manufacturing*, Vol.39, pp.157-164.

47. Li, X., Dong, S., and Venuvinod, P.K., 2000, Hybrid Learning for Tool Wear Monitoring, *The International Journal of Advanced Manufacturing Technology*, Vol.16, pp.303-307.

48. Li, X.Q., Wong, Y.S., and Nee, A.Y.C., 1997, Tool Wear and Chatter Detection Using the Coherence Function of Two Crossed Accelerations, *International Journal of Machine Tools and Manufacturing*. Vol.37, No.4, pp.425-435.

49. Liao, Y.S., and Young, Y.C., 1996, A New On-line Spindle Speed Regulation Strategy for Chatter Control, *International Journal of Machine Tools and Manufacturing*. Vol. 36, No.5, pp.651-660.

50. Liu, Y., Cheng, T., and Zuo, L., 2001, Adaptive Control Constraint of Manufacturing Processes, *The International Journal of Advanced Manufacturing Technology*, Vol.17, pp.720-726.

51. Liu, Y., Cheng, T., Zuo, L., and Wang, C., 2000, Development of an Open Parallel Intelligent CNC Milling System, Part 2: Milling Experiment, *The International Journal of Advanced Manufacturing Technology*, Vol.16, pp.542-546.

52. Liu,Y., Zuo, L., Cheng T., and Wang, C., 2000, Development of an Open Parallel Intelligent CNC Milling System, Part 1: System Structure, *The International Journal of Advanced Manufacturing Technology*, Vol.16, pp.537-541.

53. Liang, M., 2001, Fuzzy Control and Chatter Suppression, Research Notes.

54. Minis, I., and Tembo, A., 1993, Experimental Verification of a Stability Theory for Periodic Cutting Operations, *ASME, J. Ind.*, Vol.115,pp.9-14.

55. Minis, I., and Yanushevshy,R., 1993, A New Theoretical Approach for Prediction of Stability Lobes in Milling, *ASME, J. Ind.*,Vol.115,pp.1-8.

56. National Instrument, November 1992 ed., LabVIEW for Windows: Graphical Programming for Instrumentation, National Instrument.

57. National Instrument, 1998, LabWindows/CVI 5.0 user Manual, National Instrument.

58. Neve.,1996, http://www.educatorscorner.com/experiments/pdfs/exp96.pdf

59. Ohzeki, H., Mashine, A., Aoyama, H., and Inasaki, I., 1999, Development of a Magnetostrictive Torque Sensor for Milling Process Monitoring, *Journal of Manufacturing Science and Engineering*, Vol.121. Nov., pp.615-622.

60. Prickett, P.W., and Johns, C., 1999, An Overview of Approaches to End Milling Tool Monitoring, *The International Journal of Advanced Manufacturing Technology*, Vol.39, pp.105-122.

61. Rahman, M., 1988, In-Process Detection of Chatter Threshold, *Transactions of the ASME*, Vol.110. Feb.,, pp.44-50.

62. Radulescu, R., Kapoor, S.G., and DeVor, R., 1997, An Investigation of Variable Spindle Speed Face Milling for Tool-Work Structure with Complex Dynamics: Part I & II, *ASME J. Eng. Ind.*, 119,pp.266-280.

63. Ranganath, S., Narayanan, K., and Sutherland, J.W., 1999, The Role of Flank Face Interference in Improving the Accuracy of Dynamic Force Predictions in Peripheral Milling, *Journal of Manufacturing Science and Engineering*, Vol.121. Nov., pp.593-599.

64. Rober, S.J., and Shin, Y.C., 1996, Control of Cutting Force for End Milling Processes Using an Extended Model Reference Adaptive Control Scheme, *Journal of Manufacturing Science and Engineering*, Vol.118. Aug., pp.339-347.

65. Sastry, S., Kapoor, S.G., and DeVor, R.E., 2002, Floquet Theory Based Approach for Stability Analysis of the Variable Speed Face-Milling Process, *Transactions of the ASME*, Vol.124. Feb., pp.10-17.

66. Segreti, M., Moufki, A., Dudzinski, D., and Molinari, A., 2001, Modelling of Self-excited Vibration in Metal Cutting, *Proceedings of the 3rd International Conference On Metal Cutting and High Speed Machining, June 27-29, Metz, France.*

67. Shames, I.H., 1989, Introduction to Solid Mechanics, 2nd ed., Pretice-Hall, Englewood Cliffs, N.J.

68. Smith, S., and Tlusty, J., 1991, An Overview of the Modeling and Simulation of the Milling Process, *ASME, J. Eng. Ind.*, Vol.113, pp.169-175.

69. Soliman, E., and Ismail, F., 1997, Chatter Suppression by Adaptive Speed Modulation, *International Journal of Machine Tools and Manufacturing*, Vol.37, No.3, pp.355-369.

70. Stephenson, D.A., and Agapiou, J.S., 1992, Calculation of Main Cutting Edge Forces and Torque for Drills with Arbitrary Point Geometries, *Int. J.Mach.Tools Manuf.*, Vol.32, pp.521-538.

71. Tarng, S., Hwang, T., and Wang, Y.S., 1994, A Neural Network Controller for Constant Turning Force, *International Journal of Machine Tools and Manufacturing*, Vol.34, No.4, pp.453-460.

72. Tarng, Y.S., 1990, Study of Milling Cutting Force Pulsation Applied to the Detection of Tool Breakage, *International Journal of Machine Tools and Manufacturing*, Vol.30, No.4, pp.651-660.

73. Tarng, Y.S., and Cheng, S.T., 1993, Fuzzy Control of Feed Rate in End Milling Operations, *International Journal of Machine Tools and Manufacturing*. Vol. 33, No.4, pp.643-650.

74. Tarng, Y.S., Hwang, S.T., and Wang, Y.S., 1994, A Neural Network Controller for Constant Turning Force, *International Journal of Machine Tools and Manufacturing*. Vol.34, No.4, pp.453-460.

75. Tsao, Tsu-Chin., McCarthy, Mark W., and Kapoor, Shiv G., 1993, A New Approach to Stability Analysis of Variable Speed Machining Systems, *International Journal of Machine Tools and Manufacturing*. Vol. 33, No.6, pp.791-808.

76. Tung, E.D., Tomozuka M., and Urushisaki, Y., 1996, High-speed End Milling Using a Feed forward Control Architecture, *Transactions of the ASME*, Vol.118. May., pp.178-187.

77. Valley, Scotts, 1996, Borland C++ Programmer's Guide, *Borland International, Inc.*, California, USA, Version 5.0.

78. Yilmaz, A., Al-Regib, E., and Ni, J., 2002, Machine Tool Chatter Suppression by Multi-Level Random Spindle Speed Variation, *Transactions of the ASME*, Vol.124. May, pp.208-216.

79. Yun, W.-S.,and Cho, D.-W., 2000, An Improved Method for the Determination of 3D Cutting Force Coefficients and Runout Parameters in End Milling, *The International Journal of Advanced Manufacturing Technology*, Vol.16, pp.851-858.